Swiss Needle Cast and the Foliar Mycobiome of Coastal Douglas-fir (*Pseudotsuga menziesii*)

by

Emma Hayward

BSc, University of Victoria, 2021

A Thesis Submitted in Partial Fulfillment of
the Requirements for the Degree of

MASTER OF SCIENCE

in the Department of Biology

We acknowledge and respect the Lək̓ʷəŋən (Songhees and Esquimalt) Peoples on whose territory the university stands, and the Lək̓ʷəŋən and W̱SÁNEĆ Peoples whose historical relationships with the land continue to this day.

Swiss Needle Cast and the Foliar Mycobiome of Coastal Douglas-fir (*Pseudotsuga menziesii*)

by

Emma Hayward
BSc, University of Victoria, 2021

Supervisory Committee

Dr. Jürgen Ehlting (Department of Biology)
Supervisor

Dr. Paul de la Bastide (Department of Biology)
Departmental Member

Dr. Barbara J. Hawkins (Department of Biology)
Departmental Member

Dr. Ryan Gawryluk (Department of Biology)
Departmental Member

Abstract

Fungal pathogens of trees are an essential component of forest ecosystems as an ecological driver of diversity and natural selection; however, they can also have devastating effects. My research aims to understand better *Nothophaeocryptopus gaeumannii,* the causal agent of Swiss Needle Cast (SNC), a disease affecting Douglas-fir (*Pseudotsuga menziesii*). This pathogen infects the needles of its host, is associated with defoliation, and is endemic throughout the Douglas-fir range. In the Pacific Northwest of the US and Canada, a rise in the incidence and severity of SNC, which is thought to be linked to climatic changes and forestry practices, has been observed in the past few decades. There is a genetic component to SNC tolerance, enabling the selection of SNC resilient genotypes for reforestation. However, fungal load is not always correlated with needle loss, suggesting a more complex relationship. My thesis work collected SNC symptom severity data (measured as stomatal occlusion severity, needle loss severity, and relative growth rate) on a general combining ability population with a high incidence of SNC from the provincial Douglas-fir breeding program. Host phenotyping revealed a similar lack of correlation between disease signs and symptoms. Stomatal occlusion severity and relative growth rate were found to be low-moderately heritable traits within this breeding population (h_2 = 0.19-0.34 and 0.28, respectively), whereas needle loss severity had low heritability (h_2 = 0.11-0.12), and considerable variation within families and across locations in the plot. I hypothesize that this is due to this study site's endemic level of infection. SNC severity at endemic levels is likely not strong enough to drown out other biotic and abiotic factors contributing to needle loss. I propose stomatal occlusion incidence as a reasonable trait to breed for resistance under endemic-level conditions. The second part of my research investigated fungal community composition within Douglas-fir needles. Community analysis was done to determine if specific communities or taxa determine SNC

symptom response or drive this lack of correlation between SNC signs and symptoms. I used ITS amplicon metagenomics supplemented by fungal culturing to characterize the foliar mycobiome of a subset of individuals from the same Douglas-fir breeding population. The Douglas-fir foliar mycobiome was diverse, including mostly rare OTUs and a few highly abundant OTUs, such as *N. gaeumannii* (64.5% of reads). *N. gaeumannii* was found to have a negative correlation with the second most abundant OTU, belonging to the genus *Rhizosphaera,* identifying it as a direct competitor with *N. gaeumannii* in the foliar environment for some host genotypes. The genus *Rhizosphaera* exhibited associations with particular families within the breeding population, suggesting some level of genetic determination. Foliar mycobiome community assemblages differed significantly among families but not between disease severity levels or groupings. The foliar mycobiome's composition, therefore, has implications for breeding programs in the context of synthetic communities ('SynComs') as seen in the context of white spruce and its pathogen spruce budworm. Despite no clear patterns in fungal community composition based on SNC symptom severity, fungal taxa that are known foliar pathogens, as well as taxa that are known to produce beneficial bio-active compounds (*i.e.,* mycoparasitic taxa), were found within my dataset. This could explain some of the variation associated with needle loss, which was not correlated with the fungal load of *N. gaeumannii* at this site.

Table of Contents

List of Tables

List of Tables

List of Figures

List of Figures

List of Figures

Acknowledgements

I am grateful to the Pacheedaht people, whose land this research was conducted on, as well as to the Lək̓ʷəŋən people, where the University of Victoria is situated. Thank you to my supervisors, Jürgen and Paul, for making these last few years zoom by and supporting me throughout this process. I could not have asked for two more kind and knowledgeable people to have in my corner. Thanks to my family, who I would not be here without, particularly my grandad, who I'm sure would have been very excited to have another Uvic alum in the family. To my friends, thank you for keeping me sane and pretending to listen when I practiced all my presentations, particularly my partner Skyler and my roommates Kylie and Dorian, who had no place to run. To everyone in the biology department, particularly the office staff who are the backbone of this department, thank you for your help and kindness these last few years. My office mates, Claire, Becca, and Brittnie, thank you for always making me laugh and bringing the most chaotic and enjoyable energy. Finally, thank you to everyone who has helped in any aspect of this project, as this would not have been possible without you. This includes my committee, Jon Degner, Joey Tanney, PFC and MoF technicians, and Ehlting lab members, particularly Sarah, whose positivity and coffee walks kept me going, and Izzy for helping with my fungal culturing/ experiencing the joy of parenting 100's fungal babies and numerous therapy walks and bike rides.

General Introduction

Douglas-fir

Douglas-fir (Pseudotsuga menziesii (Mirb.) Franco) is one of the most important timber species in the Pacific Northwest of North America. In particular, the coastal variety, *Pseudotsuga menziesii* var. *menziesii,* is known for its high productivity and superior wood quality. Because of these attributes, it is grown extensively in plantations both within its home range as well as outside (*i.e.,* Europe, South America and New Zealand) (Hermann and Lavender, 1999). Douglas-fir accounts for approximately 22% of timber harvest for British Columbia's (BC) forestry sector, which in 2021 generated 55,715 jobs and revenue of $1.9 billion in BC (BC Ministry of Forests, 2021).

As well as being one of the most economically important tree species, Douglas-fir ecosystems hold great ecological and cultural significance. Its entire range is the largest of any commercial species, with its northern limit in central BC and its southern limit extending as far as central Mexico (Hermann and Lavender, 1999). There are two different subspecies found in British Columbia, coastal and interior, with the coastal variety existing along the southern coastal mainland and most of Vancouver Island. The interior variety occurs throughout southern British Columbia and north to Takla Lake in various BEC zones, typically including more open forests with pinegrass and moss-dominated understories (Government of BC, n.d.). While these two varieties of Douglas-fir exist in high abundance across different ecosystems in BC, specifically, two different biogeoclimatic (BEC) zones within BC are defined by this species: the Coastal Douglas-fir zone (CDF) and Interior Douglas-fir (IDF) zone. The CDF is restricted to southeastern Vancouver Island, the Gulf Islands, and a strip from Powell River along the opposite mainland

coast. It is diverse and boasts over 500 rare species restricted to this range (Straley *et al.,* 1985), making it an ecosystem of great ecological significance to BC. Along the coast, Douglas-fir forests are a host for other tree species, western red cedar (*Thuja plicata* [D.] Don.), hemlock (*Tsuga heterophylla* (Raf.) Sarg.), and grand-fir (*Abies grandis [Douglas ex D.Don] Lindl.)*, while housing understory species such as: salal (*Gaultheria shallon* Pursh), huckleberries (*Vaccinium parviflorum* Andrews), Oregon grape (*Mahonia nervosa* (Pursh) Nutt.), and sword ferns (*Polystichum munitum* (Kaulf.) C. Presl.), all of which are used in some capacity in indigenous culture. Indigenous communities have stewarded this ecosystem since the beginning of their relationship with the land, long before the establishment of Canada as a nation. Their use of fire regimes to maintain a range of successional stages of these forests, particularly for creating and maintaining Gary oak ecosystems, remains visible and culturally significant today (Doll, 2022). Douglas-fir have been traditionally used for fuel, as building material, and carved for tools such as fish hooks and handles by many indigenous groups (Government of BC, n.d.). Ultimately, the dynamic nature of Douglas-fir as a species and its role in defining ecosystems necessitates careful consideration in both management and research, a need accentuated by its global spread. Recognized for its value, Douglas-fir is extensively cultivated as an exotic species worldwide, notably in countries like France, Germany, Chile, and New Zealand (Hermann and Lavender, 1999). Because of its widespread distribution and cultivation in and outside its home range, Douglas-fir is a potential host of numerous pests and pathogens.

Fungal diseases and factors contributing to disease severity

When understanding fungal pathogens, studying the causal factors behind their emergence is crucial. The emergence of what we consider "new" diseases is primarily attributed to environmental shifts, predominantly influenced by human activities (Woods *et al.,* 2011). These

changes often stem from agricultural and ecological developments, including the establishment of plantation forests. Additionally, the impact of climate change, primarily instigated by human activities, plays a substantial role in this phenomenon (Ghelardini *et al.,* 2016). This human-driven change of how pathogen, host, and environment interact ultimately contributes to the emergence of novel disease patterns and pathogens (Ghelardini *et al.,* 2016).

In the recent past, global trade, despite its associated policies and regulations (*i.e.,* quarantine policies and phytosanitary regulations), has resulted in an unprecedented number of introduced alien species worldwide (Ghelardini *et al.,* 2016), many of which have resulted in severe disease outbreaks (*i.e.,* Dutch elm disease, chestnut blight, ash dieback, and white pine blister rust (Anderson *et al.,* 2004; Ganley *et al.,* 2008; Liebhold *et al.,* 2012; Gross *et al.,* 2014). The spread of these pathogens is often due to them having gone undetected in their home range and the historical lack of phytosanitary regulations (Migliorini *et al.,* 2015; Rigling and Prospero, 2018; Langer *et al.,* 2022). Shifts between symptomless endophytic and pathogenic forms have been observed following exposure to different environmental conditions (Delaye *et al.,* 2013). Studies have shown that exotic pathogens can exhibit broader host associations than native pathogens, which makes them more likely to cause adverse indirect effects. For example, pathogens may opportunistically jump to new hosts or destabilize existing fungal community networks (Bufford *et al.,* 2020). While posing a novel threat to new ecosystems, latent or emerging pathogens can also become more damaging within their home ranges, given the right conditions.

Swiss Needle Cast

*Nothophaeocryptopus (*formerly *Phaeocryptopus) gaeumannii (T. Rohde) Videira, C. Nakash., U. Braun & Crous* is the fungal causal agent of a foliar disease called Swiss Needle Cast (SNC), specific to Douglas-fir. *N. gaeumannii* is an example of a latent pathogen that did not jump

hosts but reached epidemic levels of infection under different environmental conditions outside of its native home range (Boyce, 1940). The name "Swiss" Needle Cast originated from its initial identification in Switzerland, where Douglas-fir had been introduced as an exotic tree species (Boyce, 1940). With Douglas-fir, *N. gaeumannii* was brought into Europe and caused an epidemic of SNC. This disease had not been previously described or noticed within Douglas-fir's native range of the Pacific Northwest of North America despite its causal agent *N. gaeumannii* being present (Boyce, 1940). While Switzerland was the catalyst for this disease's discovery, New Zealand and other European countries that introduced Douglas-fir experienced similar epidemic-level outbreaks (Boyce, 1940; Stone *et al.,* 2007). Identifying this disease in different parts of the world led to the discovery of this pathogen within its native range, suggesting the presence of *N. gaeumannii,* predating symptoms and disease concerns (Hansen *et al.,* 2000). It was only in the 1990s that significant reports of forest stand damage in Oregon and Washington caused by SNC, specifically premature needle loss, emerged (Hansen *et al*., 2000; Shaw *et al.,* 2011; Ritóková, *et al.,* 2016). Needle loss is induced indirectly by stomatal occlusions, not by direct pathogenicity of the fungus. In the late spring/early summer, spores are released and colonize the surface of newly flushed needle tissue. The fungus enters through stomates via an appressorium into the intercellular space. The fungal hyphae then colonize the interior of the needle. It is essential to note that this colonization does not cause any symptoms such as necrosis, hypersensitive response, or chlorosis. Not before the following year, pseudothecia (ascospore-producing fruiting bodies) grow out through and plug the stomates (Stone *et al.,* 2007). The life cycle of this fungi thus indirectly causes a reduction in gas exchange, which directly impacts growth and eventually wood volume due to a loss of function of photosynthetic tissue (Manter *et al.,* 2000). An incidence of 50% of stomates occluded with pseudothecia has been suggested as the threshold to cause needle abscission

(Hansen et al., 2000). However, this simple causation has been questioned recently (Montwé *et al.,* 2021).

Initially, it was believed that severe cases of the disease were primarily caused by planting Douglas-fir trees in unsuitable habitats, often sites that had previously been dominated by alder, spruce, and hemlock. Such sites are typically characterized by low elevation, high rainfall, and coastal conditions (Hansen *et al.,* 2000). Although historically present in these sites, Douglas-fir was a minor component (Hansen *et al.,* 2000). It is likely a culmination of these and other factors that have caused an unprecedented increase in the severity and range of Swiss Needle Cast. Additional factors include seed sources not adapted to local site conditions, high tree densities, and changing climate patterns that become more conducive to the disease (Hansen *et al.,* 2000; Wilhelmi *et al.,* 2017; Shaw *et al.,* 2021). In recent decades, the incidence of Swiss Needle Cast along the Pacific Northwest coast of North America has coincided with higher winter temperatures and increased spring rainfall, resulting in conditions such as increased leaf wetness that promote spore dispersal and fungal colonization (Manter *et al.,* 2005). These conditions conducive to disease are typically seen at lower elevations along the coast, where the most severe symptoms have been observed (Hansen *et al.,* 2000; Rosso and Hansen, 2003; Shaw *et al.,* 2014). Extrapolating the Manter *et al.* (2005) model to BC suggests a northward spread of SNC based on climate predictions for wet springs and warm winters, which is a cause for concern for British Columbia, in particular the west coast of Vancouver Island (A. Hamman, University of Alberta, unpublished).

Recent research has focused on better understanding Swiss Needle Cast's effects (*i.e.,* stomatal occlusion incidence, needle loss, impact on growth) on highly impacted sites. One area of long-standing research is Coastal Oregon, where aerial surveys have been conducted over

the past three decades (1996-2018) (Ritóková *et al.,* 2016; Shaw *et al.,* 2021). Similar surveys have also been conducted to a slightly lesser extent in Washington and British Columbia (Hood, 1982). These studies have consistently revealed that the disease significantly impacts sites with wetter and milder coastal conditions (Ritóková *et al.,* 2016).

While the impact of the environment on SNC severity is widely supported, researchers have also observed genetic variability in the susceptibility of Douglas-fir trees to Swiss Needle Cast (Johnson, 2002; Temel *et al*., 2005; Hood, 1982; McDermott & Robinson, 1989). Offspring originating from provenances from drier climates have shown higher susceptibility to the disease than those from wetter conditions (*e.g.,* Wilhelmi *et al.,* 2017), suggesting local adaptation to higher pathogen pressures in wetter and milder conditions. Despite numerous studies highlighting the variability in disease symptoms across populations, only a few published academic studies have quantified the heritability of these traits. They found that needle retention ranges from low to moderate and stomatal occlusion exhibits relatively low heritability (Temel *et al.,* 2005; Johnson, 2002). Further studies, however, are needed to support or refine these findings.

In 2021, Montwé *et al.* conducted a study close to the west coast of Vancouver Island, British Columbia. The aim was to assess whether screening for SNC traits is an effective strategy to identify resistant (*i.e.,* low levels of infection by SNC as determined by stomatal occlusion incidence and fungal load) or tolerant individuals (*i.e.,* low levels of needle loss regardless of high levels of infection by SNC) within a breeding population; findings which could be used to select for tolerance and/or resistance within these Douglas-fir breeding populations. Their study, which assessed the variance of SNC, found that SNC resistance (stomatal occlusion incidence) and tolerance (needle retention) vary significantly across families. Only needle loss scores strongly correlated with growth metrics such as height, stem diameter, and wood volume. In contrast,

stomatal occlusion scores did not exhibit such a correlation, nor did they correlate with needle loss scores. These findings contradict our current understanding of SNC disease interactions. Since pseudothecia block stomates, this impairs CO_2 uptake, and as pseudothecia increase, this proportionally decreases CO_2 uptake. Once these needles take in less carbon than they release (*i.e.,* they become a carbon source rather than a sink), they are abscised. This implies that a correlation between the proportion of stomata occluded with pseudothecia and needle loss should be expected, and this is what has been previously described (Manter *et al.,* 2003a; Cannell and Morgan, 1990). In contrast, Montwé *et al.* (2021) suggest more complex mechanisms to be at play, at least in that site and population. However, it remains enigmatic what other factors may be involved in modulating this plant-pathogen interaction. Besides more complex factors in plant or pathogen physiology or biochemistry, another possible explanation could be the foliar fungal endophytic community's influence on disease severity.

The role of endophytic communities in pathosystems

The definition of endophytes, describing fungi or bacteria living within plants, is inconsistent in the literature. Some describe endophytes based on their found space (*i.e., '*endo' – within 'phyte' – plant). Others more explicitly define endophytes based on the nature of their interaction type with their host (*i.e.,* fungi or bacteria within a plant that do not cause disease symptoms) (Wilson, 1995). For this thesis, I will define *endophytes* as any fungi that live within plants regardless of their host association. I choose this definition because of the continuum on which endophytes exist, with some exhibiting different host associations throughout their lives, making defining based on their relationship difficult (Newton *et al.,* 2010). For example, *N. gaeumannii* begins its life cycle as a symptomless endophyte but, given the proper environmental conditions, eventually causes disease symptoms.

Numerous ex-situ experiments have addressed the impact of endophyte communities on plant pathogens and stressors. One of the most well-studied and successful examples of this is the reduction of damage caused by insect pathogen spruce budworm (*Choristoneura fumiferana* Clemens) on its host white spruce (*Picea glauca* Moench). The native endophytic fungus *Phialocephala scopiformis* DAOM 229536 Kowalski & Kehr (Helotiales, Ascomycota) has been found to decrease survival of eastern spruce budworm by releasing anti-insect metabolites (Frasz *et al.,* 2014; Quiring *et al.,* 2019). This has proved successful, resulting in JD Irving Ltd. nurseries (New Brunswick) generating enough beneficial inoculum for tens of millions of seedlings annually to mitigate this disease. Instead of inoculating with a single beneficial endophyte, hosts can be treated with a cocktail of different endophytes in the hopes that one, or interactions of few or many, confer host tolerance towards the biotic or abiotic stress of interest. Recent studies have shown the potential of introducing symbiotic fungal endophytes as an alternative to time-intensive and costly plant breeding programs and the use of fungicides (Schardl *et al.,* 2004). Examples of this include improved drought tolerance in both *P. menziesii* and *Thuja plicata* when treated with endophyte consortia (Aghai *et al.,* 2019); and a reduction of white pine blister rust symptoms (causal agent *Cronartium ribicola*) when *Pinus monticola* seedlings were treated with endophyte communities isolated from healthy individuals (Ganley *et al.,* 2008).

Although more and more fungal endophytes are being recognized to provide various benefits to their hosts, including pathogen suppression (Schardl *et al.,* 2004), they are a taxonomically diverse group and remain poorly characterized for many plant species (Porras-Alfaro & Paul Bayman, 2011). Therefore, a detailed characterization of the endophytic microbial community is essential and holds significant economic potential for Douglas-fir and other tree species of commercial importance. Another critical gap that I hope to address with my research is

the lack of research at present on community interactions between a native pathogen and native endophytes. The SNC pathosystem is unique compared to previously studied systems (*i.e.,* White Pine Blister Rust caused by *Cronartium ribicola;* Ganley *et al.,* 2008) in the sense that *N. gaeumannii* has co-evolved with the other members of the Douglas-fir foliar mycobiome (Boyce, 1940). Understanding how these relationships change when *N. gaeumannii* switches to epidemic levels, as seen in Oregon and Washington (Ritóková *et al.,* 2016), is an essential piece of information needed to understand better foliar fungal endophyte interactions in the context of SNC disease.

Objectives

In the first data chapter, I will assess SNC sign and symptom severity levels and will analyze the heritability of and correlation between SNC disease signs, disease symptoms and plant growth rate measured from approximately 600 trees in a BC Ministry of Forests breeding population. Given Montwé et al.'s (2021) study, I hypothesize that *we will see a similar lack of correlation between SNC disease signs and disease symptoms* at this close-by study site comprised of similarly aged trees. The second data chapter will test the hypothesis that *differences in fungal endophytic communities within the Douglas-fir foliar mycobiome influence disease signs and symptoms associated with SNC.* To date, limited research has focused on the foliar mycobiome of Douglas-fir despite its significant economic and ecological importance (Carroll & Carroll 1978; Daniels *et al.,* 2018; Gervers *et al.,* 2022), and no studies have investigated these mycobiomes in the context of SNC. To describe the foliar mycobiome of Douglas-fir, I will use high throughput metagenomic ITS sequencing to look at community composition in parallel with a traditional culture-based Sanger sequencing approach. I will explore community composition across samples to determine the presence of any differentially abundant taxa among genetically distinct families

expressing different disease signs and symptoms. I will also examine how community composition may differ based on tree-relatedness within the breeding program (*i.e.,* as a consequence of vertical endophyte transmission). Lastly, I will wrap up data chapter 2 by highlighting the fungal taxa found within our study and how this compares with the few recent studies published on the Douglas-fir foliar mycobiome. This aims to provide a comprehensive overview of the Douglas-fir foliar mycobiome to better understand this complex pathosystem.

Data Chapter 1 - Phenotypic Responses to SNC and Heritability

Scientific Contribution to data chapter 1

Jürgen Ehlting and Paul de la Bastide conceived and designed the initial pilot of this study. Emma Hayward contributed to aspects of study design while working as a research technician prior to her thesis work. The study was designed to be compatible with pre-existing data collected on the Jordan River progeny trial. Two-year's worth of data was collected and compiled for this site by Dr. David Noshad (MoF) and team prior to Emma Hayward's thesis work. This data was used to supplement field data for this site collected by Emma Hayward and a team of collaborators in the years 2021 and 2022. (Keith Bird (MoF), Dr. Joey Tanney (NRCAN), Robert Kowbel (NRCAN), Annie Dicaire (NRCAN), Cameron D'Amours (NRCAN), Connor Connolly-Moyls (UVic), Dr. Jürgen Ehlting (UVic), Dr. Paul de la Bastide (UVic), Sarah Lane (UVic), Isabella Laughton (Uvic), Niya Kelpin (Uvic). Emma Hayward did all data analysis with help from Dr. Jonathan Degner with ASReml heritability analysis,

Introduction

Resistance and tolerance to Swiss Needle Cast in a breeding population

This thesis uses the definition of resistance and tolerance put forth by Temel *et al.* (2004) and the interpretation of this adapted to SNC by Montwé *et al.* (2021). Signs of disease are defined as the amounts of fungal material within the leaves (*i.e.,* fungal load) and/or the proportion of stomata occluded with pseudothecia (stomata occlusion scores hereafter). Disease symptoms are defined as needle loss. A tree with low signs of the disease (*i.e.,* stomatal occlusion score, fungal load) would be considered resistant, and a tree with few symptoms (*i.e.,* low needle loss regardless of high stomatal occlusion scores or fungal load) would be considered tolerant.

It has been a longstanding question what the most suitable phenotyping method for quantifying disease severity to Swiss Needle Cast is (Temel *et al.,* 2005). Methods explored include needle/foliage color (Temel *et al.,* 2005), needle retention (Temel *et al.,* 2005; Montwé *et al.,* 2021), foliage density (Maguire *et al.,* 2002; Johnson, 2002) proportion of stomata occluded by pseudothecia (stomatal occlusion) (Hansen *et al.,* 2000; Temel *et al.,* 2005; Montwé *et al*., 2021), and amount of *N. gaeumannii* DNA in needles, quantified through qPCR (Temel *et al.,* 2005; Montwé *et al.,* 2021). Several studies have shown differences in the severity of disease symptoms within and across populations. Variability across populations can be attributed to genetic variation (Johnson, 2002; Temel *et al.,* 2005; Montwé *et al.,* 2021). What causes this genetic variation is still largely enigmatic; few studies have tried to address this with no clear conclusions as to whether resistance (*i.e.,* trees that inhibit the level of SNC infection) or tolerance (*i.e.,* trees that grow and retain foliage despite disease infection) or both drive this variation. Larger variation in measured needle loss has led to the conclusion that needle loss (tolerance) may be the best indicator when selecting genetically more adept trees (Johnson, 2002; Temel *et al.,* 2004; Montwé *et al.,* 2021). This, however, becomes more complicated when looking at how stomatal occlusion scores interact with this variable (needle loss).

Our current understanding of SNC states that the average proportion of occluded stomata is causally correlated with the severity of needle loss in Douglas-fir. This relationship is plausible in the context of this disease, as reduced photosynthetic rates caused by increased incidence of stomatal occlusion result in premature needle abscission (Manter *et al.,* 2000). Fungal load should also be correlated with stomatal occlusion incidence because fungal load increases each year as SNC continues to colonize the same needle after the initial infection (Manter *et al.,* 2003a), and ultimately, this accumulation of fruiting bodies is what results in needle abscission as a

consequence of blocked gas exchange as described above (Temel *et al.,* 2004; Stone *et al.,* 2008). Because of this, fungal load should also correlate with needle loss, thus all the above (*i.e.,* fungal load, needle loss, and stomatal occlusion) should be acceptable ways of phenotyping this disease. In a study based out of Tillamook, Oregon, USA, Temel *et al.* (2004) found that fungal load was positively associated with needle loss in families classified as experiencing mild symptoms, negatively associated with needle loss in families classified as experiencing high symptoms, and no correlation with needle loss in families classified as experiencing moderate symptoms. In a similar study out of Vancouver Island, BC, Montwé *et al.* (2021) found no significant correlation between fungal load or stomatal occlusion incidence and needle loss. While it could be that distinct adaptations within some families conferring either tolerance or resistance explain this lack of correlation seen by Montwé *et al.* (2021), the fact that family ranks (based on sign and symptom severity) were not consistent between plantation sites suggests this may not tell the whole story. Another question not addressed by Montwé *et al.* (2021) was the heritability of needle loss, fungal load, and stomatal occlusion incidence within these breeding populations. Heritability is defined by the portion of phenotypic variation for a specific measurement (*i.e.,* needle loss, stomatal occlusion incidence, fungal load) attributed to genetic variation. Heritability can be further defined as narrow-sense (an estimate of additive genetic effects) and broad-sense heritability (an estimate of both additive and non-additive genetic effects) (Barry *et al.,* 2022), the former being my focus for this research because these narrow-sense heritability calculations (h_2 = VA/VP; VA = genetic variation due to additive genetic values, VP = variation due to phenotypic variance) have significant implications for future selections in tree breeding programs if the goal is to breed for disease resistance or tolerance of SNC.

Objectives

In this first data chapter, phenotype data will be described and analyzed for a breeding population of approximately 600 individuals within the BC Ministry of Forests Coastal Douglas-fir breeding program. The purpose is first to test the hypothesis that, similar to Montwé *et al.* (2021), there will be no clear correlation between SNC disease signs and symptoms. Additionally, variation in disease signs and symptom severity will be addressed between years and families. The second objective of this data chapter is to determine the heritability of these traits and whether there is any genetic or phenotypic correlation between them. Both objectives will add to our base knowledge of mechanisms affecting variation in SNC symptom severity (particularly in BC, where fewer studies have been conducted) and how this may influence the genetic selection of Douglas-fir families.

Methods

Site and sample collection

This study was conducted in a Douglas-fir progeny trial near Jordan River on Vancouver Island, BC (48.430120, -124.033993). It is situated in the fog belt of the west coast, close to the Pacific Ocean, where the prevalence of Swiss Needle Cast (SNC) is relatively high (fig. 1). The site falls within the Coastal Western Hemlock Biogeoclimatic (BEC) zone and was established in 2001 as a third-generation general combining ability population by the Douglas-fir breeding program of the BC Ministry of Forests (Jonathan Degner, personal communication). Forty-five families consisting of 607 trees total were sampled in June 2021, and a subset of trees (12 families, five individuals each) included in our mycobiome analysis were resampled the following year during the same period (June 2022). In cases where branches could not be collected due to excessive tree height or tree mortality, this was noted. Needle loss scores and diameter at breast

height (DBH) scores (only in 2021) were collected in the field, while the percentage of stomata occluded with pseudothecia (stomatal occlusion incidence) were obtained in the laboratory. Two years of previous data were also available for this study site (provided by Dr. David Noshad, unpublished).

Figure 1. Location of Jordan River, British Columbia, third generation general combining ability progeny trial established in 2001 by the BC Ministry of forests (48.430120, -124.033993).

Needle loss scoring

For needle loss assessment, a branch from the mid-crown, between 20 and 30 feet above the ground, preferably from the south side of the tree, was cut using 12' pole pruners and 12' orchard ladders. A score ranging from 0 to 10 was assigned to branches based on their needle loss for the past four years of growth (Y1, Y2, Y3, Y4), with 0 indicating no needle loss and 10 representing 100% needle loss (fig. 2). Scores were recorded from a lateral branch and compared to 2-3 other lateral branches to ensure accuracy. In cases of variation, an average score was estimated ad hoc. The branch leader was not assessed, as needle retention on the leader often differs from that of laterals. When possible, lateral branch scores were recorded closer to the branch leader

to avoid shaded sections near the base that might exhibit lower-than-expected needle retention. Two-year-old sections from multiple laterals were retained and transported in coolers with ice blocks and then refrigerated at 4°C until they could be processed.

Figure 2. A) SNC Symptomatic Douglas fir branch B) Non-symptomatic (healthy) tree branch. Numbers 1-3 indicate last three years of growth. Not pictured measurements for 4th year age class needles were scored as well. Each year of growth (years 1-4) was scored on a scale of 0-10 (0 indicating no needle loss, 10 indicating 100% needle loss).

Stomatal occlusion scoring

Ten two-year-old needles were randomly selected from each individual and mounted on a microscope slide with the stomatal side facing up. A label with 2.5 mm segment lines was attached to the slide, and the needles were mounted on top using double-sided tape (fig. 3). Care was exercised to touch only the ends of the needles during mounting to prevent any disruption of pseudothecia present on the needle surfaces for counting. The number of stomata occluded with

pseudothecia was counted within a 2.5 mm segment in the middle of each needle, covering the outermost four complete rows of stomata in each stomatal band. The proportion of stomata occluded with pseudothecia was calculated by dividing the number of pseudothecia by the average number of stomata in this region (425 stomata; region as described above) and will be referred to as stomatal occlusion hereafter. Results for individual needles were averaged for each tree to obtain a mean.

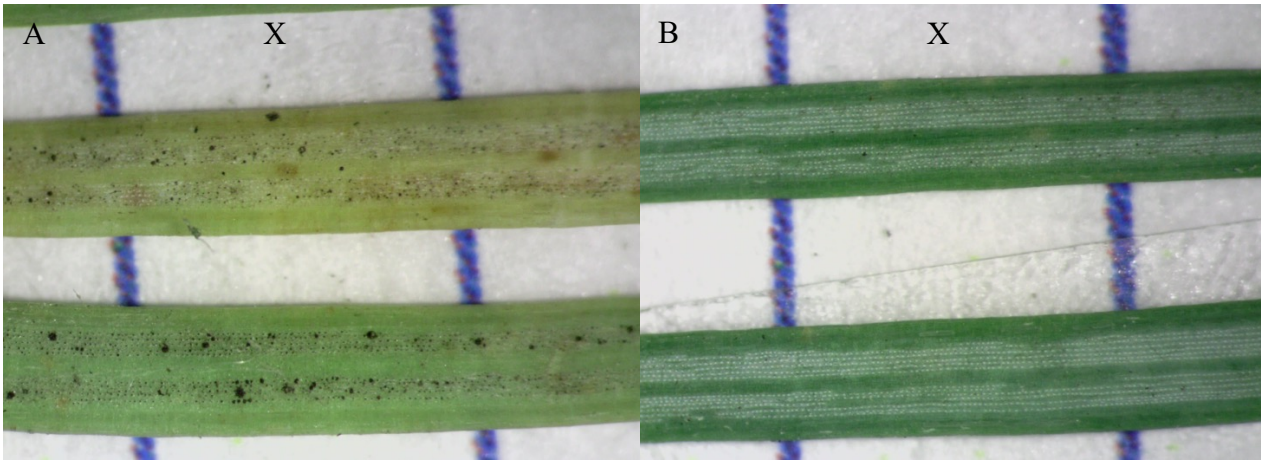

Figure 3. Douglas-fir needles mounted on microscope slides with 2.5 mm segment lines to indicate where to count. The x indicates the section where counting took place. The proportion of occluded stomata on the outermost 4 complete rows of stomata in each of the stomatal bands was counted for 10 needles per tree and averaged. (A) a tree with high stomatal occlusions (B) a tree with low/ almost no stomatal occlusions.

Relative growth rate

Relative growth rate was calculated using diameter at breast height (dbh) measurements from trees at age 11 (collected in 2012) and 20 (collected in 2021). The equation used to calculate relative growth rate was (Hoffmann and Poorter, 2002):

$$RGR = \frac{Ln\,(S_2) - Ln(S_1)}{T_2 - T_1}$$

Where:

S_1 = size at first time point

S_2 = size at second time point

T_1 = first time point (age)

T_2 = second time point (age)

Statistical analysis of phenotypic and genetic response to SNC

Unless otherwise noted, all data analysis and figures were performed and created in R (R Core Team, 2015), and plots were made in ggplot2 (Wickham, 2009).

Correlation analysis on needle loss, stomatal occlusion scores, and relative growth rate (RGR) was conducted using Spearman correlation to account for the non-normal distribution of data across all samples and years. To test whether family significantly impacts stomatal occlusion, needle loss, and RGR measurements, a linear mixed model (LMM) was applied using restricted maximum likelihood in ASReml (Butler, 2023). A LMM allows for control of the data's random effects, such as spatial biases. Replicate blocks within the plot were treated as random effects, and family as a fixed effect. Phenotype (*i.e.,* stomatal occlusion, needle loss, and RGR) scales were normalized using *scale()* in base R package. Residual plots and q-q plots were assessed for assumptions of normality and homogeneous variance of residuals, determining a good fit of the model (Zurr *et al.,* 2009). Conditional F-statistic tests (pseudo-ANOVA) were performed using the function *wald* to test for significance. LMM models were subsequently used to calculate narrow-sense heritability estimates and genetic and phenotypic correlations. Our model was designed to account for both the fixed effects of 'trait' and the random effects associated with the hierarchical structure of our data. The data is modeled as such:

[1] $\boldsymbol{y_{jki} = \mu + g_k + b_j + \varepsilon_{ijk}}$**,**

Where:

$\boldsymbol{y_{jki}}$ is the observation of the *i*th tree of the *k*th family in the *j*th block

$\boldsymbol{\mu}$ is overall mean

$\boldsymbol{g_k}$ is the fixed effect for the *k*th family

$\boldsymbol{b_j}$ is the random effect for the *j*th block

$\boldsymbol{\varepsilon_{ijk}}$ is the plot error effect corresponding to $y_{ijk.}$

To estimate genetic variance for each of the traits, an additional model was run with component g_k estimated as a random effect, incorporating pedigree information supplied by the BC Ministry of Forests (Jonathan Degner, personal communication). In this model, additive genetic variance is simultaneously estimated across parents and offspring via an "animal model" (Henderson 1984), where $g_k = \sigma^2_A \mathbf{A}$, with **A** denoting a genetic relatedness matrix. Narrow-sense heritability was estimated for each trait independently [2]. Numerous variance and covariance model structures were tested for the best fit of the data. AIC, BIC, and log-likelihood values were used to determine the best fit. Ultimately, a simple univariate model was found to have the lowest AIC and BIC scores, and this was used.

[2] $\dfrac{\boldsymbol{\sigma_A{}^2}}{\boldsymbol{\sigma_e{}^2 + \sigma_A{}^2}}$

Where:

$\boldsymbol{\sigma_A{}^2}$ is the additive genetic variance

$\boldsymbol{\sigma_e{}^2}$ is the residual variance

To estimate genetic and phenotypic correlations between all measured traits, a multivariate model was run using an unstructured genetic covariance matrix to account for covariance between the traits at the level of individual trees (due to genetic effects) and the residual level while accounting

for block effects. Variances and covariances were extracted for each trait, allowing for the calculation of both additive genetic (r_A)[3] and phenotypic correlation (r_P)[4] independent of each other.

$$[3]\ \ r_A = \frac{Cov_f(x,y)}{\sqrt{\sigma_A^2(x) \times \sigma_A^2(y)}}$$

Where:

$Cov_f(x,y)$ is the additive genetic covariance between traits *x and y*

$\sigma_A^2(x)$, $\sigma_A^2(y)$ are the additive genetic variance components for traits *x* and *y*

$$[4]\ \ r_P = \frac{Cov_f(x,y) + Cov_e(x,y)}{\sqrt{\left(\sigma_A^2(x) + \sigma_e^2(x)\right) \times \left(\sigma_A^2(y) + \sigma_e^2(y)\right)}}$$

Where:

$Cov_f(x,y)$ is the additive genetic covariance between traits *x and y*

$Cov_e(x,y)$ is the residual covariance between traits *x and y*

$\sigma_A^2(x)$, $\sigma_A^2(y)$ are the additive genetic variance components for traits *x* and *y*

$\sigma_e^2(x)$, $\sigma_e^2(y)$ are the residual variance components for traits *x* and *y*

Results

SNC phenotypic responses

607 individuals representing 45 families from a third-generation GCA population in the BC Ministry of Forests coastal Douglas-fir breeding program were phenotyped for SNC signs, symptoms, and growth traits. SNC, having known associations with climate, is variable from year to year; this can impact how results regarding disease severity are interpreted. I first assessed annual variations in SNC signs and symptoms across the site to address this. As expected, needle loss scores increased as the age of needles increased, which was consistent for all years of

measurement (fig. 4). I also observed annual variation in SNC signs and symptoms. Needle loss in 2020 (at age 19) for 3- and 4-year-old needles was higher than in any other year. Stomatal occlusion scores were higher on average in years sampled prior to my thesis work (2019 and 2020) (fig. 4). Because stomatal occlusion and needle loss measurements were consistently non-normally distributed and data transformation attempts did not significantly improve normality, non-parametric tests were used going forward for correlations and significance testing. In my analysis of average needle loss the 2019 dataset was not included because branch scoring was conducted differently that year.

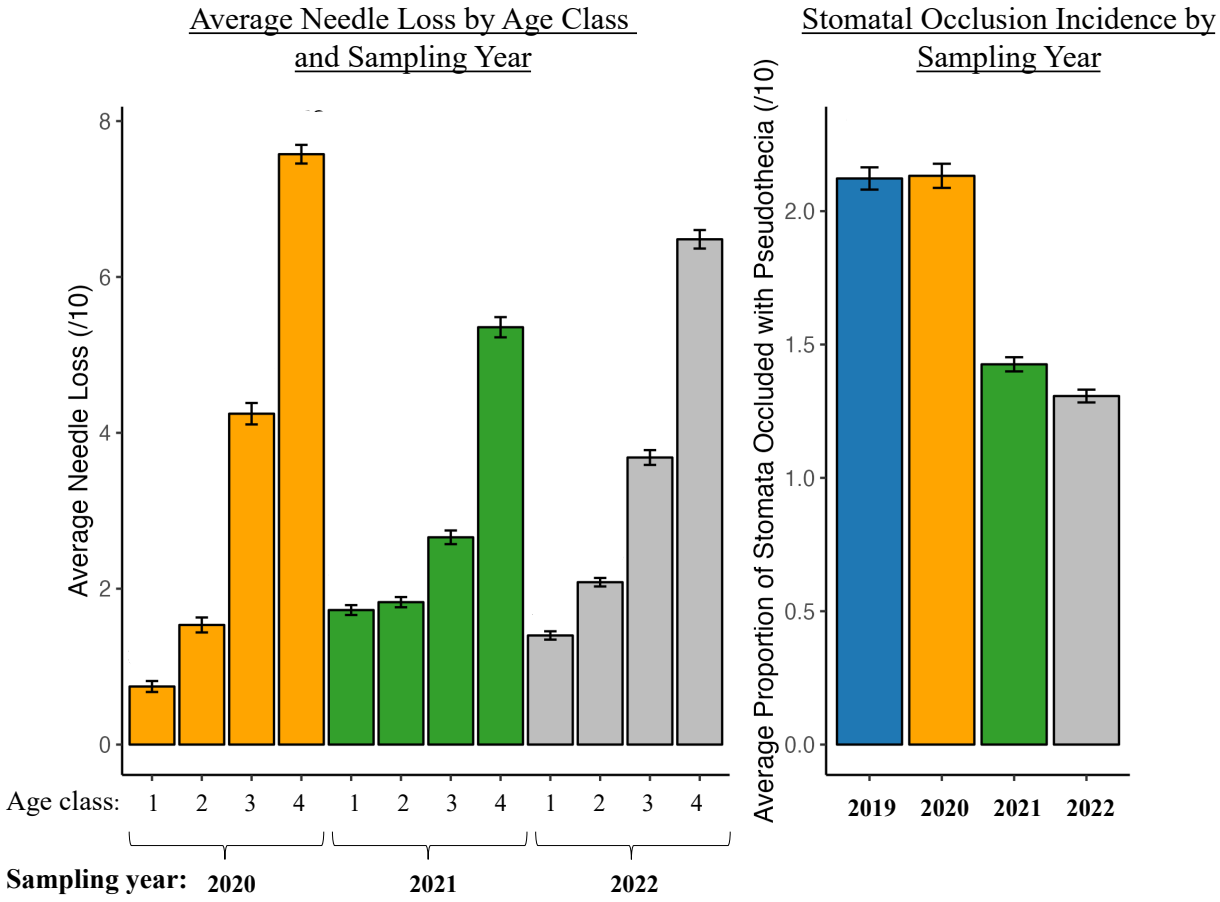

Figure 4. Average scores for each year of measurement for needle loss and proportion of stomata occluded with pseudothecia across 607 individuals (45 families) in JR GCA breeding population. For needle loss this covers 4 age classes of needle (i.e., 1y, 2y, 3y, 4y) and for stomatal occlusion all measurements were taken in 2y age class needles. The errors bars represent SE.

Phenotypic correlations in space and time

To determine whether disease signs and symptoms are correlated or not (as seen previously in other Vancouver Island breeding population stands; Montwé *et al.,* 2021), these relationships were assessed for this stand. Both needle loss scores and stomatal occlusion scores were weakly to moderately correlated between years across the whole population (607 individuals covering 45 families) (fig.5a). This was also seen in correlations based on family averages for stomatal occlusion scores but to a lesser extent in needle loss scores (fig.5b). No notable correlation was detected between stomatal occlusion scores (disease sign) and needle loss scores (disease symptom) in any comparison. This observation is notable because while stomatal occlusion in 2019 (SO2019) served as a metric for disease signs in 2-year-old branches, subsequent years' symptoms within the same age class, *i.e.,* third-year needle loss in 2020 (NL3y2020) and fourth-year needle loss in 2021 (NL4y2021), did not demonstrate correlation with this level of infection although they all represent the same infection year. A significant but weak negative correlation was seen between needle loss and relative growth rate in individual-level correlations (fig.5a).

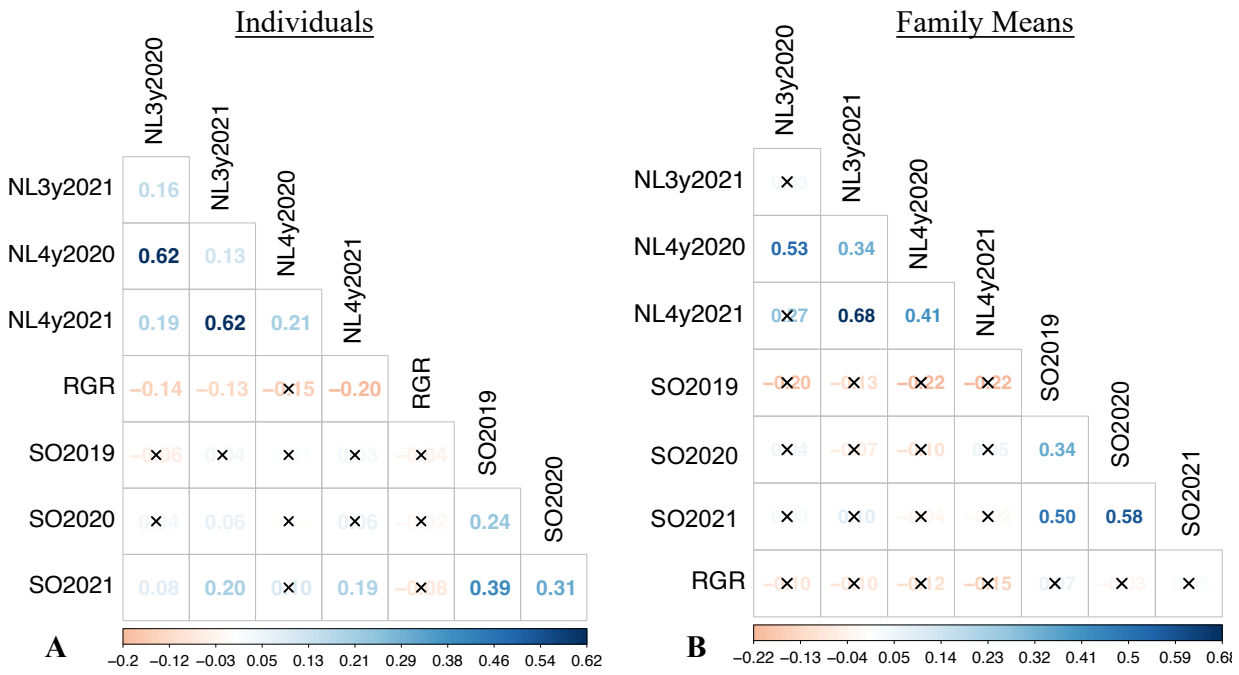

Figure 5. (left(A)) Spearman correlation (r-value = rho) of phenotypes for 607 individuals (trees) in JR GCA breeding population (right(B)) is based on average scores for the 45 families within the same population. NL (needle loss) is followed by the age class of needles (3y or 4y) and the year of sampling; SO (proportion of stomata occluded with pseudothecia followed by year of sampling); RGR (relative growth rate between ages 11 and 20). X's indicate non-significant results.

Block effects

Microenvironmental effects may impact observed phenotypes and are a confounding factor to consider when asking the question of how much phenotypic variation is due to genetics. To address this, trends in phenotypes by block were assessed. While there was some variation across blocks when considering stomatal occlusion, there was only one year where these differences in stomatal occlusion were significant (variance: **2019** = 0.072, **2020** = 0.051, **2021** = 0.025; fold change varied from 1.39-fold to 1.63-fold, fig. 6). Likewise, in one year of the two years measured (2020) there was a significant difference in mean needle loss scores by location (block) (variance: **2020** = 1.823, **2021** = 0.236; fold change varied from 2-fold to 5.8-fold, fig. 6).

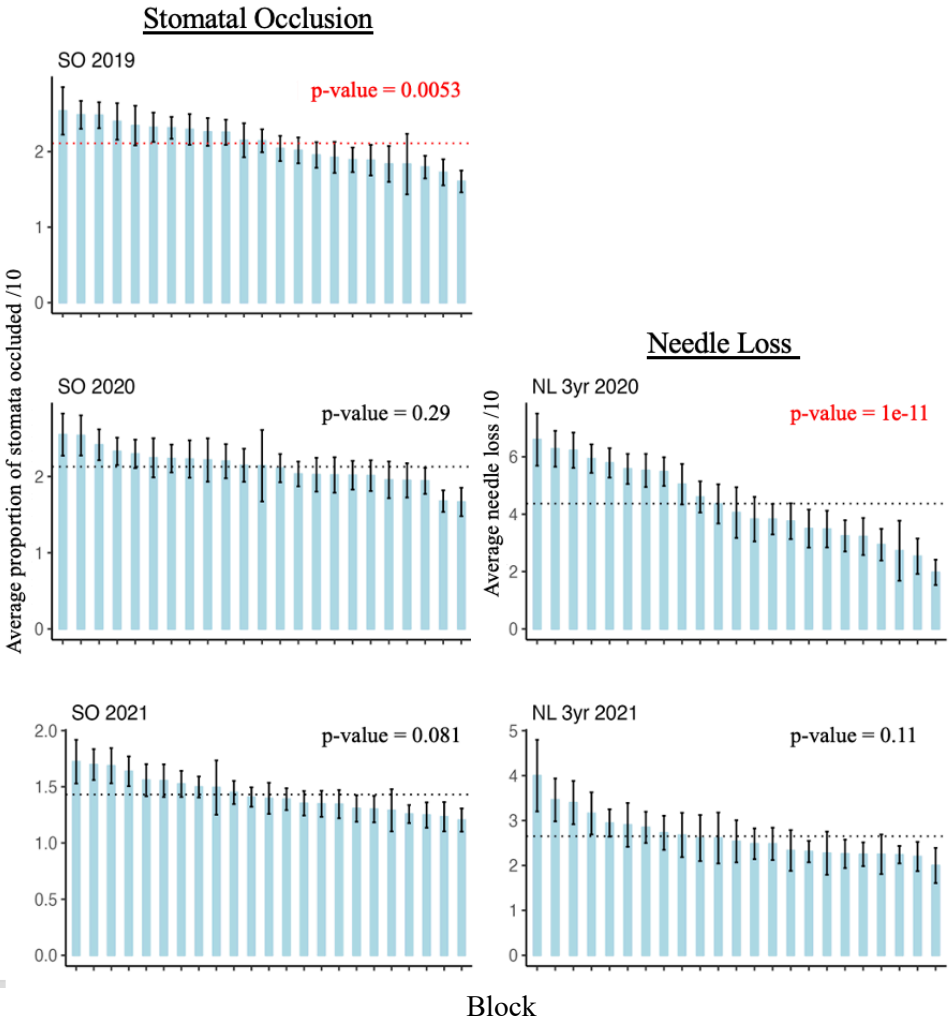

Figure 6. (Left) differences in average proportion of stomata occluded with pseudothecia (Stomatal Occlusion) for 2rd year age class needles from different blocks in JR GCA breeding population (n= 607). (Right) differences in average needle loss for 3rd year age class needles from different blocks in JR GCA breeding population (n= 607). p-values are results from a Kruskal-Wallis test. Error bars represent standard error for group averages and red line indicates the overall mean.

Family effects and heritability

To initially assess the extent to which genetic factors explain variation in SNC sign and symptom severity, I looked at differences in these measured traits across families in my study population. There were significant across-family differences in the average proportion of stomatal occlusion for all years of measurement (variance: **2019** = 0.147, **2020** =0.181, **2021** = 0.0696; fold change varied from 2.29-fold to 2.94-fold, fig. 7). There was considerable variability seen within these

families for average needle loss, with no significant differences between them (variance: **2020** = 0.998, **2021** = 0.343; fold change varied from 2.89-fold to 3.65-fold, fig. 7).

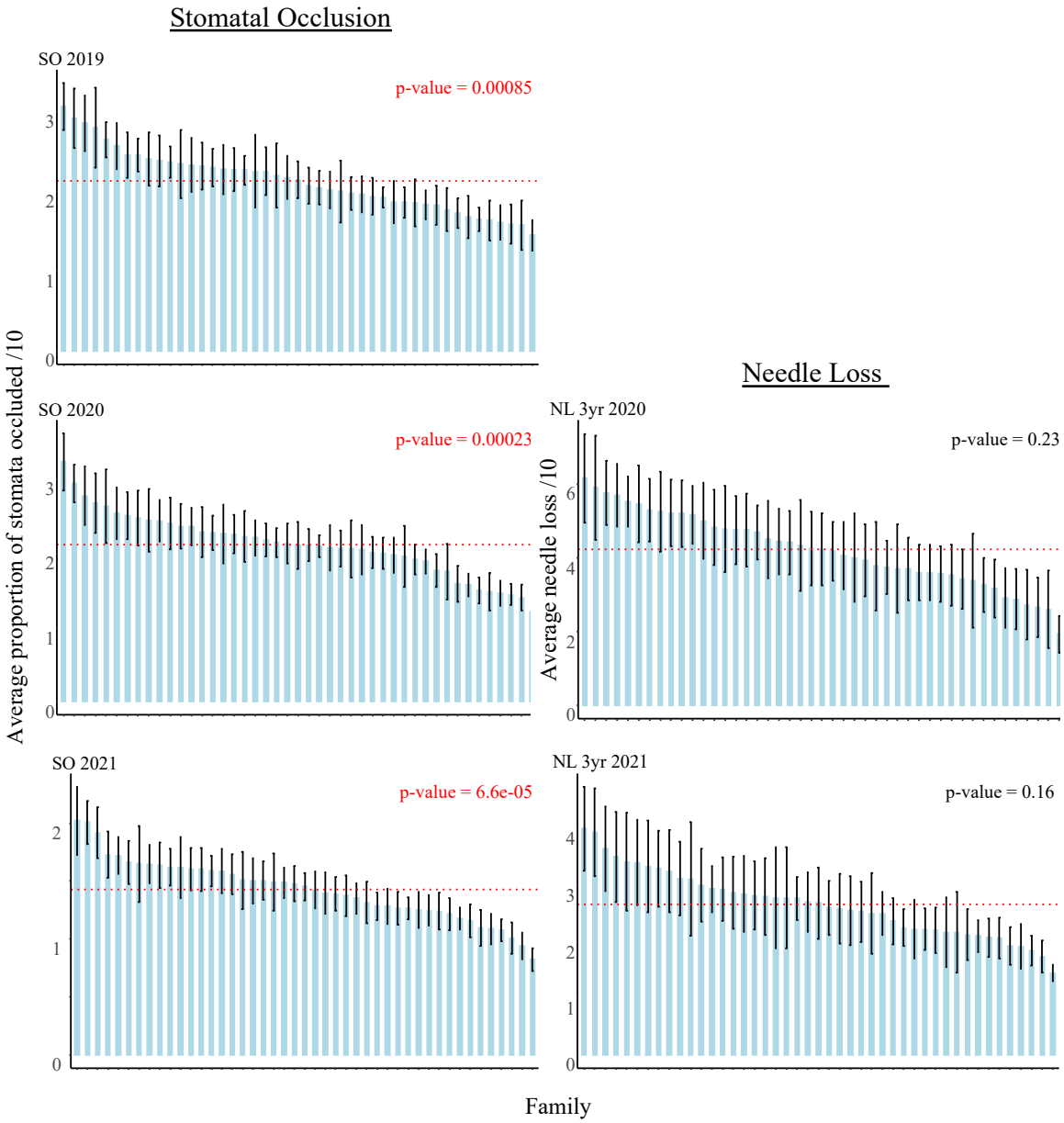

Figure 7. (Left) Family differences in average proportion of stomata occluded with pseudothecia (Stomatal Occlusion)) for 2nd year age class needles for all 45 families (n= 607) in JR GCA breeding population. (Right) Family differences in average needle loss for 3rd year age class needles for all 45 families (n= 607) in JR GCA breeding population. P-values are results from a Kruskal-Wallis test. Error bars represent standard error for group averages and red line indicates the overall mean.

Because location within the plot potentially contributed to variation within the dataset, a Linear Mixed Model (LMM) was employed to determine the fixed effect of family while considering location in the plot (block) as a random variable. This was conducted to assess whether family alone significantly affected measured phenotypes. F-tests for LMM indicate significant effects of family on stomatal occlusion across years of measurement and relative growth rate. No significant effects were seen regarding needle loss at either age class (3 or 4-year-old) (Table 1). Estimated narrow-sense heritability for SNC and growth traits (needle loss, stomatal occlusion, and RGR) were low to moderate for stomatal occlusion (0.19-0.34) and relative growth rate (0.28) and low for needle loss in three-year-old needles (0.11-0.12) (table 1).

*Table 1. Based on JR GCA breeding population (n = 607). P-values of F-tests for fixed effects of family on SNC phenotypes calculated with conditional sum of squares. Narrow-sense heritability scores for needle loss, stomatal occlusion, and relative growth rate (relative growth rate (RGR) * this is from age 11- 20). The standard error associated with that trait is given in brackets below heritability scores.*

Phenotype	SO	SO	SO	NL 3y	NL 4y	NL 3y	NL 4y	RGR
Year	2019	2020	2021	2020	2020	2021	2021	
Effect of Family	<0.001	<0.001	<0.001	0.0605	0.191	0.306	0.469	<0.001
Heritability	0.27	0.19	0.34	0.11	0.13	0.12	0.13	0.28
	(0.10)	*(0.09)*	*(0.11)*	(0.06)	*(0.07)*	(0.06)	(0.06)	(0.08)

Genetic correlations were calculated from an unstructured covariance model to determine the extent to which correlations (fig. 5) are attributed to genetics. Stomatal occlusion incidence had a high genetic correlation between all years of measurement (r-value = 0.80 to 0.90, fig. 8), suggesting that its overall phenotypic correlation year to year (fig. 5a) is driven by genetics, not environmental effects. A moderate genetic correlation was observed between years when assessing needle loss in three-year-old needles (r-value = 0.47). However, this was not significant due to

considerable variation resulting in high standard errors (fig. 8). Together with the low but significant phenotypic correlation of three-year-old needle loss across years (r-value = 0.16, fig. 5a), this suggests that environmental factors drive variability in needle loss in this population and assessment. Relative growth rate was consistently phenotypically correlated with three-year-old needle loss (r-value = -0.13 to -0.14, fig 5a). However, there was no genetic correlation (fig 8). While not phenotypically correlated with relative growth rate (fig. 5a), stomatal occlusion incidence did show a weak yet significant negative genetic correlation with relative growth rate (r-value = -0.14 to -0.28), suggesting a genetic relationship but not one strong enough to observe phenotypically (fig. 8).

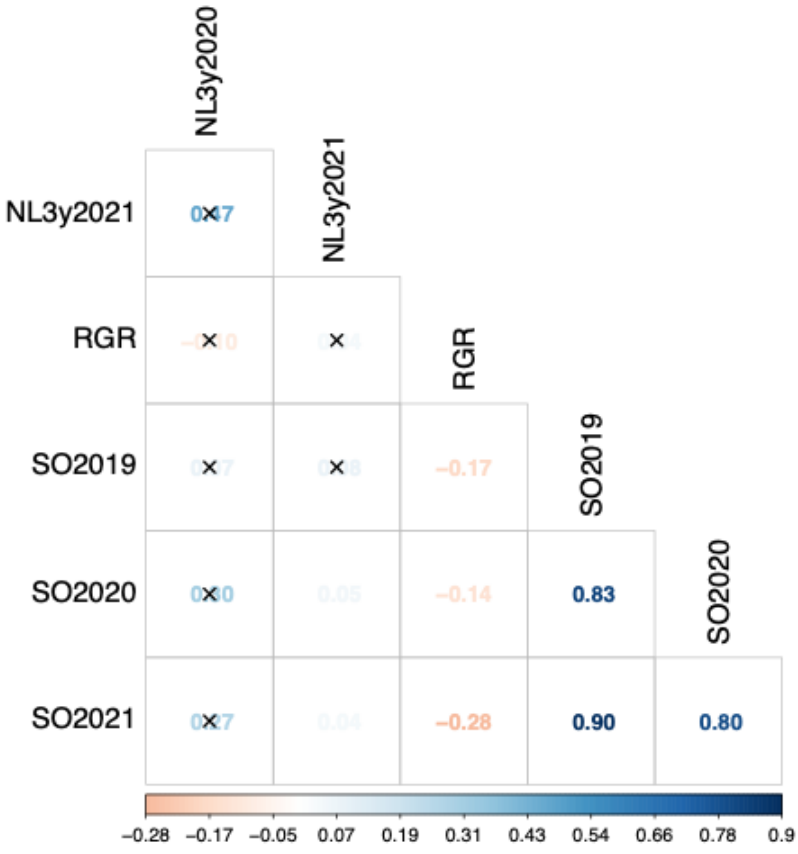

Figure 8. Based on JR GCA breeding population (n = 607). Estimated genetic correlations between Swiss Needle Cast severity traits. Calculated using an unstructured model in ASReml R and visualized using Corrgram. Colouring indicated the strength of the Pearson correlation (r-value) and X's indicate non-significant correlations (p>0.05). X's indicate non-significant results.

Discussion

This study found that for this breeding population, stomatal occlusion scores are controlled more by genetic factors and are less impacted by extrinsic factors such as microenvironment than needle loss. This could have implications because tolerance traits (needle loss) are typically being selected over resistance (stomata occlusion) for breeding programs to reduce SNC severity. Stomatal occlusion scores showed consistent correlations across years, had moderate heritability, and were found to be significantly impacted by family.

Narrow sense heritability estimates for growth were similar to what has previously been reported in the literature for similar traits within breeding programs. Douglas-fir growth and wood yield traits typically display narrow sense heritability values (h_2) ranging from 0.13 to 0.32 (Yeh and Heaman, 1987; Vargas-Hernandez and Adams, 1991; St. Clair, 1994; Ukrainetz *et al.,* 2008). Stomatal occlusion and relative growth rate displayed similar low to moderate heritability estimates in our study (h_2 = 0.19 to 0.34 and 0.28, respectively). For stomatal occlusion, this was paired with a high genetic correlation (r-value = between 0.8 and 0.9) across different years of measurement. A high genetic correlation between two traits indicates that the same gene(s) influence the expression of these traits (Lynch and Walsh, 1998), and a correlation between the same trait over years would suggest that the genetic factors influencing the trait are stable over time. However, we can't exclude the possibility that distinct genes contributing to these traits in different years are co-inherited.

Stomatal occlusion was the most consistently correlated trait across years and exhibited the smallest variability within families across numerous years of measurement. The extent of correlation observed for stomatal occlusion (r-value between 0.24 and 0.39) incidence across years is consistent with previous work on SNC in the same geographic area (Montwé *et al.,* 2021).

Increased correlation coefficients when looking at family-level correlation (r-value ranging from 0.34 to 0.58) indicate an important impact of family on this trait within this breeding population. A high genetic correlation corroborated this. At the individual level, reduced correlations are likely caused by specific microenvironmental effects that are dampened when grouped by family. There was a significant but weak correlation between years of needle loss scores for this site. In contrast, Montwé *et al.* (2021) found that needle loss was moderate to strongly correlated (r-value = 0.63-0.77) between three consecutive years of measurement. The inconsistency of these findings suggests stronger environmental variables and site-specific effects on the current site that may be playing a role in needle loss. There was high variability within families for needle loss, which may have impeded the detection of any significant familial differences. Significant differences in needle loss across blocks in the plot (used as a rough approximation of location) corroborate that location (microenvironment) does influence this phenotype. Fixed effect tests were used to isolate the effect of family on needle loss.

These fixed effect tests showed that family significantly affects stomatal occlusion and relative growth rate within this population but not needle loss for either the third or fourth-year class of needles when accounting for spatial biases (block). These findings appear to contradict an earlier study by Montwé et al. (2021) that determined that family had an effect on needle loss within two other BC Coastal Douglas-fir breeding populations, one of them very close to our study site. Unlike my study site, which is laid out in a randomized complete block design, meaning that we can account for spatial variation (Shieh and Jan, 2004), Montwé's experimental plot was laid out with all family members located within one block (non-replicated family plots) making it difficult to disentangle family from microenvironmental effects. This was a limitation of their study and why they refrained from reporting heritability values for their populations. While they

used an auto-spatial correlation within their fixed effect test to account for spatial dependencies, the plot term still confounded their family term (Cappa & Stoehr, 2016). My data suggests that the plot term likely plays a prominent role in the significant fixed effect of family on needle loss in their study. From this, I speculate that some aspects of needle loss have a genetic basis, as this has been reported in the literature with narrow sense heritability value means of 0.15 (Johnson, 2002) and 0.18 (Temel *et al.,* 2005). However, the influence of genetic factors appears to be overshadowed by more pronounced site effects, such as localized pathogens and abiotic factors, which are likely contributing to needle loss at this site. These effects will be discussed in more detail below.

Needle loss within our population was found to have low narrow-sense heritability (h_2 = 0.11 to 0.13), pointing towards the role of environmental influences in the variation for this trait. The literature for SNC reports higher heritability of needle loss-associated traits than seen in our study (Temel *et al.,* 2005). However, these study results come from substantially younger trees, ranging from two to 12 years of age (Temel *et al.,* 2005). Crown size, causing different vertical profiles, impacts infection by *N. gaeumannii,* which could have implications for comparing these data to our larger 20-year-old trees (Lan *et al.,* 2019; Gervers *et al.,* 2022). Temel *et al.* (2005) tested juvenile field and laboratory trials (two years old) as well as more mature field trial plantations (12 years old). All field trials planted in Coastal Oregon were naturally inoculated by surrounding heavily infected Douglas-fir plantations. Needle loss scores were taken from two-year-old foliage, and the means for all test groups ((field, lab (juvenile), and field (mature))) were similar, ranging from 2.15 to 2.81. These values are slightly higher but comparable to needle loss levels observed at our site for two-year-old foliage (mean = 1.53 to 2.08). While the means were similar across test groups, the range of values for needle loss in the mature field trials was smaller

than both juvenile trials and exhibited a smaller h_2 value of 0.1 compared to juvenile trials whose values were $h_2 = 0.21$ (laboratory) and $h_2 = 0.23$ (field). Temel *et al*. 's (2005) narrow-sense heritability value for the mature field trees is comparable to our study site's, where $h_2 = 0.11$-0.13.

A possible explanation for this low heritability of needle loss in older field trial trees is a combination of endemism/epidemics, stand age, and associated dynamics. SNC epidemic areas are defined by sites with less than three age classes of needles retained (Ritóková *et al.,* 2016). Where SNC is present but not causing these severe levels of needle loss, it is referred to as endemic. My site falls explicitly into the range of endemic infection, showing high levels of infection but relatively benign symptom levels. I hypothesize there is low heritability associated with needle loss within my population and Temel *et al*.'s (2005) mature field trial due to other pressures at these more mature endemic sites. It has been observed that foliar pathogenic endophytes or latent pathogens typically increase with tree age, as well as beneficial endophytic communities (Yu *et al.,* 2021). This is due to most members of the foliar mycobiome being horizontally transferred and thus increasing with systemic re-infection. However, *N. gaeumannii* is unique because it does not follow this typical trend (Ritóková *et al.,* 2020). It is known to infect young stands, likely due to its ubiquitous presence on the landscape (Ritóková *et al.,* 2020) and its ability to withstand sun-exposed sites within the canopy (Gervers *et al.,* 2022), which is more prevalent in young stands prior to crown closure. Given proper environmental conditions, this latent pathogen can reach high levels in these young stands where competition for its niche space is limited. This would explain the higher heritability and variance in needle loss in young stands of Douglas-fir infected with SNC (Temel *et al.,* 2005). Any genetically determined tolerance would be tested with reduced noise due to abiotic and other pathogen-associated reasons for needle loss. Meanwhile, more mature endemic-level stands are impacted by abiotic factors such as shading and have additional

disease pressures acting on them while at the same time having possibly more developed beneficial endophytic communities (Yu *et al.,* 2021) that could confer some benefit against SNC. Both could be driving the variance in needle loss across the population. Ultimately, while SNC may partially explain needle loss, other complex dynamics associated with needle loss at these mature sites are likely masking any quantifiable genetic differences in tolerance to SNC.

The implications for this work are that this disease's current outlooks and management strategies may need to be more flexible to understand how (and if) host factors change impacts when sites shift from endemic conditions to outbreak levels. From my research, stomatal occlusion incidence may be the optimal phenotype to select for in endemic-level stands. Strong correlations have been observed between the proportion of stomata occluded with pseudothecia and needle loss (Manter and Kavanagh, 2003). This appears to be a consistent finding across epidemic-level sites (*e.g.* Hansen *et al.,* 2000; Maguire *et al.,* 2002; Manter *et al.,* 2003a). The only exception to this is Temel *et al.,* (2004) who observed trees with severe symptoms (high needle loss and poor growth) having a negative correlation with fungal load as measured through qPCR. This correlation, however, starts to fall apart when looking at sites where SNC is present but below that epidemic threshold. Examples of this are Montwé's (2021) study, whose trees retained most of their third-year-age class needles on average, and Ritóková *et al.'s* (2021) study sites, which had 4.7 years of mid-crown needles still intact on average. Both studies are examples of sites exhibiting moderate endemic infection and low to undetectable correlation between stomatal occlusion and needle loss. These findings and my own suggest endemic sites do not have disease pressure high enough to cause an observable difference in needle loss. However, my study indicates that stomatal occlusion incidence significantly differs between families. Hence, stomatal occlusion incidence traits could reasonably be used to select more resistant trees to SNC at these endemic-level sites. I speculate

that families selected for reduced stomata occlusion will have both fewer stomata occluded and less severe needle loss under epidemic conditions, even if impacts on needle loss may not be detectable under endemic conditions.

While stomatal occlusion showed a negative genetic correlation with relative growth rate in our study, needle loss negatively correlated phenotypically with relative growth rate. This could be a potential trade-off. While selecting trees that show more resistance could mitigate SNC symptoms under future epidemic conditions, selection of resistance to one pathogen poses the risk of making hosts unintentionally more susceptible to other biotic and abiotic defoliation causes, as has been observed in agricultural settings (Gruner *et al.,* 2020). The phenotypic correlation between relative growth rate and needle loss suggests that other microenvironmental factors driving needle loss must also be considered. Hence, it is essential to understand what other foliar mycobiota may be impacting needle loss and how host genetics may impact such microbial communities.

I attributed the lack of correlation between needle loss, stomatal occlusion, and low heritability to our choice of an endemic stand. The same argument may be brought forward to explain low correlations with relative growth rate. Shaw *et al.* (2021) suggest quantifiable volume growth losses typically occur in trees with fewer than three years of retained foliage. Despite some needle loss observed for the third-year class and younger, most trees at my site still had at least some of the third-year class needles. The higher correlations with growth metrics in Montwé *et al.*'s study could be partly due to the confounding effect of position in the field in Montwé *et al*.'s (2021) study, where family blocks introduced spatial biases.

Another variable to take into consideration for needle loss variance is sampling effects. When sampling from the ground via orchard ladders and pole pruners, the height of a tree will significantly impact sampling efforts. This is an essential factor to consider as *N. gaeumannii* is known to prefer the upper, open canopy (Gervers *et al.,* 2022; Lan *et al.,*2022) and is found to be associated with higher severity in the south-facing side of the canopy (Manter *et al.,* 2003b). Although within our study, best efforts were made to sample from as high in the canopy as possible, the height of these trees when sampling from the ground could have had impacts on the quality and consistency of samples that we were able to collect. While height was not measured for my study site, height growth models suggest heights upwards of 10 meters (32.8 feet) based on the age of this site (Wang and Kimmins, 2002). Sampling heights for this study varied from 6 – 9 m, which could have resulted in sampling of the lower canopy for taller individuals. Aside from SNC presence likely being higher up in the canopy (Gervers *et al.,* 2022), the lower canopy is more likely to have branches that have started to be shaded out, likely driving needle loss scores up, independent of SNC severity. However, within our data, the needle loss scores were relatively low for second and third-year age classes, meaning that we likely were sampling from within the crown areas where needle retention is still generally high. Yet another aspect to consider when discussing tree height and sampling position is that vertical height within the crown also impacts fungal endophyte communities (Gervers *et al.,* 2022). This could affect colonization by *N. gaeumannii* and disease severity. This is an aspect I will explore in the second data chapter of this thesis.

Measuring crown density metrics through alternative ways may be useful, especially for older stands. Aerial surveys could provide a more reliable phenotype for trees of this age and size. This method has been employed successfully for the last few decades at a large scale in Oregon

(Shaw *et al.,* 2021) to assess for obvious chlorosis and thinning of crowns. While very effective in obtaining quantitative data over large areas, it is a land-scape level tool that cannot quantify SNC symptoms at the individual tree level, which is required in the context of tree breeding. Alternatively, recent work with drones is attempting to establish standards for SNC phenotyping that will allow for the delineation of specific trees and their SNC-associated symptoms, which could hopefully become a more affordable and time-efficient method for sampling these older, harder-to-sample breeding populations (Dr. Miriam Isaac-Renton, personal communication).

Summary

In summary, given high genetic correlation and reasonable heritability, I propose stomatal occlusion as a trait that has the potential to mitigate SNC disease severity under increasing disease pressure. As hypothesized, my study found no significant correlation between needle loss and stomatal occlusion. I hypothesize that this lack of correlation is predominantly linked to the absence of epidemic levels of SNC in the study site, and I speculate that stomatal occlusion (measured under endemic conditions) is a predictor of needle loss under epidemic conditions given that stomatal occlusion and needle loss correlate under epidemic conditions.

It is also plausible that the symptoms of SNC (needle loss) did not exert a significant enough influence to surpass the impact of other contributing factors within this stand. Other contributing factors may include variation in the fungal endophyte community within Douglas-fir needles. Consequently, my second data chapter will explore the contributing effects of other fungal taxa to determine if other community members could be promoting or dampening needle loss.

Data Chapter 2: Mycobiome

Contributions by others to data chapter 2

A portion of fungal culturing and processing was done at the Pacific Forestry Center (PFC) by Dr. Joey Tanney and Robert Kowbel. Emma Hayward conducted a portion of the culture-based DNA extractions and sequencing while working as a lab technician with Dr. Joey Tanney, who also aided in the identification of some of these fungal species. Isabella Laughton assisted with lab work for the second field season.

Introduction

Microbiomes

The recently coined holobiont concept refers to the association between a host and its microbiome. This model considers complex dynamics like those observed in ecological systems of higher organisms (Sánchez-Cañizares *et al.,* 2017). Related to plant microbiomes, the pioneering research on *Arabidopsis thaliana* in 2012 by Lundberg *et al.* sparked numerous studies on model plants (Tkacz *et al.,* 2015; Zgadzaj *et al.,* 2016; Alcaraz *et al.,* 2017) and crops (Peiffer *et al.,* 2013; Sugiyama *et al.,* 2014; de Souza *et al.,* 2016; Bulgarelli *et al.,* 2015) and continues to be a very active area of research. The plant microbiome can be divided into the above-ground phyllosphere and the below-ground rhizosphere. The phyllosphere coined by Last (1955) can be broken down into the different aerial portions of the plant: leaves, flowers, buds, and the vegetative foliar zone (Sánchez-Cañizares *et al.,* 2017), all of which are hosts for a variety of microorganisms that include bacteria, filamentous fungi, and yeasts (Vorholt *et al.,* 2012). Here, I aim to shed light on the foliar microbiome, focusing on the tissue that *N. gaeumannii*, the causal agent of Swiss Needle Cast (introduced in previous chapters), infects. While bacteria are important and abundant, and their role in the microbiome can benefit their plant hosts (Müller *et al.,* 2016), only fungal

community members were surveyed for this study. This focus is motivated by the anticipation of many unidentified fungal species occupying this niche and the potential role that these taxa may play in disease response (Gakuubi *et al.,* 2021). The foliar mycobiome can be categorized into two main groups: epiphytes, residing on the surface of the foliage, and endophytes, colonizing the interior of the foliage. It is worth noting that some fungi exhibit both modes within their life cycle, blurring the distinction between the two (Porras-Alfaro and Bayman, 2011). My research targets the predominantly endophytic taxa, recognizing the importance of understanding their role in the foliar mycobiome and how they interact with the endophytic foliar pathogen *N. gaeumannii*.

Foliar mycobiomes and their functions

Fungal endophytes are known to inhabit all major lineages of plants (Rodriguez *et al.,* 2009) and occupy the entire extent of possible relationships with plants, ranging from latent pathogens, mutualists, commensals, temporary residents to latent saprotrophs (Davis and Shaw, 2008; Porras-Alfaro and Bayman, 2011; Christian *et al.,* 2017; de la Bastide *et al.,* 2019). Because of this, both partners employ many different strategies to maintain or prevent these relationships (Suryanarayanan, 2013), and understanding these interactions is an essential ongoing area of research. Molecular detection techniques have allowed new insights into how these relationships manifest, finding numerous taxa exhibiting multiple relationship types with plants throughout their lifecycles. These shifts are often triggered by different life cycle stages initiated by environment, host, or microbe-specific triggers (Newton *et al.,* 2010). For example, *Phytophthora infestans* (causing potato blight) is a symptomless biotroph that may go undetected for phases of its life before causing necrosis upon a temporal trigger (Sowley *et al.,* 2010). On the other two extreme sides of this, there are strictly necrotrophic fungi that always kill host cells when growing (e.g., *Botrytis cinerea*, known as grey mold (Van Kan, 2006)) and mutualistic fungi that

can protect hosts from specific stressors (e.g., *Neotyphodium* sp., which protects the leaves of fescue grasses from herbivory by eliciting loline alkaloids (Roberts and Lindow, 2013)).

Among the possible interactions, mutualism, particularly in the context of agricultural crops, has been investigated most often in the literature. This is because of the prospect of using these mutualistic taxa as a form of biocontrol to treat pathogens or plant stressors (Grabka *et al.,* 2022). Studies have shown that endophytes can mediate disease severity by direct competition with pathogens (Olivia *et al.,* 2021) or indirectly by up/down-regulating plant defense responses via modulation of phytohormones and expression of genes related to defense and growth (Mejía *et al.,* 2014; Ahmad *et al.,* 2022). Benefits provided by foliar mycobiomes have also been observed for conifer species. Successful inoculation of Ponderosa Pine (*Pinus ponderosa*) and White Spruce (*Picea glauca*) with endophytic fungi has reduced the impacts of their respective pathogens: *Dothistroma* pine needle blight and spruce budworm (Ridout and Newcombe, 2015; Quiring *et al.,* 2019).

Drivers of foliar mycobiomes

Numerous factors influence the species diversity present in these foliar endophytic communities. Both biotic and abiotic factors, such as plant species and developmental stage (Yang *et al.,* 2022; Zahid *et al.,* 2021) or elevation, mean annual temperature, and precipitation (Huang, 2020) can impact these community assemblages. However, experimental conditions such as isolation procedure, size of sample and sampling strategy (dos Reis *et al.,* 2022; Faticov *et al.,* 2023) can affect communities. These communities are generally shaped by the horizontal transmission of endophytes via wind-dispersed spores. However, some taxa are known to be transmitted vertically via the seed coat (Mejía *et al.,* 2014). These vertically transferred endophytes are thought to play a role in seed germination and seedling growth, with some then systemically

colonizing the phyllosphere (Shearin *et al.,* 2018; Hodgson *et al.,* 2014). While these studies have elucidated some of the factors that shape these communities, little is known about community composition, dynamics, and function in most plant species, particularly in tree species.

Douglas-fir foliar mycobiome

Despite its economic value in BC, in the last decade only two papers have explored the fungal mycobiome of Douglas-fir (Daniels *et al.,* 2018; Gervers *et al.,* 2022). Earlier and pioneering research in the pre-genomics era was pivotal in identifying common endophytes of Douglas-fir (Bernstein and Carroll, 1977; Carroll and Carroll, 1978; Sherwood-Pike *et al.,* 1986), but their methods relied on traditional culture-based approaches only, which are biased towards prolific taxa that can grow in culture (Wijayawardene *et al.,* 2021). With the development of metagenomic-based approaches for identifying microbiome community compositions, we can better quantitatively identify cryptic, unculturable taxa (Wijayawardene *et al.,* 2021). Despite what we know about the benefits that endophytes can confer to their host plants (Grabka *et al.,* 2022), no literature currently details how these fungal endophyte communities may change under different environmental conditions or disease pressures in Douglas-fir, particularly with SNC. Given the lack of correlation observed between stomatal occlusion severity and needle loss in endemic-level Douglas-fir stands, as seen in data chapter 1 and previous literature (Ritóková *et al.,* 2016; Montwe *et al.,* 2021), I hypothesize that differences in the foliar mycobiome have contributed to this lack of correlation. While *N. gaeumannii* is common in these sites and infection is visible, family-level differences in mycobiome community composition could be driving heightened resistance to needle loss, or conversely, the presence of other pathogenic species could cause even more severe needle loss.

Objectives

In this second data chapter, the foliar mycobiome will be characterized for a subset of the population from data chapter 1 (n = 60, 5 individual trees each from 12 families). Characterization will be done using metagenomics and complemented and cross-validated with a traditional culture-based approach. My first objective is to examine differences in diversity and community composition related to SNC and whether this is related to host genotype. Ultimately to test my hypothesis that *differences in endophyte community composition are influencing the observed lack of correlation between SNC disease signs and symptoms within this endemically infected population of Douglas-fir*. To do this, I will compare alpha and beta diversity metrics from the metagenomic data across levels of SNC disease severity and among different families within the breeding population. I will also determine the presence of any differentially abundant taxa and whether these differences correlate with disease severity groupings or families. The second objective of this data chapter is to compare endophyte community data observed in my study with the two other publicly available datasets on the foliar mycobiome of Douglas-fir; one study employed culture-based methods (Daniels *et al.,* 2018) and the other a metagenomic method (Gervers *et al.,* 2022). Pioneering studies on Douglas-fir endophytes (Bernstein and Carroll, 1977; Carroll and Carroll, 1978; Sherwood-Pike *et al.,* 1986) were excluded from this portion of the analysis. This decision is attributed to the likelihood of taxonomic reassignment of numerous species since the publication of these studies and the unavailability of DNA sequences for comparison with our current study. I will determine to what taxonomic level the fungal diversity is conserved across these different studies and geographic regions in the same host organism. Overall, this second data chapter aims to determine differences in endophyte community composition of Douglas-fir in a BC Coastal Douglas-fir breeding population in the context of an

economically important pathogen and to provide baseline knowledge of the Douglas-fir mycobiome.

Methods

Cultured fungal endophytes protocols

Surface sterilization and culture isolation

Two-year-old needles collected from the field during phenotyping (refer to data chapter 1) were stored for up to 2 weeks at 4°C before surface sterilization. Second-year needles were surface-sterilized via immersion in 95% ethanol for one minute, seven minutes in 3% bleach, and one minute in 70% ethanol, followed by a sterile distilled water rinse. This series was done twice. The sterilized samples were then cut into approximately one cm long sections and aseptically transferred to 2% malt extract agar (MEA). Plates were incubated at 20°C to allow fungal growth within the sterilized tissue. If distinctly different mycelial colonies were present on a plate for a single needle, these were assumed to be different isolates and were aseptically transferred to fresh Petri dishes containing 2% MEA media. This was done as many times as necessary to obtain pure cultures. Cultures were observed for morphological characteristics (*i.e.,* growth rate, colour, texture, aerial mycelia, sporulation), and a number of distinct morphotypes were selected for further analysis by DNA extraction, PCR amplification, and DNA barcode sequencing to determine the taxonomic affinity.

Culture preservation and storage

To maintain viable cultures, cultures were stored in duplicate for future use. Plugs of hyphae were taken using core borers. Cores were stored in both water (short-moderate term storage) and in 10% glycerol-distilled water solution for long term storage.

Fungal DNA extraction

Approximately 10-20 mg of fungal biomass collected aseptically from pure, solid medium cultures was transferred to 2 mL screw cap microtubes (Starstedt) containing 70 µL Prepman Ultra extraction buffer (Applied Biosystems) and 30 µg of Zirconia/Silica beads (0.5 mm diameter; Fisher Scientific). Each tube was agitated for 30 s with a Mini BeadbeaterTM (Biospec Products Inc.), followed by centrifugation for 30 s at 14,000 g; this process was repeated twice. The resulting homogenates were incubated at 100℃ for 10-15 min, cooled at room temperature (2 min), and centrifuged for 5 min at 14,000 g. A 40 µL volume of supernatant containing extracted DNA was transferred to a new 1.5 mL tube and stored at -20℃ until used. The purity and concentration of selected DNA extractions were determined using the Nanodrop ND-100 spectrophotometer (Thermo Fisher Scientific) before preparing DNA template dilutions for subsequent PCR reactions. If DNA concentrations were too high, samples were diluted 1/10 with sterile, distilled water. All DNA samples were stored at -20℃ until used.

PCR and nucleotide sequence analysis

The internal transcribed spacer region (ITS) of the rDNA region was amplified using forward primer ITS1F-KY02 (5'-TAGAGGAAGTAAAAGTCGTAA -3'; Toju *et al.,* 2012) and reverse primer ITS4 (5'- TCCTCCGCTTATTGATATGC -3'; White *et al.,* 1990) or forward primer V9G (5'- TTACGTCCCTGCCCTTTGTA -3') and LS266 (5'- GCATTCCCAAACAACTCGACTC -3'; Gerrits van den Ende and Hoog, 1999) (fig. 9). The PCR reaction volume was 50 uL using DreamTaqTM DNA Polymerase (ThermoFisher Scientific). Each reaction contained 31.5 uL dH20, 1.0 uL dNTPs (10mM), 5.0 uL buffer (10x), 2.5 uL forward primer (10 µM), 2.5 uL reverse primer (10 µM), 2.5 uL BSA (10 mg/mL), 2.5 uL DMSO, 0.5 uL Taq (10X), and 2.0 uL DNA (1 µg). Reactions were completed in a thermocycler (S1000 Thermal

Cycler, Bio-Rad) and included an initial 3 min denaturation step (2 min at 94°C), followed by 35 cycles of denaturation (45 s at 94°C), annealing (30 s at 55°C), extension (40 s at 72°C), and a final extension (10 min at 72°C). Post-reaction samples were held at 10°C until processed. Positive amplicons were visualized by agarose gel electrophoresis. Amplicons were purified with the Column Pure PCR Clean-up Kit (Applied Biological Materials Inc.) following the manufacturers protocol. Amplicons were Sanger-sequenced in both directions by the sequencing facility at University of Laval (CHUL) (Montreal, QB, Canada). Forward and reverse nucleotide sequences were aligned using Geneious (Biomatters) and edited manually. Final consensus sequences were subject to a BLASTn (nucleotide query) search with default parameters using the National Centre for Biotechnology Information database.

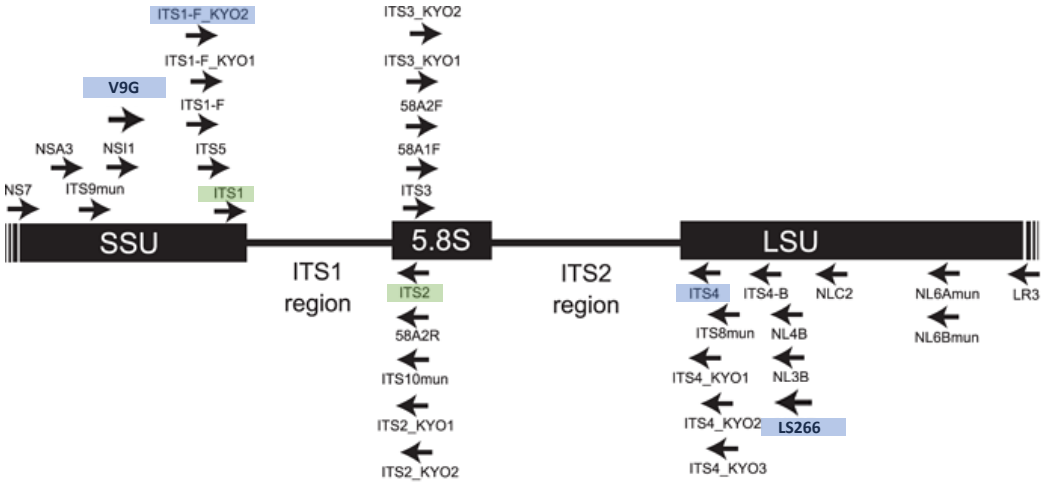

Figure 9. Internal transcribed spacer region (ITS) of the rDNA with primers used for amplification. Blue highlights primers used for culture-based methods and green highlights primers used for metagenomic based methods. Adapted from Ben Hassine Ben Ali and Kluthe (2016).

ITS amplicon metagenomics protocols

Total DNA extractions

60 trees from 12 families (five trees per family) covering the full ranges of all phenotypes were selected for this portion of the analysis.

To avoid an overrepresentation with DNA from *N. gaeumannii* pseudothecia and to minimize epiphytes, all needles were cleaned prior to extraction by soaking in 0.01% Tween 20 (Phytotech Labs) for 5 minutes and agitated by vortexing to remove surface contaminants and debris. Needles were then wiped clean with a Kimwipe paper. This was done for approximately 15 needles randomly selected from 2-year-old branch sections for each tree. Plant material was ground in liquid nitrogen and stored at -20℃ until processing.

DNA extractions were performed using a CTAB-based protocol described as follows: Extraction buffer (50 mL Tris-HCL [1 M, pH 8.0], 10 g PVP-40, 175 mL Sodium Chloride [4 M], 20 mL Disodium Salt EDTA [0.5 M], 20 g CTAB, 5 g PVPP, 50 uL RNase A, dH_2O to final volume of 500 mL) was prewarmed to 65℃ and 224 mg of Extraction powder (0.48 g Aurintricarboxylic acid [1 mM], 2.16 g Dithiothreitol [10 mM], 0.48 g Thiourea [5 mM], 28.8 g PVPP, 1.44 g Activated Charcoal) was added to a 28 mL aliquot of the prewarmed extraction buffer. Approximately 100 mg of the ground frozen issue was transferred to a prechilled 2 mL screw cap tube with 1 mL of extraction buffer with extraction powder per sample. Two glass beads were added, and the sample was homogenized in a bead beater (2 x 45 s). The sample was incubated at 65℃ for 15 min and then centrifuged at 12 000 x g for two minutes at 4℃. The supernatant was transferred to a new centrifuge tube and washed with Chloroform:Isoamyl alcohol (24:1). This was repeated twice. The supernatant was transferred into a new tube with a 2-2.5x volume of prechilled (-20℃) 100% ethanol. The sample was mixed and centrifuged at 12 000 x g at 4℃ for two minutes. The supernatant was discarded, and 1 mL of wash buffer (400 ml Ethanol [95%], 3300 uL Ammonium Acetate [1.5 M], dH2O to 500 mL) was added to the pellet. This was centrifuged at 12 000 x g at 4℃ for 30 min. The supernatant and wash buffer were discarded. The

DNA pellet was dried and resuspended in nuclease-free H_20. Samples were stored at -20°C until needed.

ITS amplicon library production and high-throughput sequencing

PCR amplification of fungal ITS regions (as described above) and gel electrophoresis were performed to confirm the presence of quality fungal genomic DNA from Douglas-fir needle extractions.

High-quality genomic DNA samples were sent to the Sequencing and Bioinformatics Consortium at the University of British Columbia (Vancouver, Canada) for quality control and ITS1 amplicon library preparation using the Illumina MiSeq v3 2x300bp kit with a target of 30,000 paired-end reads per sample. The service facilities standard operating procedure were as follows: extracted DNA was quantified using Qubit fluorometry. ITS fragments were PCR amplified using primers ITS1F (5'- CTTGGTCATTTAGAGGAAGTAA-3'; Gardes and Bruns, 1993) and ITS2 (5'-GCTGCGTTCTTCATCGATGC-3'; White *et al.,* 1990) (fig.8). These amplicons were then converted to sequencing libraries using an 8-cycle indexing PCR with Illumina DNA/RNA UD index primers (Illumina). These libraries were sequenced on MiSeq v3 flow cells (Illumina) to generate paired-end 300 bp reads. Raw base call data (bcl) were converted into FastQ format using the bcl2fastq conversion software from Illumina.

To validate the use of metagenomics-based read abundance to measure species abundance, I quantified *N. gaeumannii* fungal load using an alternative approach, namely qPCR. The kit used was Luna qPCR Master Mix (New England BioLabs Inc.), and I followed methods as described by Montwé *et al.* (2021) to amplify and quantify the LEAFY gene (*P. menziesii*) and β-tubulin gene (*N. gaeumanii*). This was done for a subset of 18 DNA extracts prepared for Illumina

sequencing as described above and was replicated three times to account for variation. A Spearman correlation was conducted to compare the proportion of *N. gaeumannii* DNA to *P. menziesii* DNA determined by qPCR with the relative abundance of *N. gaeumannii* reads from Illumina Miseq metagenomic data.

Bioinformatics analysis

Paired-end sequences were assessed for quality using FastQC (v0.11.9; Babraham Bioinformatics), and low-quality data were removed (using a median quality score threshold of less than 30). Primer sequences were trimmed using CutAdapt (v3.5; Martin, 2011) within QIIME2 (Boylen *et al.,* 2019), Using ITSxpress (Rivers *et al.,* 2018) implemented as a QIIME2 plug-in, the ITS1 region was extracted from these reads, which were then aligned to the 2023-25-07 UNITE Fungi release with singletons included (Abarenkov *et al.,* 2023)) using VSEARCH (Rognes *et al.,* 2016). If alignments to the fungal references had an identity score of >0.5, they were considered fungal sequences and retained. Utilizing DADA2, amplicon sequence variants (ASVs) were generated. DADA2 corrects for errors in the sequencing reads using an error model based on quality scores; merges overlapping forward and reverse reads into consensus sequences; and denoises the sequences, employing statistical methods to distinguish true biological variation from sequencing errors and noise (Callahan *et al.,* 2016).

Taxonomic assignment

ASVs were clustered into operational taxonomic units (OTUs) to reduce the number of erroneous ASVs using the LULU R package (Frøslev *et al.,* 2017), with parameters as follows: minimum match = 97% similarity and minimum relative occurrence = 95%. OTUs were then classified using *classify-consensus-blast* in QIIME2 by alignment with the 2023-25-07 UNITE Fungi release database with singletons included (Abarenkov *et al.,* 2023). Default parameters were

used (query cover = 0.8, percent identity = 0.8) except for the e-value threshold, which was set to 10^{-10} (a less stringent approach was used to enable the classification of OTUs at a higher taxonomic level). Before alignment, the ITS1 region was extracted from this UNITE database for this query (using ITSXpress, Rivers *et al.,* 2018). All OTUs with assigned taxonomy, a frequency table, and metadata for each sample as described in Chapter 2 were exported, and all further analysis was done in R studio (R Core Team, 2015) using the microbiome analysis package Phyloseq (McMurdie and Holmes, 2013). Any OTU's without classification were removed from the dataset. To filter out taxa with low abundance, a rule adopted from Milici *et al.* (2016) was used: Only taxa with an abundance level higher than 0.001 were kept. Among those, only taxa that satisfied at least one of the following conditions were retained: 1) were present in at least one sample at a relative abundance higher than 1% 2) were present in at least 2% of samples at a relative abundance higher than 0.1% for a given sample or 3) were present in at least 5% of samples at any abundance level.

Community composition and ecological analysis

In order to compare samples, each sample library's features were normalized through rarefaction (without replacement) to a consistent depth determined by visual inspection of species accumulation curves (Sanders, 1968; Cameron *et al.,* 2021). A depth of 7000 was chosen to select a depth accommodating the maximum number of samples while preserving diversity and read counts as indicated by the curves plateauing. To address potential biases caused by the very high abundance of *N. gaeumannii*, an additional data set that excluded *N. gaeumannii* was rarefied without replacement as described above (to a depth of 1500) and was used in further analysis. All plots were created in R using ggplot2 (Wickham, 2009), and all *functions* used, unless otherwise noted, are from the packages Vegan (Oksanen *et al.* 2023) and Phyloseq (McMurdie and Holmes, 2013).

Disease groupings

For visualizations of data and analysis where discrete variables were necessary the following groupings based on phenotype data collected in data chapter 1 were used: **stomatal occlusion severity**: l**ow** = less than or equal to 10% of stomata occluded, **medium** = greater than 10% stomata occluded, but less than 15% stomata occluded, **high** = greater than or equal to 15% of stomata occluded; **needle loss severity: low** = less than or equal to 40% of needles lost, **medium** = greater than 40% of needles lost, but less than 70% of needles lost, **high** = greater than or equal to 70% of needles lost). An additional category aimed at understanding overall disease expression grouped individual trees as **non-tolerant and non-resistant** (needle loss and stomatal occlusion scores greater than average across all individuals), **tolerant and non-resistant** (needle loss scores less than the average, and stomatal occlusion scores greater than the average), or **tolerant and resistant** (needle loss scores less than the average and stomatal occlusion scores less than the average), **non-tolerant and resistant** (needle loss scores greater than the average and stomatal occlusion scores less than the average.)

Differentially abundant genera

To determine if any genera were differentially abundant across different groupings, OTUs were collapsed into their respective genus using the function *taxa_glom()*, and a Kruskal-Wallis test was performed using the R base package to test for significant differences between groups. This was done on mean centered log ratio (clr) transformed data (Aitchison, 1982). Clr transformed data was chosen instead of relative abundance transformed or rarefied data to account for the compositionality of data (Gloor *et al.,* 2017) while still considering any low occurrence of differentially abundant taxa that may not have been addressed using rarefied data. P-values were

adjusted to control for the false discovery rate due to multiple comparisons using a Benjamini-Hochberg correction (Benjamini and Hochberg, 1995).

α-diversity

To determine whether alpha diversity varied among levels of disease symptom severity (discrete categories as described above) or between different families, Observed Richness and Shannon entropy were estimated for each sample using the *estimate_richness()* function in *phyloseq.* Variation in these estimates was tested using analysis of variance (ANOVA) F-tests (*AOV()* function) across all levels of previously defined groups to determine if any had an impact on diversity within samples. Assumptions of normality (*Shapiro_test()* in package Rstatix) and homoscedasticity (*levenTest()* in package Car; Fox and Weisberg, 2019) were investigated prior to testing, and error adjustments were added if needed. If significant, a Tukey honest significant differences test (alpha = 0.05) was performed using the R base package to determine which levels in the respective grouping were significantly different. Spearman rank correlations were additionally employed to understand if alpha diversity is correlated with stomatal occlusion or needle loss severity when treated as a continuous variable.

β-diversity

A Bray-Curtis dissimilarity (Bray and Curtis, 1957) matrix was calculated for all trees based on OTU abundance data. To test for significant differences in community composition based on family and disease symptoms permutational analysis of variance (PERMANOVA; Anderson, 2001; Bakker, 2024) using the *adonis2()* function was run. *Betadisper()* (using PERMDISP2; Anderson *et al.,* 2006) was used to assess the homogeneity of variances among different levels of disease symptoms and between families. The *permutest()* function was employed to test for significant differences between *betadisper()* results to determine if differences in group dispersion

impacted differences in fungal community composition. These tests each employed 999 random permutations; unless otherwise noted, this was the case for all permutational tests. Distance-based redundancy analyses (dbRDA) of the community dissimilarity matrix were constrained on disease symptoms and family using the function *capscale()*. This aimed to determine how much variation in the foliar mycobiome is explained specifically by phenotypes or family data. For both ordination methods, the function *envfit()* in the package Vegan (Oksanen *et al.,* 2023) was used to measure the strength and direction of the linear relationship between environmental variables and the untransformed relative abundance of OTUs with the ordination axes. Significant taxa in explaining these ordinations were uploaded to FUNguild database (Nguyen *et al.,* 2016) for fungal functional prediction.

Association network visualization

Association networks using the R package NetCoMi (Peschel *et al.,* 2020) were employed to understand co-occurrence or competition with *N. gaeumannii* and identify network hubs. Network hubs using this package are identified by Eigenvector centrality (nodes with a centrality value above the empirical 95% quantile) (Peschel *et al.,* 2020). Data was aggregated to genus, and clr transformations (adding pseudo values where zeros were present) were performed to avoid compositional effects. Networks were constructed using the function *netConstruct(),* which employed Pearson correlations with a threshold of 0.40 to exclude weak correlations from the network. The network was visualized using the function *netAnalyze(),* and network hubs indicative of interconnected nodes and genera strongly associated with *N. gaeumannii* were noted.

Role of Rhizosphaera

Rhizosphaera was recognized as a taxon of interest due to its significant presence in the dataset and negative correlation with *N. gaeumannii.* To confidently identify the two OTUs

associated with this genus to species, alignments and phylogenetic trees were generated (using Clustalw multiple alignment, Gblocks, and PhyML maximum likelihood; Dereeper *et al.,* 2008). Sequences were trimmed before alignment to only include the ITS region as applicable. Reference *Rhizosphaera* sequences from all known species within this genus, as described in Taylor and Koukol (2023), were combined in an alignment of whole ITS sequences for *Rhizosphaera* sequenced from culture (described in Chapter 2) and the resulting phylogenetic tree was visualized using ITOL (Letunic and Bork, 2007). Subsequent alignments of the two *Rhizosphaera* OTUs (only ITS1) from the metagenomic dataset were generated with culture derived sequences to assess their taxonomic placement.

Mycobiome meta-analysis

OTUs classified by presence or absence data were compiled from available studies (Daniels *et al.,* 2018; Gervers *et al.,* 2022) and collapsed to the most appropriate taxon, based on the levels of resolution possible by using function *tax_glom()* in Phyloseq. Classes present in these different studies were mapped to a recently published fungal phylogenetic tree (James *et al.,* 2020) to visually inspect any trends in taxa present between different studies, locations, and methodology (*i.e.,* culture-based versus metagenomics).

Results

Cultured endophytes

As a means of complementing ITS amplicon metagenomics analysis, cultures of endophytic fungi were isolated from a subset of 100 individuals within the breeding population, covering a range of disease incidence and symptoms. In total, over one thousand subcultures were grown from 500 initial cultures, from these 100 trees. These cultures were sorted roughly into 72 morphotypes based on macroscopic features (*i.e.,* growth rate, colour, texture, aerial mycelia,

sporulation) (Table 2). Approximately 200 isolates that included the observed morphotypes were chosen for genomic DNA extraction, subsequent amplification of the whole ITS region, and sent for Sanger sequencing. Of these, 97 cultures produced sufficient quality sequences that could be identified to at least fungal class. 14 cultures could not be identified to species level despite quality sequences due to no close matches in the database. The successfully identified sequences covered 38 species, 30 genera, 19 families, 14 orders, and 7 Classes. Of the 38 unique isolates identified at the genus level, all but three were Ascomycetes with almost half (46%) of these taxa belonging to the class Sordariomycetes (fig. 10). Of these sequenced cultures the most abundant were found to be *Jackrogersella* multiformis, *Rhizosphaera* sp., *Xylaria hypoxylon, Plectania melastoma, Hypoxylon fuscum, Rhabdocline parkeri, Nothophaeocryptopus gaeumanni,* and *Sydowia polyspora* (Table 3). Based on representative culture sequences, the morphotypes containing *Rhabdocline parkerii* and *Nothophaeocryptopus gaeuamannii* dominated this dataset. However, there were a few cases where numerous taxa within a singular morphotype were seen (*i.e., Rhabdocline parkeri;* Table 2). This indicates the presence of distinct yet morphologically similar taxa within a morphotype group, so some of these estimates may be slightly inflated (table 3). The majority of cultures were preserved for future work that may require viable cultures of these fungal taxa (*e.g.,* bio assays, metabolomics and controlled inoculation studies).

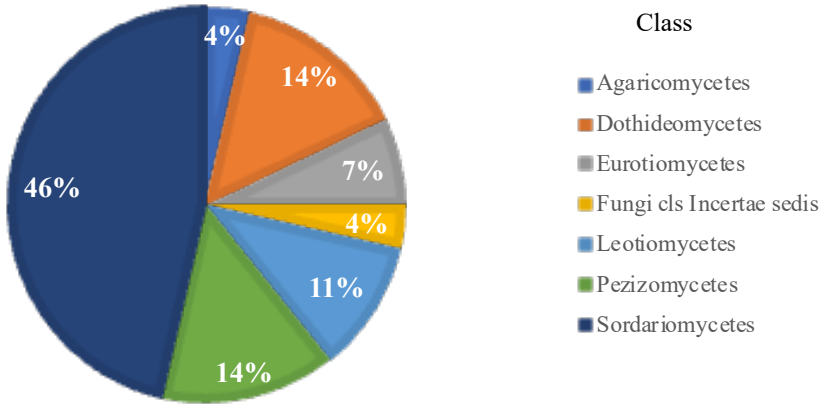

Figure 10. Fungal endophytes from JR GCA breeding population surface sterilized needles. Graph shows proportion of fungal classes represented by fungal culture sequencing of the whole ITS region.

Table 2. Most abundant of the 72 described morphotypes cultured from JR GCA breeding population. Grouped based on growth and hyphal morphology. The accession number of DNA sequence matching these cultures is provided when a close match was found. Some morpho-groups contained more than one taxa indicating similar morphology between these taxa.

Morphotype	Species	Culture
Black	*Rhizosphaera sp.* (ON784043)	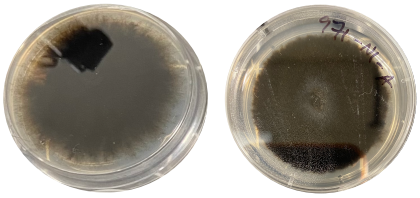
Light Yellow	*Lachnum virgineum* (MZ087787.1)	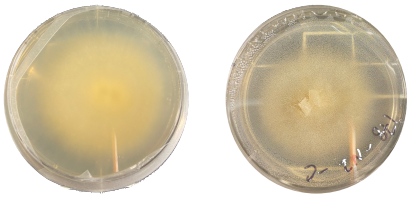
Black-grey	*Jackrogersella Multiformis* (ON453667.1) *cf. Coleospora* (GQ153148.1) *Sydowia polyspora* (KP152486.1)	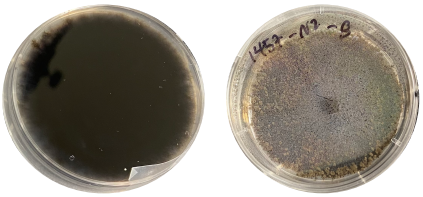
Rings-white	*Jackrogersella muliformis* (ON453667.1)	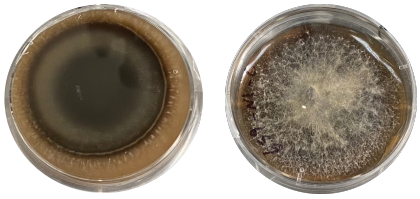
White-powdery	*No close hits*	
White-brown-spots	*Clypeosphaeria mamillana* (HQ228266.1)	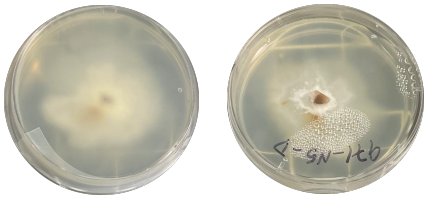

Morphotype	Species	Culture
White-black-1	*Xylaria hypoxylon* (MK577428.1, MH864103.1)	
Black-brown-ring	*Rhizosphaera sp.* (ON784043)	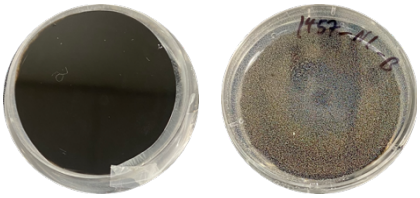
Brown-white-spores	*Penicillium glaucoalbidum* (MG490875.1)	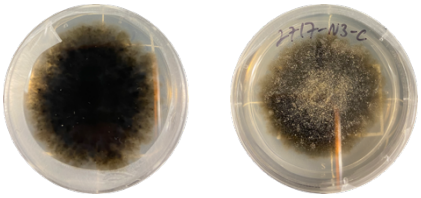
Yellow-brown-2	*Mollisia cf. melaleuca* (MH861785.1)	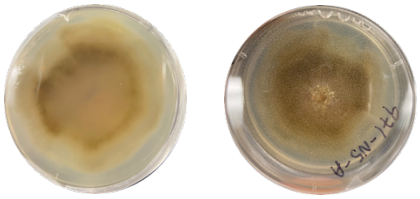
White-radial	*Xylaria hypoxylon* (MK577428.1, MH864103.1)	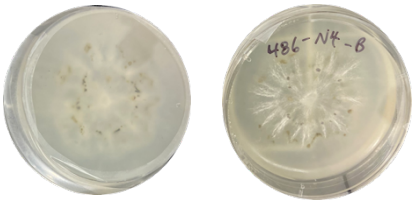
Black-Slow growing	*Nothophaeocryptopus gaeumannii* (MT154259.1)	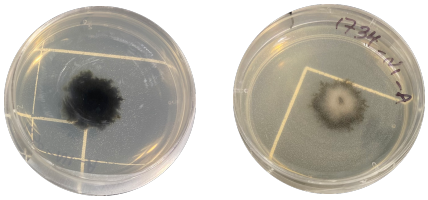

Morphotype	Species	Culture
Phenotype suggestive of *Rhabdocline parkeri* (Dark yellow, light yellow, dark green, light green)	*Rhabdocline parkeri* (AF462426.1) *Coniochaeta lignaria* (OM337547.1) *Hypoxylon fuscum* (MW367856.1, OQ831970.1) *Trichophaea hybrida* (AF351582.1)	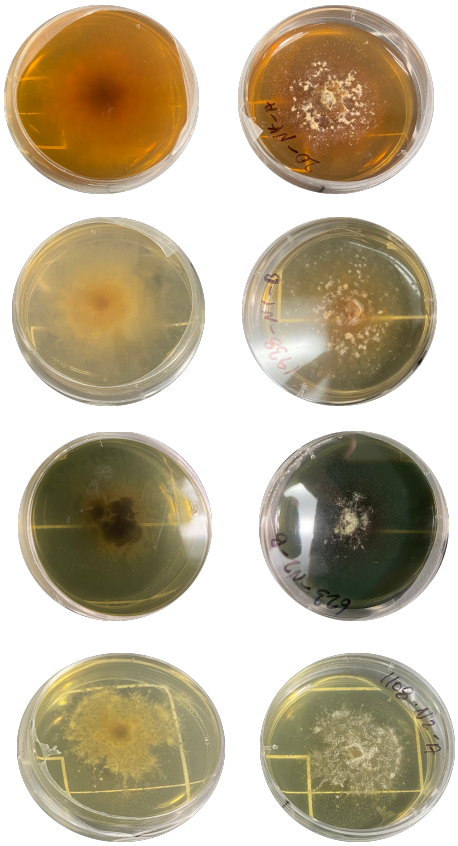

Table 3. Taxonomic assignment and frequency from 97 cultures derived from surface sterilized Douglas-fir needles grown on 2% MEA media. Sequences were reported at 95% identity match unless otherwise noted.

Species	Frequency	Accession Number(s)
Biscogniauxia bartholomaei	1	AF201719
Botrytis fabae	1	CP136209
Caliciopsis pseudotsugae	1	MT334518
Chromelosporium carneum	1	MG098273.1
cf. Clypeosphaeria mamilana[1]	3	HQ228266.1
Coleospora sp.	1	GQ153148.1
Coniochaeta taeniospora	1	KU762325.1
Coniochaeta ligniaria	3	OM337547.1
Coprinellus micaceus	1	MT644910.1
Diaporthe sp.	1	OP783986.1
Diaporthe crousii	2	MK792299.1
Diaporthe eres	1	MW040531.1
Helminthosporium velutinum	1	KY984354.1
Heterobasidion occidentale	2	KC492946.1
Hypoxylon fuscum	5	MW367856.1, OQ831970.1
Hypoxylon rubiginosum	2	OQ831968.1

Species	Frequency	Accession Number(s)
Jackrogersella multiformis	12	ON453667.1
Lachnum virgineum	1	MZ087787.1
Lasiosphaeria lanuginosa	1	MZ435277.1
Xylariales aff. Linteromyces[1]	2	no close match
Mollisia melaleuca	1	MH861785.1
Mollisiaceae sp.[1]	1	no close match
Sordariomycetes sp.	2	FN548158.1, JQ761451.1
Nemania serpens	3	OQ831989.1
Nothophaeocryptopus gaeumanni	6	MT154259.1
Penicillium sp.	1	MF942967.1
Penicillium glaucoalbidum	2	MG490875.1
Phialocephala scopiformis	1	KP972465.1
Plectania melastoma	5	OR778447.1, OQ694434.1
Cladosporium aff. Pseudocladosporiodes[1]	1	OP590136.1
Rhadocline parkeri	7	AF462426.1
Rhizosphaera merioides	2	ON784015.1
Rhizosphaera sp.	8	ON784043
Sydowia polyspora	3	KP152486.1
Trichoderma gamsii	1	KM491887.1
Trichoderma caerulescens	1	MT217122.1
Trichophaea hybrida	1	AF351582.1
Xylaria hypoxylon	8	MK577428.1, MH864103.1

[1]Taxonomic affinity as indicated by dr. Joey Tanney
cf ("compare with", indicating uncertainty)
aff (short for "species affinis", indicates a potentially new or undescribed species)

ITS amplicon metagenomics approach

Foliar mycobiome composition and diversity

12 families consisting of 5 individuals each (n = 60) were selected to cover the full range of SNC signs and symptoms, representing all possible combinations (*i.e.,* tolerant and non-resistant, tolerant and resistant, non-tolerant and non-resistant, non-tolerant and resistant). ITS amplicon metagenomic data were obtained for a total of 59 individuals (one was lost due to sampling error). Initial number of reads across all 59 samples was 1,801,928 with a mean of 30,541 and a median of 27,627 per sample. The number of reads was reduced to 1,694,167 after ITS1 region extraction, meaning nearly 110,000 (6%) reads were not found to contain the ITS1 region. Merging sequences into amplicon sequence variants (ASV) resulted in 1,820 distinct ASV's. To eliminate any non-fungal ASVs, sequences with a global alignment <0.5 identity against UNITE

reference database were removed, which reduced the number of fungal ASVs to 1,780. Collapsing ASVs that were more than 97% similar into operational taxonomic units (OTUs) yielded 1,512 OTU's. This was done to minimize intragenomic or artifactual ASVs. Aligning these OTUs against the UNITE reference sequence database resulted in 941 OTUs with at least some level of taxonomic identification while 571 OTUs remained 'unassigned'. The final filtering step was to remove low abundance OTUs to reduce noise in subsequent analyses, and this resulted in 232 distinct OTUs (Table 4).

Table 4. Number of reads, ASVs or OTUs after respective quality control or filtering steps of ITS1 amplicon sequence data (Illumina Miseq) from JR GCA breeding population.

	Initial reads	ITS reads	Trimming and ASV generation	Fungal ASVs	OTUs	OTUs w/ blast result	Contingency Filtered Fungal OTUs
Package	-	ITSexpress	DADA2	VSEARCH	LULU	QIIME2	R studio
Number Reads *(% retained)*	1,801,928 *(100%)*	1,694,167 *(94%)*	1,441,840 *(80%)*	1,438,057 *(80%)*	1,337,348 *(74%)*	1,087,261 *(60%)*	1,080,099 *(60%)*
ASVs/OTUs			1,820	1,780	1,512	941	232

Species accumulation curves (species referring to OTUs) generated from the Biodiversity package (Kindt and Coe, 2005) indicate that each tree was adequately sampled (fig. 11). Four samples showed a considerably low number of reads (<7000) and were removed from the dataset for subsequent analysis by rarefaction. Rarefying decreased read counts from 1,080,099 to 385,000 for the 232 OTUs (fig. 11A). Reads from *N. gaeumanni* were the most frequent in the dataset, making up more than 60% of the reads. To avoid possible biases introduced by the high abundance of *N. gaeumannii* reads, all analyses were performed with and excluding *N. gaeumannii* reads.

Rarefaction of the dataset without *N. gaeumannii* reads to 1,500 decreased read counts from 399,706 to 82,500 (fig. 11B). Species accumulation curves show species counts and associated reads before (left) and after (right) rarefaction. Species retained after rarefaction (right) in datasets including and excluding *N. gaeumannii* reads display similar trends in species regardless of differences in sequencing depth (fig. 11).

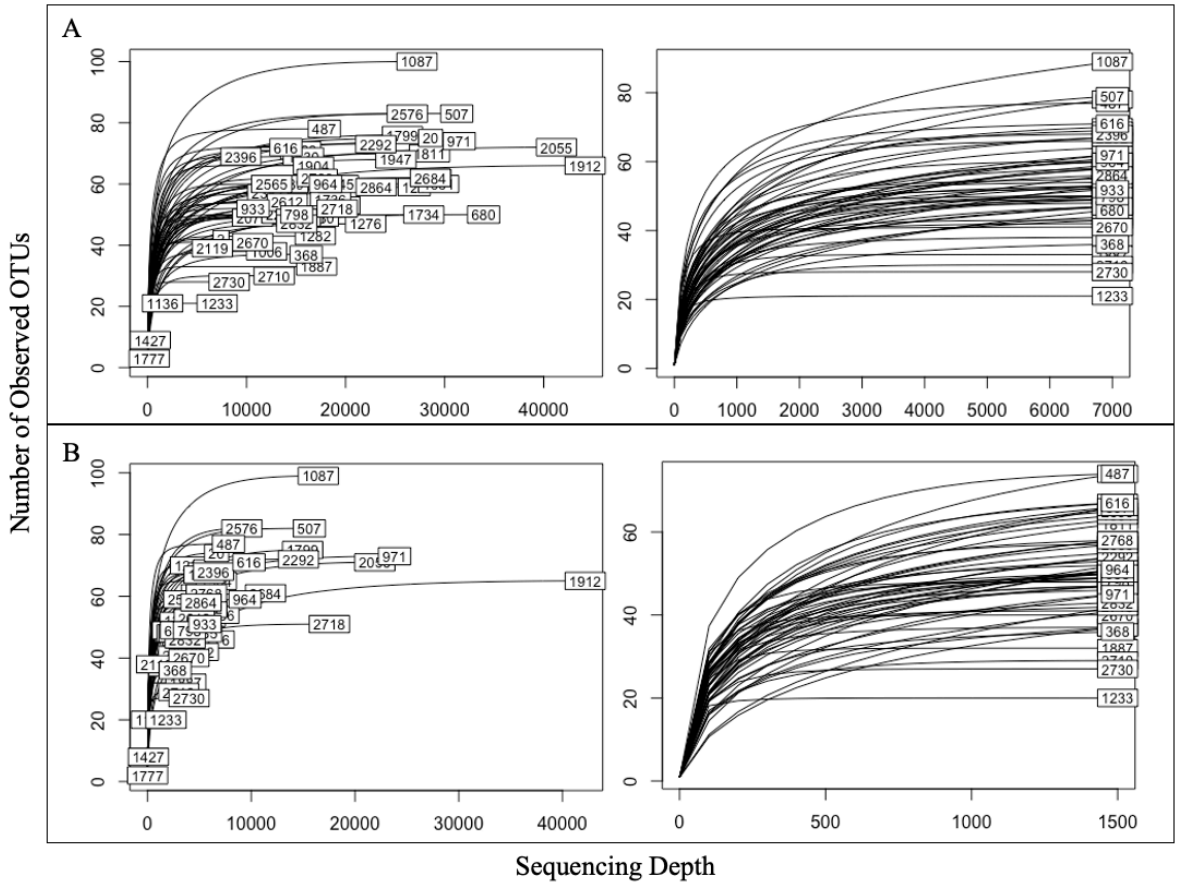

Figure 11. Rarefaction curves show the number of OTUs present in each sample as a function of sequencing depth before (left) and after (right) rarefaction. (A) shows rarefaction of the dataset including N. gaeumannii normalized to a depth of 7000, and (B) shows rarefaction of the dataset excluding N. gaeumannii (normalized to a depth of 1500).

The number of unique OTUs within rarefied samples ranged from 21 – 88 with an average of 54.3 unique OTUs and a standard deviation of +/- 13.3 per individual tree. Across the whole dataset, the by far most abundant OTU (corresponding to 64.5%) was *N. gaeumannii* (Mycosphaerellales, Dothideomycetes). The second most abundant OTU, *Rhizosphaera merioides* (Dothideales, Dothideomycetes), was more than ten time less abundant and represented by 5.6% of reads. This was followed by Chaeotothyriales sp. (3.6%) (Chaetothyriales, Eurotiomycetes), *Zasmidium* sp. (3.22%) (Mycosphaerellales, Dothideomycetes), *Rhizosphaera sp. 2* (2.26%) (Dothideales, Dothideomycetes), *Rhabdocline pseudotsugae* (1.94%) (Helotiales, Hemiphacidiaceae), and *Exobasidium* sp. (1.38%) (Exobasidiales, Exobasidiaceae). In total only nine, that is less than one tenth of all OTUs identified, achieved relative abundances of greater than 1%. This means that most of the fungal diversity observed is among rare species each less than 1% abundant (appendix 6). *N. gaeumannii* was found in all 54 samples, yet with a wide variance, ranging from 91% to only 4% abundance for each sample. Yet, *N. gaeumannii* was only found with a relative abundance less than 50% in 11 of the 55 samples. I validated the approach of using metagenomics based read abundance as a measure of species abundance by quantifying fungal load using an alternative approach, namely qPCR as described earlier (Montwé *et al,* 2021). I observed an overall positive correlation between *N. gaeumannii* abundance determined by qPCR and metagenomics-based sequence read abundance (appendix 4, fig. 1). This supported relative read abundance as a reasonable measure for fungal abundance.

The other eight most abundant OTUs (relative abundance greater than 1%) were found consistently across samples (*i.e.,* found in 18 to all of the 55 samples). When *N. gaeumannii* reads were excluded from the dataset, 23 genera were found to have read abundances greater than 1% (fig. 12). OTUs were grouped by genus for this portion of analysis due to lower number of

successful identifications to the species level. Specifically, 143 OTUs (61%) were identified to genus while only 19 (8%) OTUs could be identified to species. Six genera had abundances that significantly differed (*alpha* = 0.05) between families (Kruskal-wallis p-values of: *Exobasidium* = 8.09e-05*, Rhizosphaera* = 2.00e-03, *Tremellales gen Incertae sedis* = 7.45e-03, *Orbiliales gen Incertae sedis* = 1.37e-02, *Rhabdocline* = 2.31e-02, *Retiarius* = 3.17e-02, *alpha* = 0.05*),* however, when p-values were corrected for multiple testing (Benjamini-Hochberg method) only *Exobasidium* significantly differed across families (p-adjust = 0.006; fig. 13). No genera showed significant abundance differences across any disease phenotype classification grouping (*i.e.,* non-tolerant and non-resistant, non-tolerant and resistant, tolerant and resistant, tolerant and non-resistant) or when categorized by stomatal occlusion or needle loss severity (as described in Methods).

Figure 12. Relative abundance of fungal genera comprising the foliar mycobiome of 59 Douglas-fir trees (12 families) in a GCA breeding population, Jordan River BC. A) is including highly abundant genera Nothophaeocryptopus B) is excluding Nothophaeocryptopus. Taxa found at an abundance of <1% in a sample are assigned together. NA represents taxa that could not be resolved to genus level.

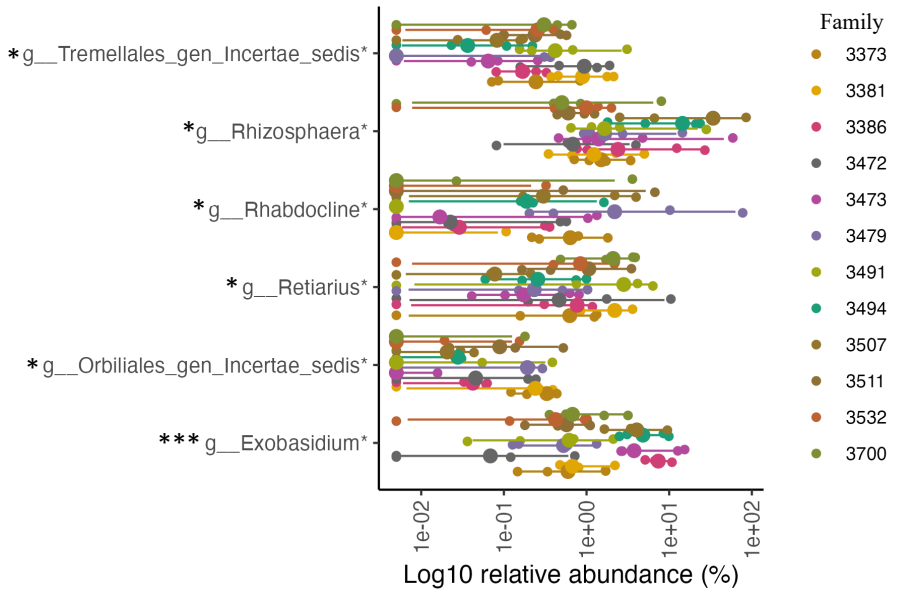

*Figure 13. Differentially abundant genera across different families within the JR GCA breeding population. Plotted is log_{10} relative abundance transformed data; however, significance testing was done using CLR transformed data to account for the compositionality of the data. * Signifies Kruskal-wallis test p-values < 0.05. *** Signifies p-values adjusted for multiple comparisons (using Benjamini-Hochberg correction) < 0.05.*

Alpha Diversity

Alpha Diversity (Shannon and Observed) was not significantly different across any levels of disease severity or family groups (Table 5, fig.14; Observed in appendix 1). For all groupings, except for family, Shannon diversity p-values increased when *N. gaeumannii* reads were removed from the dataset prior to rarefaction (Table 5). While not significant, Shannon diversity was observed to be higher in samples grouped based on low incidence of stomatal occlusion, in comparison to samples with high incidence of stomatal occlusion. A similar trend was seen in terms of disease interaction classification with 'tolerant and resistant' displaying higher alpha diversity compared to other groupings (fig. 14). I observed a significant negative correlation between stomatal occlusion incidence and Shannon diversity when treated as a continuous variable (r-value = -0.285, p = 0.0388) (fig.15). However, no statistically significant correlation was found

between the observed richness and the severity of stomatal occlusion (r-value = -0.139, p = 0.320). This suggests that evenness of these species, not richness, is what decreases with increased stomatal occlusion pressure.

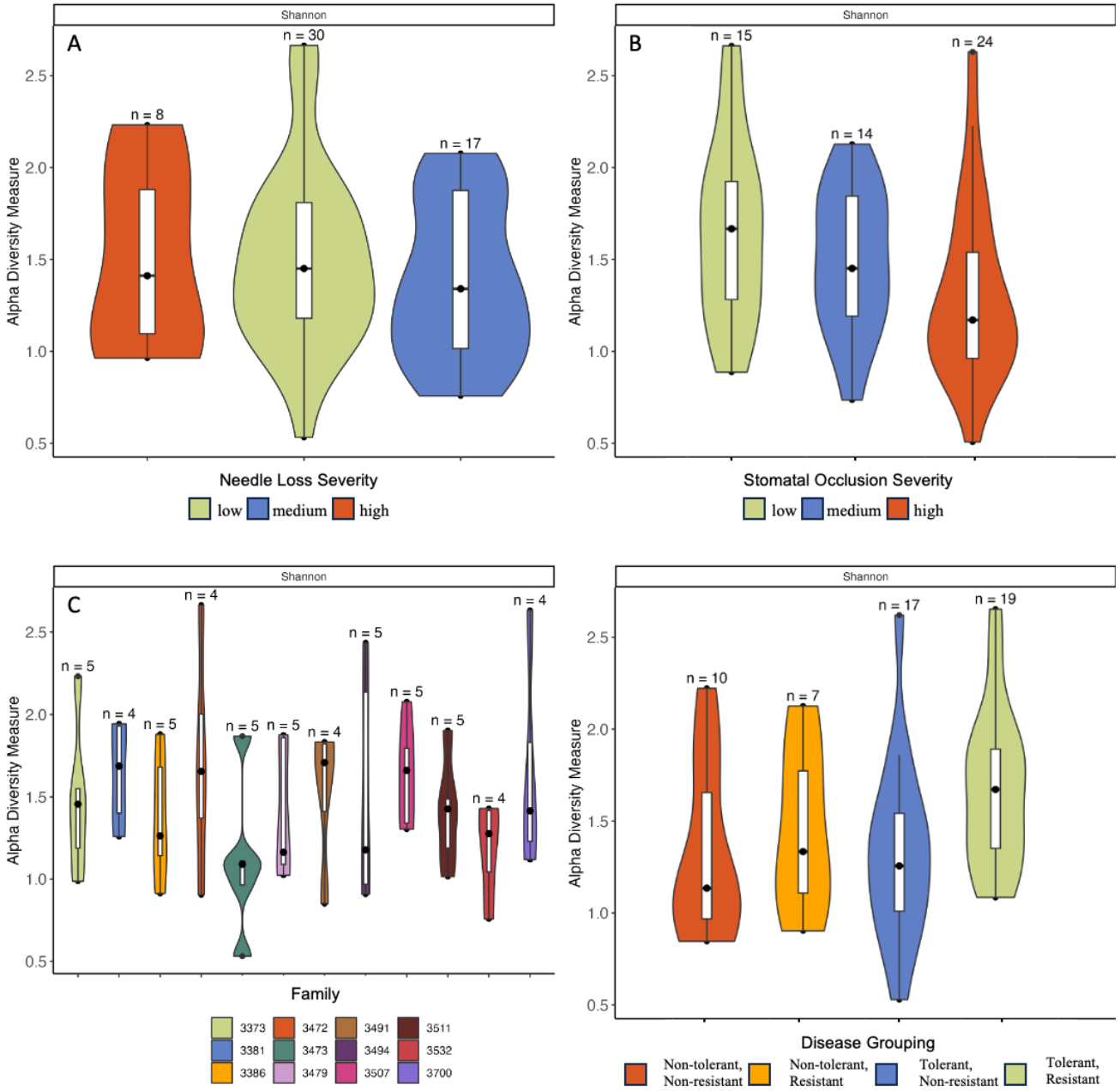

Figure 14. Comparison of Alpha Diversity metrics based on Shannon Diversity Indices for individual disease phenotypes (i.e., needle loss and stomatal occlusion: low, medium, and high), disease grouping (based on tolerance and resistance), and family. The dataset was rarefied to a depth of 7000 (N = 55, with 4 to 5 individuals per each of the 12 families).

Table 5. ANOVA results comparing Shannon Diversity Indices for disease groupings and family as described in figure. 14 (alpha < 0.05). Top refers to dataset with N. gaeumannii (rarefied to depth of 7000) and bottom refers to dataset excluding N. gaeumannii reads (rarefied to depth of 1500).

	Df	**Sum Sq**	**Mean Sq**	**F value**	**Pr(>F)**
With *N. gaeumannii*					
Needle Loss 3rd Year 2022	2	0.21	0.11	0.47	0.63
residual	*52*	*11.85*	*0.23*		
Stomatal Occlusion 2021	2	1.10	0.55	2.56	0.087
residual	*50*	*10.75*	*0.22*		
Family	11	1.71	0.16	0.64	0.78
residual	*43*	*10.36*	*0.24*		
Disease Grouping	3	1.35	0.45	2.09	0.11
residual	*49*	*10.51*	*0.21*		
Relative Growth Rate	*3*	*0.94*	*0.16*	0.72	0.54
residual	*51*	*11.61*	*0.23*		
Without *N. gaeumannii*					
Needle Loss 3rd Year 2022	2	0.015	0.008	0.029	0.97
residual	*52*	*13.64*	*0.26*		
Stomatal Occlusion 2021	2	1.12	0.56	2.33	0.11
residual	*50*	*11.99*	*0.24*		
Family	11	3.84	0.35	1.53	0.16
residual	*43*	*9.82*	*0.23*		
Disease Grouping	3	0.91	0.30	1.22	0.31
residual	*49*	*12.20*	*0.25*		
Relative Growth Rate	3	0.50	0.17	0.73	0.54
residual	*53*	*12.06*	*0.23*		

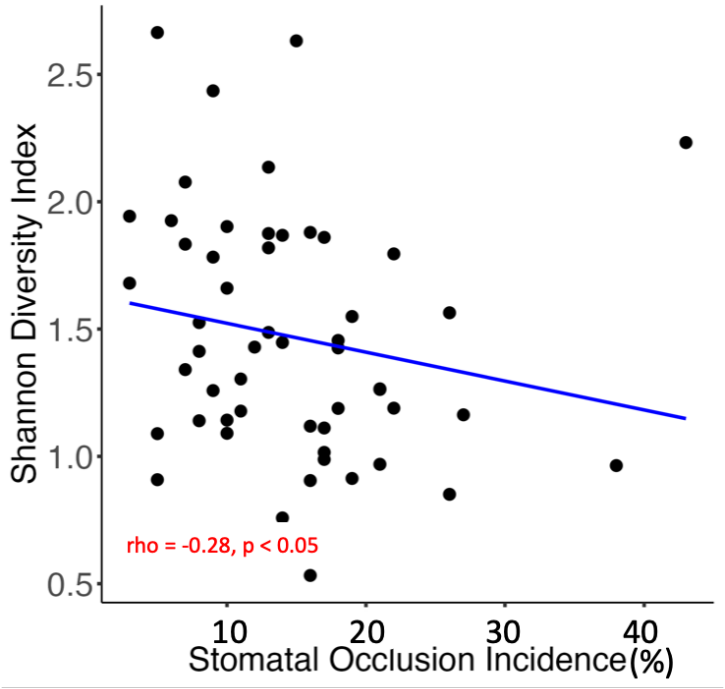

Figure 15. Spearman correlation (r-value = rho) of stomatal occlusion incidence (% out of 100) with Shannon diversity index based on rarefied ITS1 amplicon data from 55 trees within JR GCA breeding population.

Beta Diversity/ Community Composition

Analysis of variance showed that foliar mycobiome community assemblages differed significantly between different families but not between different disease severity groupings. This was observed both for data sets including *N. gaeumannii* ($F = 1.63$, $P = 0.036$, $R^2 = 0.297$) and when excluding *N. gaeumannii* ($F = 2.28$, $P = 0.001$, $R^2 = 0.361$) (Table 6). Analysis of variance was conducted with multiple normalization methods, and consistent results indicate robustness of the observation that mycobiomes differ among families (appendix 2). Analysis of multivariate homogeneity of group dispersions (PERMDISP2, Anderson, 2006) confirmed that this was not influenced by unequal variance within families).

Table 6. Permutational multivariate analysis of variance of the compositional dissimilarity between foliar mycobiome fungal assemblages associated with Douglas-fir 2nd year age class needles (n = 55) in a subset of JR GCA breeding population. The analysis is based on rarefied data including (top) and not including N. gaeumannii reads (bottom). The compositional dissimilarity between assemblages was assessed with the Bray-Curtis dissimilarity index.

	Df	**Sum Sq**	**R^2**	**F value**	**Pr(>F)**
With *N. gaeumannii*					
Family	11	1.375	0.297	1.633	**0.036***
Block	21	1.919	0.414	1.194	0.279
Needle Loss 2nd Year 2021	1	0.018	0.004	0.230	0.973
Needle Loss 3rd Year 2022	1	0.038	0.008	0.490	0.807
Stomatal Occlusion 2021	1	0.106	0.023	1.389	0.237
Relative Growth Rate	1	0.025	0.005	0.320	0.95
Disease Grouping	3	0.160	0.035	0.697	0.767
Residual	*13*	*0.995*	*0.215*		
Total	*52*	*4.636*	*1*		
Without *N. gaeumannii*					
Family	11	4.849	0.361	2.279	**0.001****
Block	21	4.577	0.341	1.127	0.196
Needle Loss 2nd Year 2021	1	0.213	0.016	1.104	0.336
Needle Loss 3nd Year 2022	1	0.146	0.011	0.754	0.721
Stomatal Occlusion 2021	1	0.222	0.017	1.149	0.289
Relative Growth Rate	1	0.141	0.010	0.727	0.739
Disease Grouping	3	0.758	0.056	1.306	0.136
Residual	*13*	*2.515*	*0.187*		
Total	*52*	*13.422*	*1*		

Non-metric multidimensional scaling of the Bray-Curtis dissimilarity matrix obtained for the rarefied metagenomic sequencing dataset generally showed overlap between families (Figure 15). However, the spread of the hulls varies between certain families, indicating distinct patterns in the distribution of data within these families. Despite these differences, no pairwise comparisons between families were significantly different after controlling for multiple comparisons (using Benjamini-Hochberg adjustment; Benjamini and Hochberge, 1995). Visualized in the NMDS plot, the majority of points clustered along the ordinate axes indicate low mycobiome community composition dissimilarity among trees, which appears to be correlated with presence of *N. gaeumannii (*r-value = 0.888, p-value < 0.05; fig. 16). Few non-clustered community assemblages are associated with the presence of genera such as *Rhizosphaera merioides, Rhabdocline pseudotsugae, and Cosmospora* sp. (r-values = 0.901, 0.783, 0.707; p-values < 0.05; fig. 16).

Because family was the only grouping that explained community composition differences, a distance-based redundancy analysis (dbRDA) was run. The aim of this analysis was to explain variation in community composition when constrained on the explanatory variable, Family. The community dissimilarity between the 12 families explained 28% of the total variance (fig.17). For the latter, *N. gaeumannii* had the strongest correlation (r-value = 0.96, p-value = 0.001) with community dissimilarity, followed by *Rhizosphaera* (r-value= 0.92, p-value = 0.001). Community composition appears to be driven by *Rhizosphaera* and *Exobasidium* for families 3494, 3507, 3473, and 3386, which are the only families that display separation on the ordinate axis (fig. 17). This is supported by the high abundance of these taxa in fig. 12, where *Exobasidium* is high in 3386 and 3473 versus *Rhizosphaera* in 3494 and 3507.

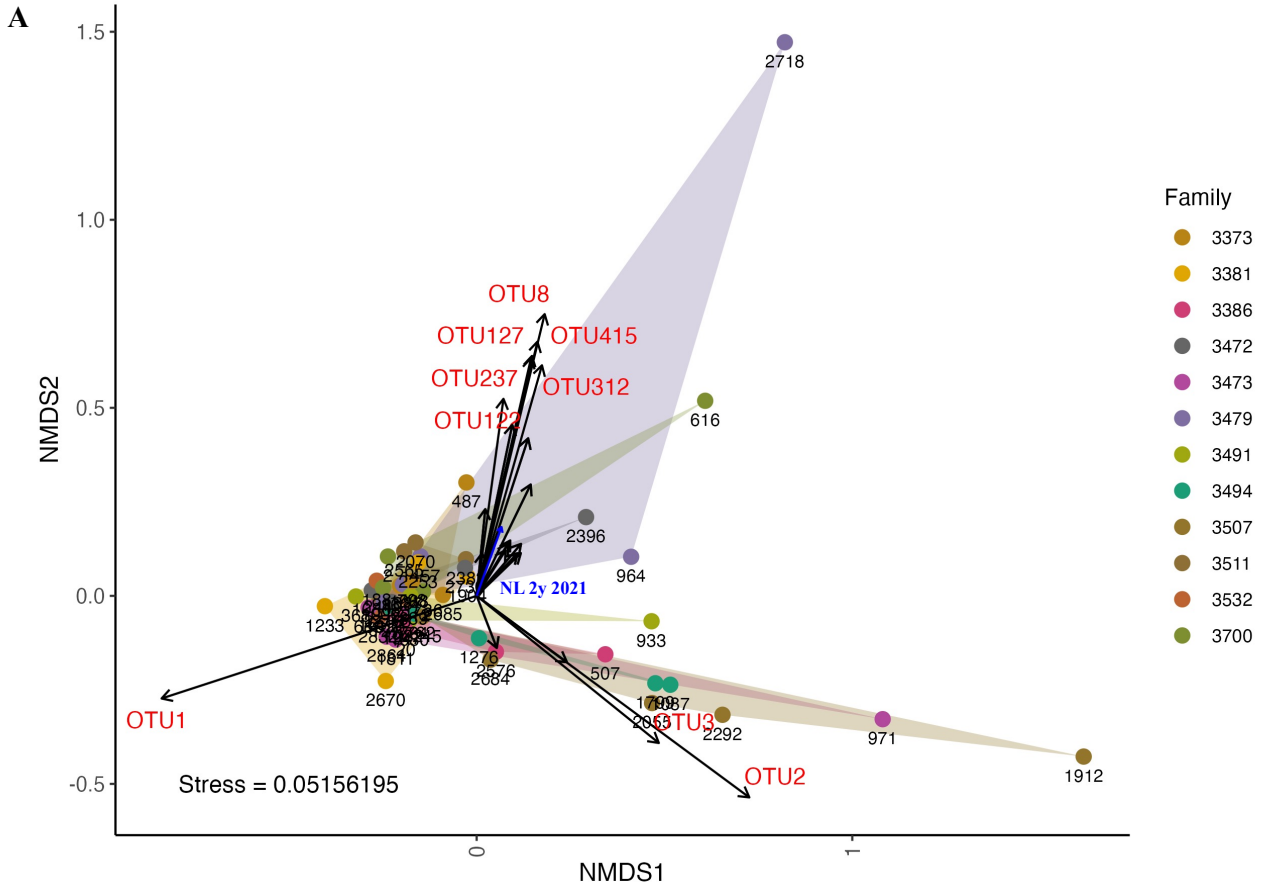

B

Name	Direction	R-value	P-value	Genus	Species	Query Cover	% Identity	Accession Number	Guild
OTU1	↙	0.888	0.001	*Nothophaeocryptopus*	*gaeumannii*	100	100	ON783984.1	Plant Pathogen-Undefined Saprotroph
OTU8		0.783	0.002	*Rhabdocline*	*pseudotsugae*	100	98.62	AF462420.1	Plant Pathogen
OTU312		0.707	0.021	*Cosmospora*	*sp.*	98	95.24	MK795729.1	Fungal Parasite
OTU237		0.666	0.015	*Erythrobasidiales* (order)	*sp.*	100	99.07	MK281685.1	
OTU127		0.620	0.002	*Heterocephalacria*	*sp.*	97	100	MN066369.1	
OTU122	↑	0.583	0.016	*Microcyclospora*	*tardicrescens*	100	97.35	MN065467.1	
OTU415		0.572	0.012	*Helotiales*	*sp.*	100	94.47	KY742551.1	
OTU85		0.462	0.019	*Calycina*	*sp.*	100	96.82	OR882763.1	Undefined Saprotroph
OTU321		0.430	0.008	*Taphrina*	*purpurascens*	100	99.04	MH857503.1	Plant Pathogen
OTU103		0.325	0.026	*Microcyclospora*	*tardicrescens*	100	99.12	MN065467.1	
OTU291		0.179	0.041	*Neomicrosphaeropsis*	*sp.*	100	98.60	OM745345.1	Animal Pathogen-Plant Pathogen-Undefined Saprotroph
OTU175		0.179	0.037	*Leucosporidium*	*intermedium*	100	96.19	KY104188.1	Soil Saprotroph-Undefined Saprotroph
OTU260		0.166	0.035	*Bannozyma*	*yamatoana*	100	90.87	KY101711.1	
OTU157		0.154	0.045	*Bannozyma*	*sp.*	100	100	MN128415.2	
OTU37		0.152	0.045	*Cladosporium*	*delicatulum*	100	100	MT548673.1	
OTU29		0.136	0.049	*Niesslia*	*endophytica*	100	100	NR_189406.1	Undefined Saprotroph
NL 2y 2021		0.189	0.042						
OTU2		0.901	0.001	*Rhizosphaera*	*merioides*	100	100	ON784015.1	Plant Pathogen
OTU3	↓	0.612	0.001	*Rhizosphaera*	*sp.*	100	100	ON784044.1	Plant Pathogen
OTU44		0.280	0.040	*Thysanophora*	*penicillioides*	100	99.53	AB175249.1	Undefined Saprotroph
OTU25		0.146	0.043	*Exobasidium*	*sp.*	100	90.72	ON787635.1	Plant pathogen

Figure 16. NMDS plot of foliar mycobiome fungal assemblages within 54 Douglas-fir trees representing 12 families within JR GCA breeding population. Community dissimilarity between samples was assessed with a Bray-Curtis dissimilarity matrix of fungal ITS metabarcoding sequences. Vectors indicate a significant correlation between individual OTUs or disease phenotype and ordination axes (alpha =0.05), the length of the vector signifies the strength of the correlation. Only ***OTUs with a r-value > 0.5*** *are visualized, table below summarizes all significant correlations with OTUs and disease phenotypes with classification from FUNguild.*

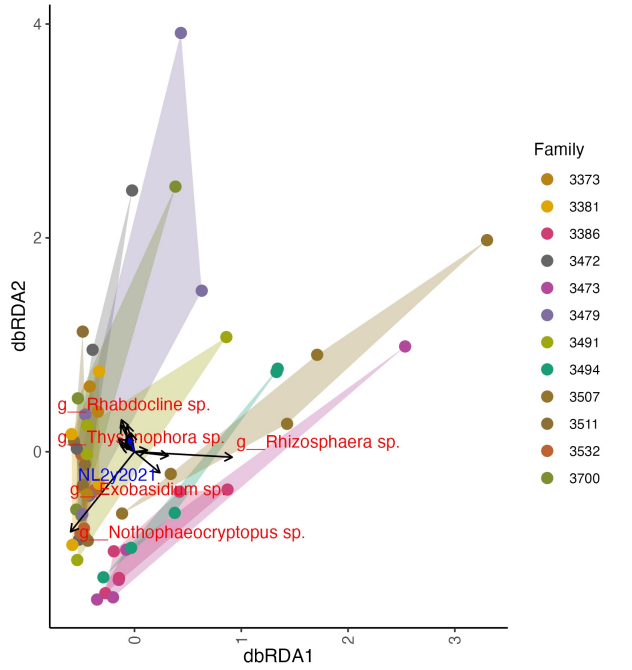

Genus	Direction	R-value	P-value
Nothophaeocryptopus	↙	**0.96**	**0.001**
Rhizosphaera		**0.92**	**0.001**
Thysanophora	→	**0.32**	**0.002**
Exobasidium		**0.31**	**0.001**
Penicillium		0.12	0.041
Rhabdocline		**0.32**	**0.006**
Tremellomycetes gen Incertae sedis		0.28	0.006
Fusicolla	↖	0.26	0.026
Kurtzmanomyces		0.19	0.019
Fellozyma		0.18	0.012
Microcyclospora		0.18	0.039
Catenulostroma		0.17	0.011
Orbiliaceae gen Incertae sedis		0.15	0.018
Tremella		0.13	0.046

Figure 17. Distance-based redundancy analysis of Douglas-fir foliar mycobiome constrained on family. This ordination describes 28 % of variation in community composition. Vectors indicate a significant correlation between genera or disease phenotype and ordination axes (alpha =0.05), the length of the vector signifies the strength of the correlation. Each point denotes an individual tree's mycobiome and are coloured based on Family. Genera with a significant correlation (p <0.05) and an ***r-value >0.3*** *are plotted while weaker associations are listed.*

Abundance correlations between all taxa identified at the genus level were analysed to test for co-occurrence or competition with *N. gaeumannii.* Hub taxa were determined based on Eigenvector centrality (Peschel *et al.,* 2020), *i.e.* nodes were considered hubs if they are connected to other central nodes in the network. Hub-OTUs were identified as genera *Sloofia, Fusicola, Agaricostilbales gen Incertae sedis* and *Kriegeriales gen Incertae sedis.* Importantly, *Rhizosphaera* was the only genus found to have a strong negative correlation with *Nothophaeocryptopus* (R-value = -0.43, p-value < 0.05) (fig. 18).

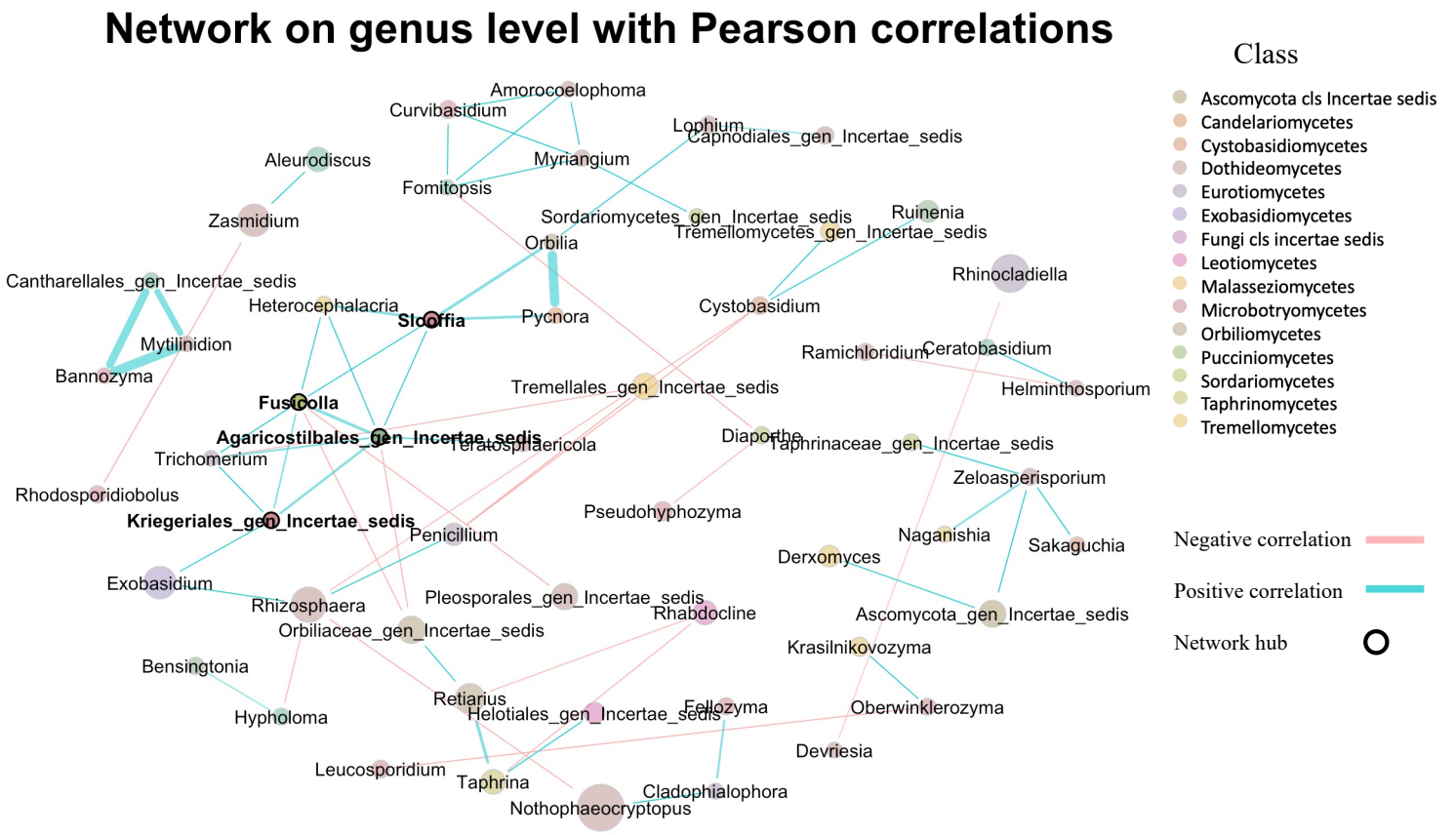

Figure 18. (Pearson correlation) Co-occurrence network of fungal genera detected in a SNC infected GCA breeding population of Douglas-fir. The network was generated using R package NetCoMi. Edge colour represents negative (red) and positive (blue) associations. Hub-taxa nodes have a black outline. Node size represents differences in relative read abundance. Only correlations with an absolute value (r-value) of 0.4 or greater were used to calculate edges.

Two distinct species were identified belonging to the negatively correlated genus *Rhizosphaera.* These two species obtained from metagenomics data were aligned with other previously published *Rhizosphaera* sequences (Taylor and Koukol, 2023) as well as sequences obtained from my cultures of *Rhizosphaera*. One OTU closely aligned with a *Rhizosphaera* sp. described by Taylor and Koukol (2023) and one to *Rhizosphaera merioides* (fig. 19). Abundance of the two *Rhizosphera* species both exhibited strong negative correlations with *N. gaeumannii* (r-values = -0.572, -0.433; p-values = 2.25 x 10^{-06}, 6.21 x10^{-04}; fig.19). To determine if this directly impacted disease severity, correlations between both *Rhizosphaera* OTUs and stomatal occlusion and needle

loss were analysed. No strong or significant correlations were found, indicating that they do not measurably impact disease symptoms in our experimental setting (appendix 3, table 1). Additionally, there was a strong positive correlation observed between the two *Rhizosphaera* species (r-value = 0.680, p-value = 3.19e-09; fig. 20).

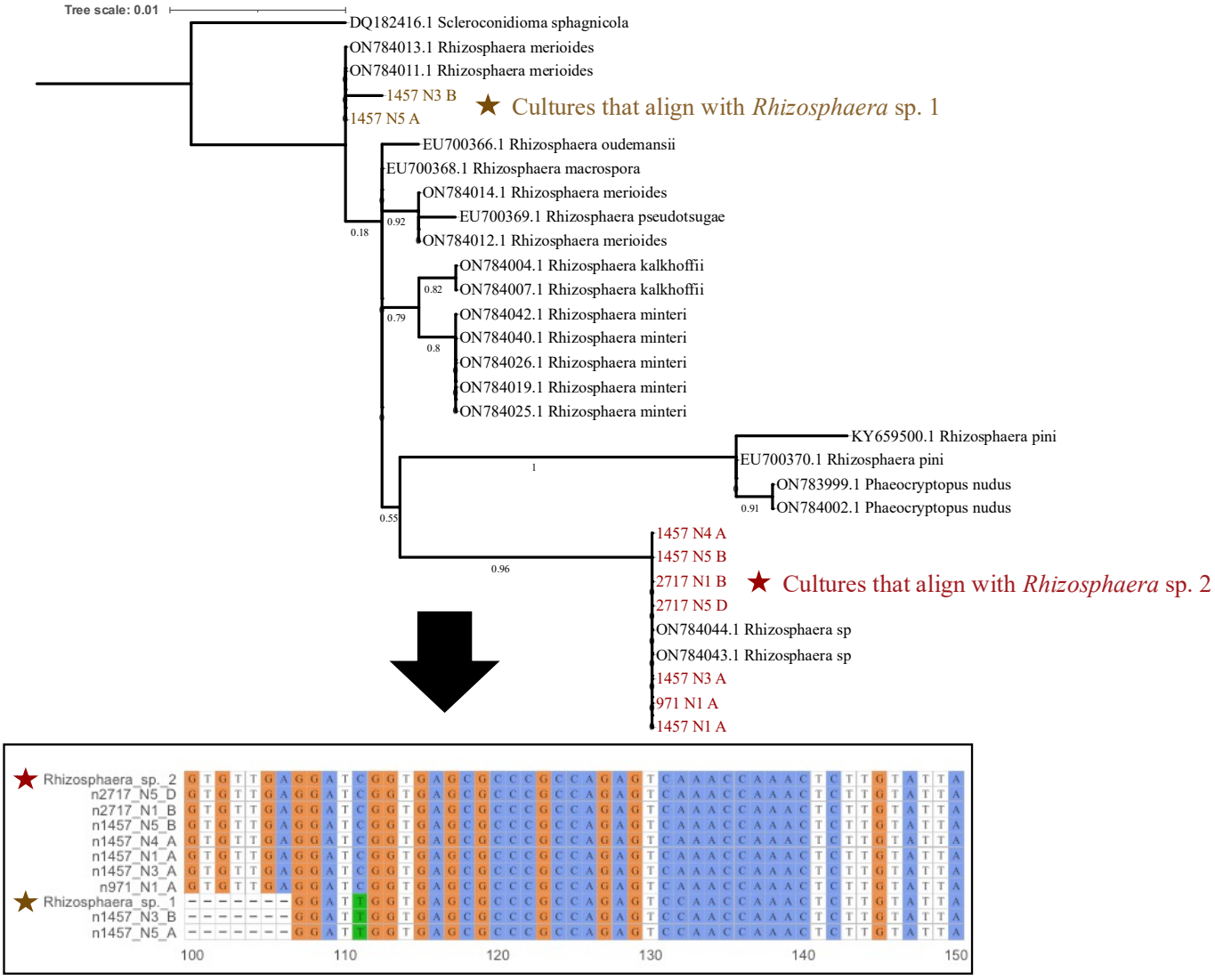

Figure 19. Phylogenetic relationship of Rhizosphaera cultures with published Rhizosphaera sequences (Taylor and Koukol, 2023) based on whole ITS region. Sequences were aligned using ClustalW and visualized using iTOL. Seperate alignment of my cultures and metagenomic sequences show that Rhizosphaera sp.1 is most similar to cultures grouped with Rhizosphaera merioides and Rhizosphaera sp. 2 is most similar to cultures grouped with Rhizosphaera sp.

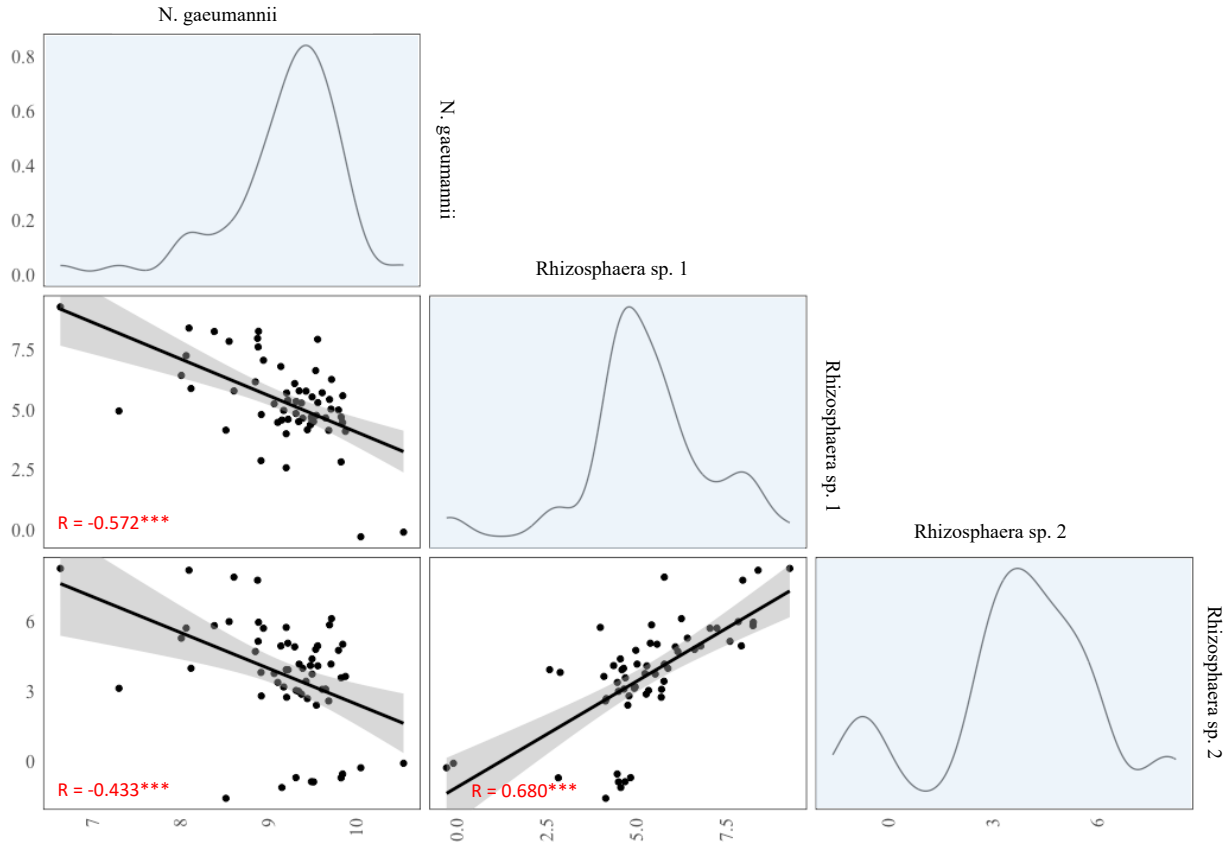

*Figure 20. Pearson correlations of clr transformed data from JR GCA metagenomics for both Rhizosphaera species and N. gaeumannii reads. The lower triangle reports r-value (corr) and significance denoted by asterisks * (alpha < 0.05). Blue graphs show density plots for each respective taxa representing the distribution across all (59) samples. Data was clr transformed to account for compositionality.*

Mycobiome Meta-analysis

The most holistic approach to capturing fungal community diversity is via the complementary use of culture-based and non-culture-based (metagenomic) methods. Through culture methods I identified 37 unique species comprising 28 genera. Through metagenomics 143 OTUs out of 232 could be identified to the genus level of which 76 unique genera were identified. However, only 19 of these OTUs could be identified to species due to the limited resolution of just the ITS1 region or the absence of close matches in the databases. To supplement this data I have compiled information from two more publications allowing for comparisons across geographical regions and methods. The goal of this meta-analysis is to provide a comprehensive look at what taxa constitute the Douglas-fir foliar mycobiome based on all currently available data.

Fungal Class Sordariomycetes comprised the largest percentage of taxa found in my culture-based data (fig. 21) and the same class was most abundant in culture-based studies from Oregon and Washington (Daniels *et al.,* 2018). While this class was present in my metagenomics data, the abundance of Sordariomycetes was substantially lower compared to many other taxonomic groups. This was seen both in count and abundance data. Despite sequencing fewer cultures than Daniel *et al.* (2018), the diversity and proportion of fungal classes represented in my data set and theirs remain similar, suggesting that diversity in culturable fungi, at least at this taxonomic level, is comparable across large geographic distances (fig.17). Daniel *et al.'s* (2018) study found the genera *Diaporthe*, *Penicillium*, *Rhabdocline,* and *Xylaria* as some of the most commonly occurring across their sites, which was also observed in my culture-based data.

In terms of metagenomics, I identified only one other published study that has used this method to characterize the foliar mycobiome of Douglas-fir. Gerver *et al.'s* (2022) study addressed community composition in six individual old-growth Douglas-fir in central Oregon. They similarly found *N. gaeumannii* to be the most abundant species, followed by *Rhabdocline parkerii*. *Rhabdocline parkerii,* while present in my metagenomic dataset, was at a much lower level. Similar to my study, the majority of Gerver *et al.'s* (2022) reads were associated with a limited number of taxa, while the remainder were distributed among numerous less abundant taxa, including *Phyllosticta abietis*, *Rhabdocline pseudotsugae*, *Raustoria pseudotsugae*, and *Hormonema macrosporum* (Gervers *et al.,* 2022). Of these species the only one found within my metagenomic data was *Rhabdocline pseudotsugae* at an abundance 1.94% of all reads. Fungal classes between my study and Gervers *et al.'*s (2022) were similar (fig. 21). However, this became less the case for the family, genus, and species level, suggesting the role of more localized taxa within these more commonly associated higher-level groupings. The use of a different ITS region

(ITS2) in Gerver *et al.*'s (2022) study and study design differences (*e.g.,* stratified sampling and different surface sterilization techniques) did not allow for further comparison.

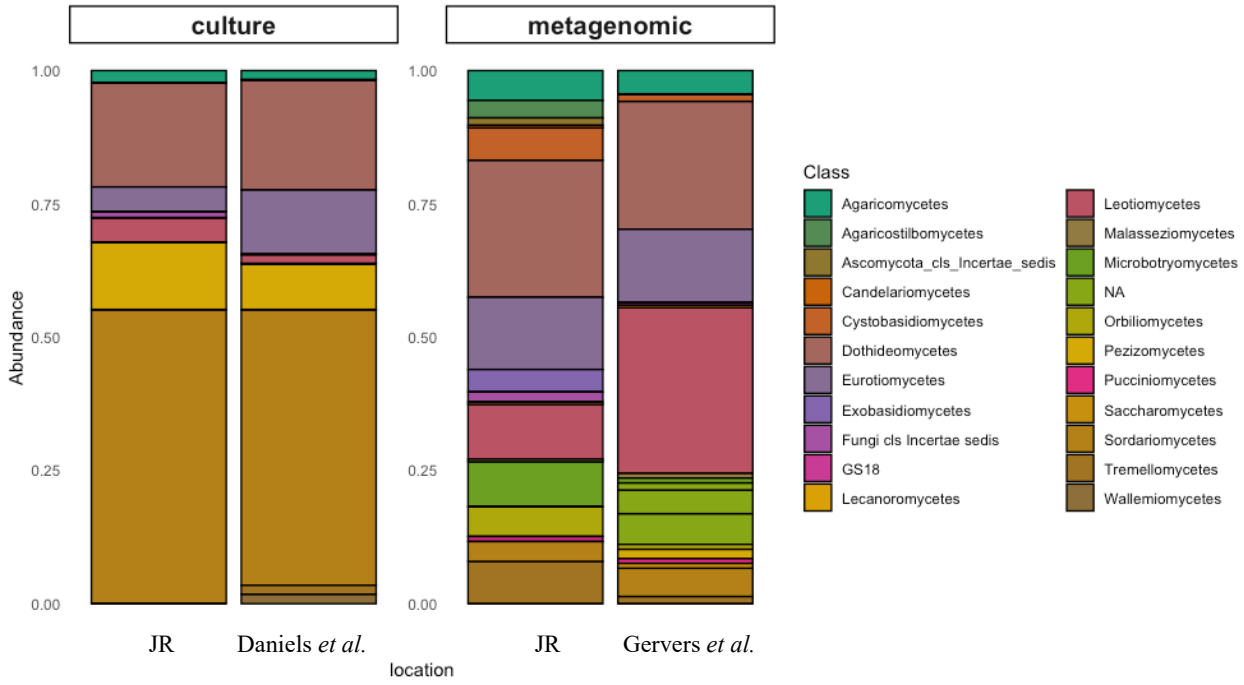

Figure 21. Taxa represented in Jordan River GCA breeding population culture and metagenomic sequences data compared to other available studies using these respective techniques: metagenomics (Gervers et al., 2022) and culture-based (Daniels et al., 2018).

To summarize what is currently known about the Douglas-fir foliar mycobiome I mapped all fungal classes and orders represented in the studies discussed above as well as my own to a recent and complete fungal phylogenetic tree (James *et al.,* 2020). The taxa represented in the Douglas-fir mycobiome are wide spread across the subkingdom Dikarya (composed of Ascomycota, Basidiomycota and Entorrhizomycota) within the fungal phylogeny and exclude the early diverging fungal taxa (Mucoromycota, Zoopagomycota, Chytridiomycota, Monoblephardomycota, and Blastocladiomycota were not found in any study's data). Overall, the diversity of fungal taxa represented by metagenomics is far higher than that of culture-based approaches, and it captures more within the Basidiomycota (fig. 22).

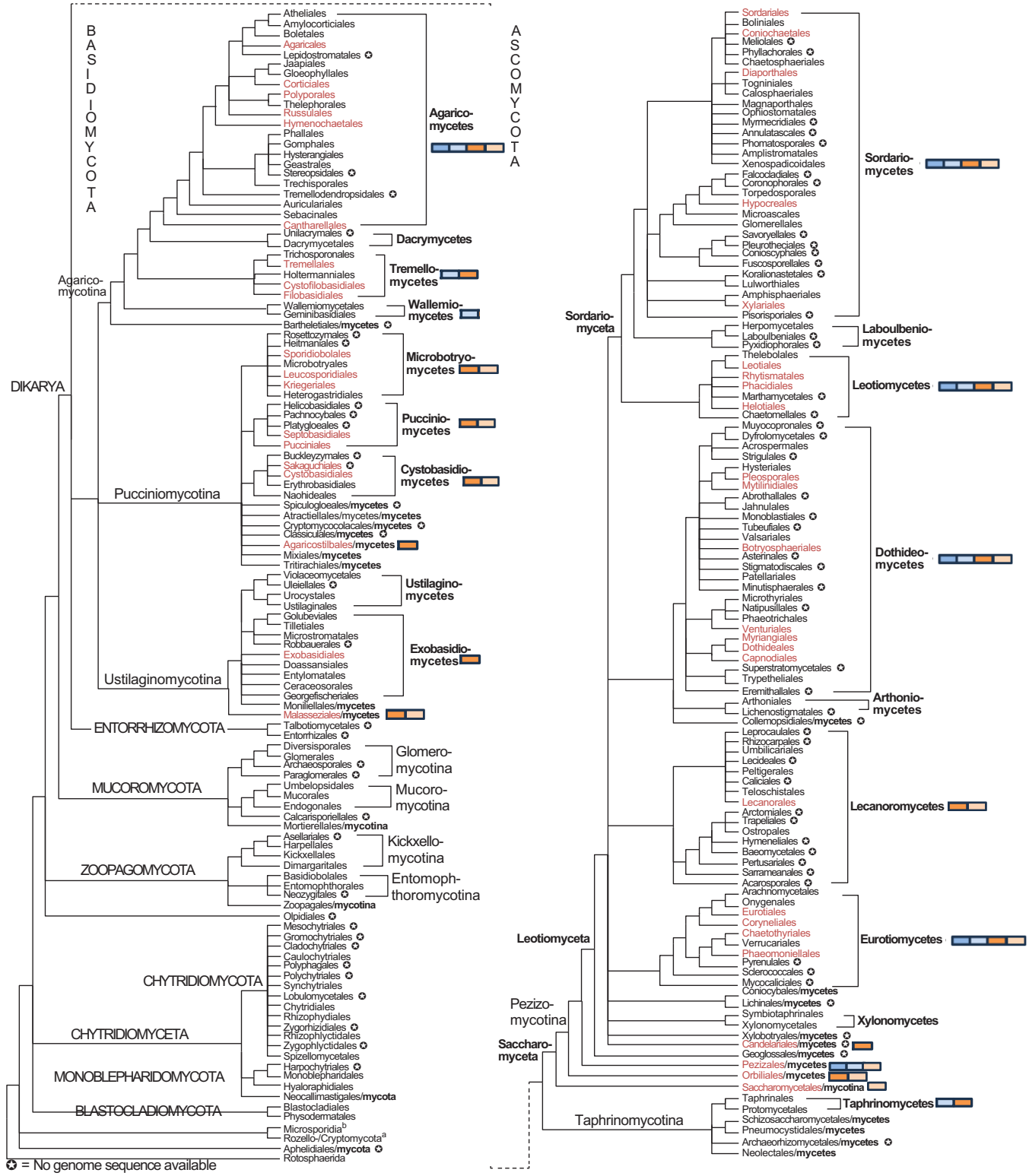

J D I G Culture (**D** = Daniels *et al*., 2018 , **J** = Jordan River, BC), NGS (**I** = Jordan, River, BC, **G** = Gervers *et al*., 2022)

*Order associated with Douglas-fir foliar mycobiome

Figure 22. Fungal taxonomic tree from James et al. (2020) modified to include fungal class and orders present in my study and two other available studies that used metagenomics (Gervers et al., 2022) and culture-based approaches (Daniels et al., 2018) to characterize the foliar mycobiome of Douglas-fir. Orders not represented by this tree but present were: Cladosporiales, Mycosphaerellales, Taphriles, Triblidiales, Wallemiales, Zeloasperisporiales.

Discussion

A novel finding of this study was the genus *Rhizosphaera*'s significant negative correlation with the Swiss Needle Cast causing fungus *N. gaeumannii.* Considering *N. gaeumannii's* abundance, exceeding that of any other fungal OTU, including *Rhizsophaera,* by at least a ten-fold factor, a fungal taxon that could alleviate some of the fungal pressure imposed by *N. gaeumannii* is of great interest. *Rhizosphaera* was the second most abundant genus within the metagenomic dataset and was represented by two distinct OTUs. Given these findings, I will first discuss the taxonomic placement of these two species of *Rizosphaera* and what ecological roles they may play.

The genus *Rhizosphaera* is currently described to contain around a dozen species, many of which are known pathogens of plants (Taylor and Koukol, 2023). Known hosts of the genus *Rhizosphaera* include conifer species of the genera *Pinus, Abies, and Picea,* as well as *P. menziesii.* Different species exhibit different lifestyle preferences, with some found to be associated with diseased tissue (pathogenic), green/ healthy tissue (latent pathogen or endophytic), and some with dead tissue (suggesting saprotrophic life styles) (Taylor and Koukol, 2023). Two distinct species of *Rhizosphaera* were found in my metagenomic data: *Rhizosphaera* sp. 1 (relative abundance of 5.64%) identified as *R. merioides* (ON784015.1) and R*hizosphaera sp.* 2 (relative abundance of 3.59%) identified as *Rhizosphaera sp.* (ON784044.1) (Taylor and Koukol, 2023). A recent study characterized *R. merioides* as a latent saprotroph (isolated from dead Douglas-fir leaf litter) and proposed *R. merioides* as a new name for two suspected conspecific species: *Hormonema merioides* and *Rhizosphaera pseudotsuga* (Taylor and Koukol, 2023). Pathogenicity has been suspected but not proven for both original species (Funk *et al.,* 1985; Butin and Kehr, 2000). *Rhizosphaera* sp. was described by Taylor and Koukol (2023) as a pathogen

because it was isolated from alive but diseased tissue of Douglas-fir; however, this has not been confirmed using Koch's postulate and remains speculative.

The moderate negative correlation between both *Rhizosphaera* OTUs and *N. gaeumannii* fungal load suggests a potential relationship between these genera, representing the only significant negative co-occurrence observed in my metagenomic results. Two Douglas-fir families (3494 and 3507) showed consistent elevated abundance of *Rhizosphaera* despite their scattered distribution across the plot, indicating a genetic influence on associations with this genus. Further exploration, considering potential heritability and the negative correlation with *N. gaeumannii*, is warranted. Possible additional avenues include confirming the presence or absence in other Vancouver Island plantations and investigating the presence of inhibitory bioactive compounds (*e.g.,* fungicides; Adeleke and Babaloala, 2021). Conducting a comprehensive study on the histopathology of this genus is warranted to understand how and if its lifecycle may compete with *N. gaeumannii.* Knowledge about *Rhizosphaera* is largely derived from studies on *Rhizosphaera kalkhoffii*, which causes a disease highly similar to SNC in spruce. *R. kalkhoffii's* lifecycle shares similarities with *N. gaeumannii*, including favored environmental conditions, infection through stomata of new tissue, and overwintering as an endophyte (Hansen *et al.,* 2018; Brazee, 2015). While the pathogenicity of *R. merioides* remains uncertain, its described lifecycle is comparable to that of *R. kalkhoffii's* (Funk *et al.,* 1985; Butin and Kehr, 2000). *Rhizosphaera* sp.'s remains completely unknown to date. This is a gap that needs to be filled to understand how the species present within our site may interact with and impact *N. gaeumannii.*

Despite the negative correlation between both *Rhizosphaera* species and *N. gaeumannii,* no correlation was observed with disease signs and symptoms such as stomatal occlusion incidence

and needle loss severity (see appendix 3). However, this lack of correlation is not unexpected given the weak and non-significant correlations between *N. gaeumannii* reads and disease signs and symptoms. The role of this genus (and the respective species identified in this study) in foliar health remains uncertain and warrants further study.

In addition to findings associated with *Rhizosphaera,* this study showed that Douglas-fir needles host a highly diverse community of fungal species dominated by Ascomycetes. Despite very high species richness, a small number of fungal taxa comprised the majority of reads associated with the foliar mycobiome. Most of the observed diversity is based on rare species, consistent with a previous mycobiome metagenomic study in Douglas-fir (Gervers *et al.,* 2022). Numerous fungal taxa remain unknown or unresolved to lower taxonomic levels (*i.e.,* genus and species), meaning numerous endophytes remain to be identified, emphasizing the need for better characterization and a more complete reference database(s). This is similarly seen in my culture based data in which numerous cultures could not be identified to lower taxonomic levels, indicating poor resolution of the ITS region alone or a potentially undescribed species. In addition to poor characterization of some fungal OTUs, high abundance of *N. gaeumannii* relative to all other taxa may have obscured the impact of these less abundant taxa, even when employing data transformations (*e.g.,* centered log ratio transformations) to deal with sparse, right-skewed, high-dimensional, compositional data (Pan, 2021). Consequently, when *N. gaeumannii* is not considered, this leaves even the metagenomics dataset quite small and sparse, impacting the statistical power and conclusions that can be drawn based on the many rare taxa I observed.

Ultimately, phenotypes (as defined in my study; page 48) had no significant impact on both alpha and beta diversity of fungal species in the foliar mycobiome of Douglas-fir in this stand. However, significant differences in beta diversity across families indicate that genetics could play

a role in determining specific taxa that constitute the foliar mycobiome. As discussed above, two families in particular, appear to have unique community compositions correlated with two genera, namely the previously discussed *Rhizospheara* and the genus *Exobasidium* (discussed in more detail below).

The degree to which host genotype affects the community composition within the plant mycobiome is an understudied but active area of research. Substantial work has been done to elucidate this interaction in commercially important crops such as cereals (*e.g.,* Sapkota et al., 2015), maize (*e.g.,* Wagner et al., 2020), and in model organisms such as Arabidopsis (*e.g.,* Horton et al., 2014). Research on the root-associated microbiota has identified plant developmental stages, weather events, and host genotypes as driving factors (*e.g.,* Walters et al., 2018). Genotypic differences are speculated to be driven by specific gene loci (Deng *et al.,* 2021). These findings have sparked similar research in trees, where host genotypes also impacted the foliar microbiome (Cordier *et al.,* 2012; Bálint, 2013; Rajala *et al.,* 2013; Bálint, 2014; Cregger *et al.,* 2018; Redondo *et al.,* 2022). Phyllosphere mycobiome research has identified genes associated with immune receptors in hosts thought to control mycobiome community composition (VanWallendael *et al.,* 2022). One study found that genetic distance between trees was a more significant driver of fungal mycobiome community dissimilarity between European beech trees (*Fagus sylvatica*) than the geographic distance between these trees (Cordier *et al.,* 2012). This is consistent with the results of my community analysis, in which no dissimilarity was observed in the mycobiome community assemblage based on location (block) within the plot. However, significant differences were associated with maternal half-sibling families (*i.e.,* genetically similar individuals). Redondo *et al.*'s (2022) more recent study found a similar effect, in which different Norway Spruce clones had

significant dissimilarities in fungal mycobiome assemblage, but more genetically similar clones were more similar.

A major implication for foliar mycobiomes being genetically determined is the possibility of breeding for specific endophytic taxa (Mueller and Linksvayer, 2022). Possible candidates are taxa that act antagonistically to *N. gaeumannii* or other identified beneficial endophytes or consortia that could result in genetic gains within the breeding program. The term Synthetic Communities is used to describe the selection of these beneficial taxa ('SynComs') (Großkopf and Soyer, 2014). SynComs are small consortia of microorganisms designed to mimic the structure and function observed under natural conditions, with the rationale of these communities incorporating desired traits into their host organism (de Souza *et al.,* 2020). For example, identifying natural communities of microbes associated with specific plant stress tolerance (*i.e.,* salt tolerance; Schmitz *et al.,* 2022) could be applied to make plants more adaptable in saline conditions. SynComs have, for the most part, been applied to agricultural crops (Singh and Trivedi, 2017). However, in the context of reforestation practices in BC this may be a suitable option in forestry systems as well. To date, this method has been successfully employed at an industry scale to improve tolerance to spruce budworm (JD Irving, 2017). Inoculations are done with up to five fungal endophytes known to reduce damage caused by spruce budworm, including *Phialocephala scopiformis*. Successful inoculation has been shown to have long-lasting positive effects on the host's fitness against spruce budworm (Calhoun *et al.,* 1992; Frasz *et al.,* 2014; Quiring *et al.,* 2019). In agricultural crops, studies have shown significant differences between microbiomes of commercial genotypes and their relative wildtype genotypes, with wildtype genotypes typically showing more resilience to environmental stresses (Nerva *et al.,* 2022). Acknowledging that crops differ from trees is essential (*i.e.,* faster growth, shorter life span, and more established selective

breeding). Because of this, some trends will likely not translate between these separate groups. However, research in agricultural crops is more extensive than in trees and could help structure future research questions to be addressed in the context of trees.

Given that the coastal Douglas-fir breeding program in British Columbia is the most advanced program in BC, established in the 1950s (BC Ministry of Forests, n.d.), the cultivation and recurrent selection of individuals within this breeding program has likely already caused shifts in the associated mycobiota of these populations (Nerva *et al.,* 2022). While research regarding the foliar mycobiome is lacking, research on rhizosphere soil microbial communities in plantation versus natural stands suggests that microbial co-occurrence networks are more complex and robust in the latter (Nakayama *et al.,* 2019). Given that foliar mycobiomes are shaped in part by the horizontal dispersion of fungi (Mejía *et al.,* 2014) and host genotype is thought to impact foliar microbiomes (Cordier *et al.,* 2012; Cregger *et al.,* 2018; Redondo *et al*., 2022) single-age plantation-style forestry and genetic selection should drive some level of microbiome determination. To address this knowledge gap, comparisons to wild stands and their associated disease responses could elucidate how fungal dynamics may shift between wild and genetically selected individuals and to what benefit or detriment. This study only addressed one cultivated stand of Douglas-fir. There are likely more complex community dynamics to discover at a broader scale. To address the ecological complexity within the Douglas-fir foliar mycobiome for this second half of the discussion, I will describe what is known about some of the differentially abundant and most abundant taxa found within my study site and will discuss if and how they could impact SNC disease severity. Understanding some of these taxa's functional roles could help explain the lack of correlation between SNC disease signs and symptoms. I will also compare my

findings to two previously published studies and discuss how culture-based and metagenomic methods may give different perspectives on these community dynamics.

The genus *Exobasidium* comprises over 170 globally distributed species, many of which are pathogenic, causing various plant diseases such as leaf lesions, leaf and flower galls, and leaf blight. *Exobasidium* is commonly associated with hosts within the Ericaceae, Escalloniaceae, Theaceae, and Symplocaceae (Dong *et al.,* 2019), but there is no published literature indicating Douglas-fir as a host for this genus. However, *Vaccinium parvifolium*, a member of the Ericaceae family, often coexists with Douglas-fir in the Coastal Western hemlock (CWH) BEC zone (Pojar *et al.,* 1991). Although no literature mentions interactions between Douglas-fir and *Exobasidium*, their co-occurrence within the same BEC zone suggests the potential for Douglas-fir to serve as an alternate or intermediary host. *Exobasidium* is known to overwinter on the stems of its known hosts (Wilson and Cline, 2022), indicating an epiphytic phase is part of its life cycle. This behavior aligns with our data, where *Exobasidium* was not found in any culture data (which is limited more to strictly endophytes).

Rhabdocline pseudotsugae, a known pathogen of Douglas-fir needles (Van Vloten, 1932), was the sixth most abundant OTU (1.94% of normalized reads). It was not found consistently across trees but dominated one sample, tree 2718, and was a large component in another (tree 964, fig. 12). This high incidence in a low number of samples coincided with higher than average needle loss for this age class of needles (2718 and 964 respective needle loss scores of 9 and 4 in 2-year-old needles, mean = 1.83; fig.4) and likely explains why 2-year-old needle loss measured in 2021 was the only variable that correlated with community composition (fig.16). While I did not notice a high incidence of *Rhabdocline* needle cast disease signs, which morphologically is very distinct

from *N. gaeumannii* infection (Van Vloten, 1932), it does appear to be present at this site, potentially influencing the variance observed in needle loss at this site.

Among the most abundant OTUs were numerous taxa described to the order Chaetothyriales (OTU4 = 3.6% reads, OTU17 = 1.04%, OUT19 = 0.91% of normalized reads), which is recognized for containing black yeasts and filamentous relatives, some known for causing infections in humans. Species-level resolution for this order is sparse, with many species likely undescribed (Quan *et al.,* 2020).

Zasmidium sp. (represented by one OTU not identified to the species level) constituted 3.2% of the reads from the metagenomic dataset. Belonging to the order Capnodiales and within the same family as *N. gaeumannii* (Dothideomycetes), the genus comprises approximately 150 different species (Wijayawardene *et al.,* 2020). Although the closest match within NCBI to the OTU found in this study was *Zasmidium commune* (KY979763.1) with a 97.9% percent identity, the OTU is more likely to be *Zasmidium pseudotsugae*. *Z. pseudotsugae* is known to associate with Douglas-fir foliage (González-Montiel *et al.,* 2020) and has been identified in another metagenomic study of the Douglas-fir foliar mycobiome; Gervers *et al.,* 2022). While *Zasmidium*, in the context of my study, did not exhibit significant correlations with differences in community compositions or *N. gaeumannii* reads, its significance lies in recent research on the secondary metabolites it produces (González-Montiel *et al.,* 2020). These secondary metabolites include Perylenequinone small molecules, which are thought to influence the virulence of plant pathogens on their hosts by absorbing light energy and creating reactive oxygen species, resulting in necrosis (Chooi *et al.,* 2017; Hu *et al.,* 2018). While in cases harmful to their hosts, the production of these bioactive compounds can also play important roles in resilience to biotic and abiotic stressors (Omomowo *et al.,* 2023).

Among the frequent taxa described through metagenomics (appendix 5, table 1) was *Niesslia endophytica*, a suspected mycoparasitic species (fungi that parasitize other fungi; Jefferies, 1995). *N. endophytica* is an endophyte recently isolated and described from *Picea mariana* and *P. glauca*. *N. endophytica* and others within this genus produce resorcyclic acid lactones, products recognized as being antifungal (Ayer *et al.,* 1980; Ayer and Penarodriguez 1987; Tanney *et al.,* 2023). The exact role of *N. endophytica* is unknown, but other microparasitic species within this genus that also produce resorcyclic acid suggest that *N. enophytica* may play a similar role (Tanney *et al.,* 2023). From culture, numerous taxa belonging to the family Mollisiaceae, known to produce secondary metabolites that inhibit pests and pathogens, were identified (Tanney and Seifert, 2020). Among these cultures, one had a suspected taxonomic affinity to *P. scopiformis,* as discussed earlier, which confers resistance to eastern spruce budworm in spruce by the production of a bio-active pigment called rugulosin (Quiring *et al.,* 2019)

Other frequent endophytes included taxa previously identified as members of the Douglas-fir foliar mycobiome in previous studies, such as *Xylaria hypoxylon*, known for its antimicrobial properties (Canli *et al.,* 2016; Daniels *et al.,* 2018); *Penicillium*, a genus recognized for its potential as a biocontrol agent against phytopathogens (Daniels *et al.,* 2018; Toghueo and Boyom *et al.,* 2020; Gervers *et al.,* 2022); and *Diaporthe*, a diverse genus with members reported as plant endophytes, pathogens, and saprobes (Gomes *et al.,* 2013; Daniels *et al.,* 2018; Gervers *et al.,* 2022). These commonalities suggest consistent relationships between Douglas-fir and these species and genera across geographical scales, with some potentially aiding the plant in defending against pathogens and others potentially behaving as pathogens themselves.

The most abundant endophyte observed in the culture based approach (apart from *N. gaeumannii)* was the endophyte *Rhabdocline parkeri.* Like *N. gaeumannii, R. parkeri* is a species

that is ubiquitous in Douglas-fir (Sherwood-Pike *et al.,* 1986). Unlike the common pathogen *R. pseudotsugae* mentioned earlier, *R. parkeri* occurs as a localized non-pathogenic endophyte on dying or dead needles and prefers the lower, shaded canopy (Sherwood-Pike *et al.,* 1986; Gervers *et al.,* 2022). *R. parkeri* infects single epidermal cells and remains latent until the onset of leaf senescence (Sherwood-Pike *et al.,* 1986). While abundant among the cultured endophytes, *R. parkeri* was found in relatively low abundance within the metagenomic data (OTU41 = 0.21% of normalized reads; appendix 5, table 1). Only a few representative strains were sequenced from culture for this species, but morphology based groupings indicated a very high incidence at our study site. *R. parkeri* infects epidermal cells, and infection by *R. parkeri* increases with needle age (Stone, 1987). However, despite a high incidence, the percentage of infected epidermal cells remains very low, never exceeding 5% in any age class of needles in that study. While my first thought was that the low incidence in the metagenomic data was due to inherent sequencing biases, it could be that the high incidence, but low abundance lifestyle of *R. parkeri* is what makes this species highly abundant in cultures but rare within our metagenomics dataset. *R. parkeri* stops growing once it has infected one of the epidermal cells and does not continue growing again until leaf senescence (Stone, 1987). Since the metagenomic data originates from 2-year-old live needles, where the incidence of *R. parkeri* is likely lower (as it has not yet resumed growth), there will be significantly less genetic material available for amplification. In comparison, *R. parkeri* was prolific in my cultures. I speculate this results from its preferred life history to exploit resources and proliferate when given the opportunity (as seen during post senescence; Stone, 1987). This leads me to my last point of discussion on how these two different but complementary methods (culture-based and metagenomic) can give us very different results and interpretations of community dynamics.

In traditional fungal taxonomy, culture-based methods are crucial for linking sexual and asexual forms, identifying synanamorphs, and discovering bioactive secondary metabolites. However, these methods have limitations, especially in understanding community dynamics, as some taxa remain unculturable (the so-called 'dark taxa') (Wijayawardene *et al.,* 2021). Culture-independent or metagenomic approaches reveal these taxa, but the trade-off is that classification can be difficult without morphology and based on partial ITS sequence data alone. In addition, follow-up experimental work with identified taxa of interest is not possible for metagenomic work. An example of the discrepancy between these two methods can be seen when looking at *R. parkeri.* My culture-based studies showed high *R. parkeri* levels, likely due to its high incidence (despite overall low abundance), faster growth, and better utilization of the MEA media. Analyzing only culture-based data might have suggested communities dominated by *N. gaeumannii* and *R. parkeri* while acknowledging metagenomic data reveals a dramatically different community structure with lower *R. parkeri* prevalence. While it has become increasingly common to use these techniques as compliments to each other (Schmertmann *et al.,* 2019; Shivaji *et al.,* 2022), metagenomic methods were most suitable for examining community structure dynamics in my research due to their ability to provide a more comprehensive and quantitative representation of fungal diversity (National Research Council (US) Committee on Metagenomics: Challenges and Functional Applications, 2007). Although my primary focus was on metagenomic methods for data analysis, cultures were still cultivated and maintained to offer better species-level resolution when necessary, as observed with *Rhizosphaera*. In addition, they served both as a general point of comparison and a tangible record of the culturable fungal species present, providing an accessible 'hard copy' version for any potential future work.

While metagenomics (culture-independent technique) was chosen preferentially for the large amount of data it produces, it is essential to understand that these culture-independent approaches do come with their challenges. With numerous steps in this process, from collecting the sample, sample storage, sample prep, DNA extractions, amplification, and sequencing of target gene regions, to subsequent data quality control and normalization, there are many places where errors or biases can be introduced into this workflow (Bharti and Grimm, 2021). In addition, with the onslaught of ways and still evolving gold standards to analyze the mass amounts of data that this method produces, accurate interpretations and meaningful comparisons between studies become difficult (Nearing *et al.,* 2022). The selection of primers also has implications, particularly when trying to compare studies. While ITS is the standard barcode region to study fungal diversity (Roe *et al.,* 2010; Dentinger *et al.,* 2011; Schoch *et al.,* 2012), Illumina sequencing only allows for sequencing of either the ITS1 or the ITS2 region due to sequencing length constraints. The choice of locus introduces biases into the data as some taxa are known to be detected exclusively by sequencing of either the ITS1 or ITS2 region (Mbareche *et al.,* 2020). Future work should include additional loci to ensure that the complete fungal diversity is being captured. Ultimately, while both methods introduce their own biases (Wijayawardene et al., 2021), and while metagenomics has more moving parts that could introduce error, it also has the most potential to yield more meaningful results in the context of community composition. This trade-off has been consistently observed in the literature as e-DNA and -omic microbiome studies become increasingly abundant.

Summary

Here, my investigation examined the influence of foliar mycobiome community composition on Swiss Needle Cast (SNC) symptom severity within a Douglas-fir breeding population, specifically a population lacking clear correlations between disease signs and

symptoms. Metagenomic analysis of the ITS rRNA region, supplemented by traditional culturing, revealed a highly diverse fungal community dominated by Ascomycetes in Douglas-fir needles, with *N. gaeumannii* being the most abundant fungus followed by species within the genus *Rhizosphaera.* While disease phenotypes were not significantly influenced by fungal diversity, an inverse correlation between *Rhizosphaera* and *N. gaeumannii* suggested a potential competitive relationship. My study also highlighted host genetic influences on mycobiome composition, with specific families exhibiting unique compositions correlated with particular genera. The findings underscore the potential for genetic manipulation of the mycobiome to enhance disease resistance in breeding programs. Additionally, comparisons between culture-based and metagenomic methods revealed complementary insights into community dynamics, emphasizing the importance of employing both approaches for comprehensive analysis despite inherent biases and challenges associated with each method. Next steps should include further characterization of the Douglas-fir foliar mycobiome across a broader geographical scale, representing healthy, epidemic, and endemic levels of SNC infection and between natural and cultivated stands. Coordination in methods across studies and research groups will be essential to ensure that data is comparable. In addition, a better understanding of *Rhizosphaera* and the role of this genus in the Douglas-fir foliar mycobiome is necessary, as it appears to be a commonly occurring genus that may suppress *N. gaeumannii.* The frequent occurrence of *Rhizosphaera* within specific families and the dissimilarity in community composition linked to these families prompts inquiry into the underlying factors driving this pattern. A future study that looks at the seed mycobiome or different field sites with the same families of trees present could elucidate whether family differences in mycobiota are driven by horizontal or vertical transmission. Regarding the mass of data and fungi I have collected and cultivated, additional work on identifying the fungi in this culture collection

is necessary. Basic morphological groupings overlook diversity, as was displayed in my data. Additional sequencing will be required to identify the fungal diversity within that dataset as well as the identification of fungal taxa that could not be described to species.

General Conclusion

The degree of stomatal occlusion caused by *N. gaeumannii* infection is heritable and comparable to known Douglas-fir growth and wood yield traits (Yeh and Heaman, 1987; Vargas-Hernandez and Adams, 1991; St. Clair, 1994; Ukrainetz *et al.,* 2008). While not intuitive, it may be the trait of choice to breed for when it comes to selecting Douglas-fir for stands experiencing an endemic level of infection. This has implications for our current breeding program in BC as this is not a trait that is currently selected for. Further studies at other endemic and epidemic levels are needed to confirm and complement my interpretations and speculations. Assessing heritability and correlation of SNC signs and symptoms at epidemic level sites could provide important insight into how my findings shift under increased disease levels.

In terms of the foliar mycobiome, my study suggests that genetics drives community composition, at least in part. The role of genetics in microbiome community assemblage is recognized within the literature (Cordier *et al.,* 2012; Bálint, 2013; Rajala *et al.,* 2013; Bálint, 2014; Cregger *et al.,* 2018; Redondo *et al.,* 2022); suggesting that the findings of this thesis are plausible. The extent of genetic determination of the foliar mycobiome requires further study, particularly regarding how recurrent selection of Douglas-fir within breeding populations may affect or has already affected these communities. The genus *Rhizosphaera* warrants specific attention due to its negative correlation with *N. gaeumannii* and its association with specific families. This association with specific families may indicate vertical transmission of this endophyte or genetic-based preferential selection of this genus as a horizontally transmitted endophyte. Future studies on seed-associated mycobiota (Bergmann and Busby, 2021), which could be collected from this study site, could help elucidate this.

Community composition difference, based heavily on the relative abundance of present taxa, did not explain different levels of SNC disease signs and symptoms. However, this could result from overabundant taxa overwhelming the effect of rare taxa. The presence of specific genera and species that exhibit pathogenic life strategies or are known to produce beneficial bioactive compounds (*i.e.,* fungicides) within this population hints at effects that could not be derived from abundance-based analyses of this dataset. Larger sample sizes and additional analysis strategies, such as more targeted association network analyses, could help disentangle the role of these rare but interesting taxa. Continued use of culture-based methods and incorporating additional media types could expand the culture collection that we currently have to include less-competitive, more substrate-specific taxa. This, alongside metagenomics, is necessary as this research expands to allow for species-level identification and future work that may require viable cultures of these fungal taxa (*e.g.,* bio-assays, metabolomics, and controlled inoculation studies).

In conclusion, this thesis has contributed to our knowledge of Swiss Needle Cast dynamics in BC in the context of novel microbiome research. I hope this research continues and can build upon our knowledge of these microbial communities, which play essential roles in the health of our forests. Ultimately, the goal is to consider microbiome health when breeding for or managing healthy and productive forests.

References

Abarenkov, K., Zirk, A., Piirmann, T., Pöhönen, R., Ivanov, F., Nilsson, R. H., & Kõljalg, U. (2023). *UNITE general FASTA release for Fungi* [Application/gzip]. UNITE Community. https://doi.org/10.15156/BIO/2938067

Adeleke, B. S., & Babalola, O. O. (2021). Pharmacological potential of fungal endophytes associated with medicinal plants: A review. *Journal of Fungi*, *7*(2), 147. https://doi.org/10.3390/jof7020147

Aghai, M. M., Khan, Z., Joseph, M. R., Stoda, A. M., Sher, A. W., Ettl, G. J., & Doty, S. L. (2019). The effect of microbial endophyte consortia on *pseudotsuga menziesii* and *thuja plicata* survival, growth, and physiology across edaphic gradients. *Frontiers in Microbiology*, *10*, 1353. https://doi.org/10.3389/fmicb.2019.01353

Ahmad, I., Jiménez-Gasco, M. D. M., Luthe, D. S., & Barbercheck, M. E. (2022). Endophytic *Metarhizium robertsii* suppresses the phytopathogen, *Cochliobolus heterostrophus* and modulates maize defenses. *PLOS ONE*, *17*(9), e0272944. https://doi.org/10.1371/journal.pone.0272944

Aitchison, J. (1982). The statistical analysis of compositional data. *Journal of the Royal Statistical Society: Series B (Methodological)*, *44*(2), 139–160. https://doi.org/10.1111/j.2517-6161.1982.tb01195.x

Alcaraz, L. D., Peimbert, M., Barajas, H. R., Dorantes-Acosta, A. E., Bowman, J. L., & Arteaga-Vázquez, M. A. (2017). *Marchantia* liverworts as a proxy to plants' basal microbiomes. *Scientific Reports*, *8*(1), Article 1. https://doi.org/10.1038/s41598-018-31168-0

Anderson, M. J. (2001). A new method for non-parametric multivariate analysis of variance. *Austral Ecology*, *26*(1), 32–46. https://doi.org/10.1111/j.1442-9993.2001.01070.pp.x

Anderson, M. J., Ellingsen, K. E., & McArdle, B. H. (2006). Multivariate dispersion as a measure of beta diversity. *Ecology Letters*, *9*(6), 683–693. https://doi.org/10.1111/j.1461-0248.2006.00926.x

Anderson, P. K., Cunningham, A. A., Patel, N. G., Morales, F. J., Epstein, P. R., & Daszak, P. (2004). Emerging infectious diseases of plants: Pathogen pollution, climate change and agrotechnology drivers. *Trends in Ecology & Evolution*, *19*(10), 535–544. https://doi.org/10.1016/j.tree.2004.07.021

Ayer, W. A., Lee, S. P., Tsuneda, A., & Hiratsuka, Y. (1980). The isolation, identification, and bioassay of the antifungal metabolites produced by *Monocillium nordinii*. *Canadian Journal of Microbiology*, *26*(7), 766–773. https://doi.org/10.1139/m80-133

Ayer, W. A., & Penarodriguez, L. (1987). Minor metabolites of *Monicillium nordinii. Phytochemistry, 26*(5), 1353–1355. https://doi.org/10.1016/S0031-9422(00)81811-7

Bakker, J. D. (2024). *PERMANOVA*. https://uw.pressbooks.pub/appliedmultivariatestatistics/chapter/permanova/

Bálint, M., Bartha, L., O'Hara, R. B., Olson, M. S., Otte, J., Pfenninger, M., Robertson, A. L., Tiffin, P., & Schmitt, I. (2014). Relocation, high-latitude warming and host genetic identity shape the foliar fungal microbiome of poplars. *Molecular Ecology*, *24*(1), 235–248. https://doi.org/10.1111/mec.13018

Bálint, M., Tiffin, P., Hallström, B., O'Hara, R. B., Olson, M. S., Fankhauser, J. D., Piepenbring, M., & Schmitt, I. (2013). Host genotype shapes the foliar fungal microbiome of Balsam Poplar (*Populus balsamifera*). *PLOS ONE*, *8*(1), e53987. https://doi.org/10.1371/journal.pone.0053987

Barry, C.-J. S., Walker, V. M., Cheesman, R., Davey Smith, G., Morris, T. T., & Davies, N. M. (2022). How to estimate heritability: A guide for genetic epidemiologists. *International Journal of Epidemiology*, *52*(2), 624–632. https://doi.org/10.1093/ije/dyac224

BC Ministry of Forests. (n.d.). *Tree breeding and improvement—Province of British Columbia*. Province of British Columbia. Retrieved February 7, 2024, from https://www2.gov.bc.ca/gov/content/industry/forestry/managing-our-forest-resources/tree-seed/forest-genetics/tree-breeding-improvement

BC Ministry of Forests. (2021). *2021 Economic State of British Columbia's Forest Sector*.

Ben Hassine Ben Ali, M., & Kluthe, B. (2016). Reliable protocols for DNA extraction from freeze-dried macrofungal samples used in molecular macrofungal systematics studies. *Current Research in Environmental & Applied Mycology*, *6*(1), 45–50. https://doi.org/10.5943/cream/6/1/5

Benjamini, Y., & Hochberg, Y. (1995). Controlling the false discovery rate: A practical and powerful approach to multiple testing. *Journal of the Royal Statistical Society: Series B (Methodological)*, *57*(1), 289–300. https://doi.org/10.1111/j.2517-6161.1995.tb02031.x

Bergmann, G. E., & Busby, P. E. (2021). The core seed mycobiome of *Pseudotsuga menziesii* var. *Menziesii* across provenances of the Pacific Northwest, USA. *Mycologia*, 1–12. https://doi.org/10.1080/00275514.2021.1952830

Bernstein, M. E., & Carroll, G. C. (1977). Internal fungi in old-growth Douglas-fir foliage. *Canadian Journal of Botany*, *55*(6), 644–653. https://doi.org/10.1139/b77-079

Bharti, R., & Grimm, D. G. (2021). Current challenges and best-practice protocols for microbiome analysis. *Briefings in Bioinformatics*, *22*(1), 178–193. https://doi.org/10.1093/bib/bbz155

Bolyen, E., Rideout, J. R., Dillon, M. R., Bokulich, N. A., Abnet, C. C., Al-Ghalith, G. A., Alexander, H., Alm, E. J., Arumugam, M., Asnicar, F., Bai, Y., Bisanz, J. E., Bittinger, K., Brejnrod, A., Brislawn, C. J., Brown, C. T., Callahan, B. J., Caraballo-Rodríguez, A. M., Chase, J., … Caporaso, J. G. (2019). Reproducible, interactive, scalable and extensible microbiome data science using QIIME 2. *Nature Biotechnology*, *37*(8), 852–857. https://doi.org/10.1038/s41587-019-0209-9

Boyce, J. S. (1940). *A needle-cast of Douglas-fir associated with Adelopus gaeumannii*. *30*, 649–659.

Bray, J. R., & Curtis, J. T. (1957). An ordination of the upland forest communities of Southern Wisconsin. *Ecological Monographs*, *27*(4), 325–349. https://doi.org/10.2307/1942268

Brazee, N. (2015). *Rhizosphaera Needle Cast* [Text]. Center for Agriculture, Food, and the Environment. https://ag.umass.edu/landscape/fact-sheets/rhizosphaera-needle-cast

Bufford, J. L., Hulme, P. E., Sikes, B. A., Cooper, J. A., Johnston, P. R., & Duncan, R. P. (2020). Novel interactions between alien pathogens and native plants increase plant–pathogen network connectance and decrease specialization. *Journal of Ecology*, *108*(2), 750–760. https://doi.org/10.1111/1365-2745.13293

Bulgarelli, D., Garrido-Oter, R., Münch, P. C., Weiman, A., Dröge, J., Pan, Y., McHardy, A. C., & Schulze-Lefert, P. (2015). Structure and function of the bacterial root microbiota in wild and domesticated barley. *Cell Host & Microbe*, *17*(3), 392–403. https://doi.org/10.1016/j.chom.2015.01.011

Butin, H., & Kehr, R. (2000). *Rhizosphaera pseudotsugae* sp. Nov. And related species. *Mycological Research*, *104*(8), 1012–1016. https://doi.org/10.1017/S0953756299002415

Butler, D. G., Cullis, B. R., Gilmour, A. R., Gogel, B. J., & Thompson, R. (2023). *ASReml estimates variance components under a general linear*.

Calhoun, L. A., Findlay, J. A., David Miller, J., & Whitney, N. J. (1992). Metabolites toxic to spruce budworm from balsam fir needle endophytes. *Mycological Research*, *96*(4), 281–286. https://doi.org/10.1016/S0953-7562(09)80939-8

Callahan, B. J., McMurdie, P. J., Rosen, M. J., Han, A. W., Johnson, A. J. A., & Holmes, S. P. (2016). DADA2: High-resolution sample inference from Illumina amplicon data. *Nature Methods*, *13*(7), Article 7. https://doi.org/10.1038/nmeth.3869

Cameron, E. S., Schmidt, P. J., Tremblay, B. J.-M., Emelko, M. B., & Müller, K. M. (2021). Enhancing diversity analysis by repeatedly rarefying next generation sequencing data describing microbial communities. *Scientific Reports*, *11*(1), Article 1. https://doi.org/10.1038/s41598-021-01636-1

Canli, K., Akata, I., & Altuner, E. M. (2016). In vitro antimicrobial activity screening of *Xylaria hypoxylon*. *African Journal of Traditional, Complementary, and Alternative Medicines*, *13*(4), 42–46. https://doi.org/10.21010/ajtcam.v13i4.7

Cannell, M. G. R., & Morgan, J. (1990). Theoretical study of variables affecting the export of assimilates from branches of *Picea*. *Tree Physiology*, *6*(3), 257–266. https://doi.org/10.1093/treephys/6.3.257

Cappa, E. P., & Stoehr, M. U. (2016). A combined analysis in complementary progeny tests: Effects on breeding value accuracies. *Silvae Genetica*, *65*(1), 38–48. https://doi.org/10.1515/sg-2016-0005

Carroll, G. C., & Carroll, F. E. (1978). Studies on the incidence of coniferous needle endophytes in the Pacific Northwest. *Canadian Journal of Botany*, *56*(24), 3034–3043. https://doi.org/10.1139/b78-367

Chooi, Y.-H., Zhang, G., Hu, J., Muria-Gonzalez, M. J., Tran, P. N., Pettitt, A., Maier, A. G., Barrow, R. A., & Solomon, P. S. (2017). Functional genomics-guided discovery of a light-activated phytotoxin in the wheat pathogen *Parastagonospora nodorum* via pathway activation. *Environmental Microbiology*, *19*(5), 1975–1986. https://doi.org/10.1111/1462-2920.13711

Christian, N., Whitaker, B. K., & Clay, K. (2017). Chapter 5 a novel framework for decoding fungal endophyte diversity. In J. Dighton & J. F. White (Eds.), *Mycology* (pp. 63–78). CRC Press. https://doi.org/10.1201/9781315119496-6

Cordier, T., Robin, C., Capdevielle, X., Desprez-Loustau, M.-L., & Vacher, C. (2012). Spatial variability of phyllosphere fungal assemblages: Genetic distance predominates over geographic distance in a European beech stand (*Fagus sylvatica*). *Fungal Ecology*, *5*(5), 509–520. https://doi.org/10.1016/j.funeco.2011.12.004

Cregger, M. A., Veach, A. M., Yang, Z. K., Crouch, M. J., Vilgalys, R., Tuskan, G. A., & Schadt, C. W. (2018). The *Populus* holobiont: Dissecting the effects of plant niches and genotype on the microbiome. *Microbiome*, *6*(1), Article 1. https://doi.org/10.1186/s40168-018-0413-8

Daniels, H., Cappellazzi, J., & Kiser, J. (2018). Microbiome diversity of endophytic fungi across latitudinal gradients in west coast Douglas-Fir (*Pseudotsuga menziesii*) Foliage. *Journal of Biodiversity Management & Forestry*, *07*(04). https://doi.org/10.4172/2327-4417.1000203

Davis, E. C., & Shaw, A. J. (2008). Biogeographic and phylogenetic patterns in diversity of liverwort-associated endophytes. *American Journal of Botany*, *95*(8), 914–924. https://doi.org/10.3732/ajb.2006463

de la Bastide, P. Y., LeBlanc, J., Kong, L., Finston, T., May, E. M., Reich, R., Hintz, W. E., & von Aderkas, P. (2019). Fungal colonizers and seed loss in lodgepole pine orchards of British Columbia. *Botany*, *97*(1), 23–33. https://doi.org/10.1139/cjb-2018-0153

de Souza, R. S. C., Armanhi, J. S. L., & Arruda, P. (2020). From microbiome to traits: Designing synthetic microbial communities for improved crop resiliency. *Frontiers in Plant Science*, *11*. https://www.frontiersin.org/articles/10.3389/fpls.2020.01179

de Souza, R. S. C., Okura, V. K., Armanhi, J. S. L., Jorrín, B., Lozano, N., da Silva, M. J., González-Guerrero, M., de Araújo, L. M., Verza, N. C., Bagheri, H. C., Imperial, J., & Arruda, P. (2016). Unlocking the bacterial and fungal communities assemblages of sugarcane microbiome. *Scientific Reports*, *6*(1), Article 1. https://doi.org/10.1038/srep28774

Delaye, L., García-Guzmán, G., & Heil, M. (2013). Endophytes versus biotrophic and necrotrophic pathogens—Are fungal lifestyles evolutionarily stable traits? *Fungal Diversity*, *60*(1), 125–135. https://doi.org/10.1007/s13225-013-0240-y

Deng, S., Caddell, D. F., Xu, G., Dahlen, L., Washington, L., Yang, J., & Coleman-Derr, D. (2021). Genome wide association study reveals plant loci controlling heritability of the rhizosphere microbiome. *The ISME Journal*, *15*(11), 3181–3194. https://doi.org/10.1038/s41396-021-00993-z

Dentinger, B. T. M., Didukh, M. Y., & Moncalvo, J.-M. (2011). Comparing COI and ITS as DNA barcode markers for mushrooms and allies (Agaricomycotina). *PLoS ONE*, *6*(9), e25081. https://doi.org/10.1371/journal.pone.0025081

Dereeper, A., Guignon, V., Blanc, G., Audic, S., Buffet, S., Chevenet, F., Dufayard, J. F., Guindon, S., Lefort, V., Lescot, M., Claverie, J. M., & Gascuel, O. (2008). *Phylogeny.fr: Robust phylogenetic analysis for the non-specialist* (Nucleic Acids Res) [Computer software].

Doll, S. (2022). *The story of Coastal Douglas-fir forests: Places that have been millennia in the making*. Raincoast. https://www.raincoast.org/2022/04/the-story-of-coastal-douglas-fir-forests-places-that-have-been-millennia-in-the-making/

Dong, Z., Liu, W., Zhou, D., Li, P., Wang, T., Sun, K., Zhao, Y., Wang, J., Wang, B., & Chen, Y. (2019). Bioactive exopolysaccharides reveal *Camellia oleifera* infected by the fungus *Exobasidium gracile* could have a functional use. *Molecules*, *24*(11), Article 11. https://doi.org/10.3390/molecules24112048

dos Reis, J. B. A., Lorenzi, A. S., & do Vale, H. M. M. (2022). Methods used for the study of endophytic fungi: A review on methodologies and challenges, and associated tips. *Archives of Microbiology*, *204*(11), 675. https://doi.org/10.1007/s00203-022-03283-0

Faticov, M., Abdelfattah, A., Hambäck, P., Roslin, T., & Tack, A. J. M. (2023). Different spatial structure of plant-associated fungal communities above- and belowground. *Ecology and Evolution*, *13*(5), e10065. https://doi.org/10.1002/ece3.10065

Fox, J., & Weisberg, S. (2019). *R Companion to Applied Regression* (Third edition) [Computer software]. https://socialsciences.mcmaster.ca/jfox/Books/Companion/.

Frasz, S. L., Walker, A. K., Nsiama, T. K., Adams, G. W., & Miller, J. D. (2014). Distribution of the foliar fungal endophyte *Phialocephala scopiformis* and its toxin in the crown of a mature white spruce tree as revealed by chemical and qPCR analyses. *Canadian Journal of Forest Research*, *44*(9), 1138–1143. https://doi.org/10.1139/cjfr-2014-0171

Frøslev, T. G., Kjøller, R., Bruun, H. H., Ejrnæs, R., Brunbjerg, A. K., Pietroni, C., & Hansen, A. J. (2017). Algorithm for post-clustering curation of DNA amplicon data yields reliable biodiversity estimates. *Nature Communications*, *8*(1), 1188. https://doi.org/10.1038/s41467-017-01312-x

Funk, A., Woods, T. A. D., & Hopkinson, S. J. (1985). *Hormonema merioides* n.sp., on Douglas-fir needles. *Canadian Journal of Botany*, *63*(9), 1579–1581. https://doi.org/10.1139/b85-219

Gakuubi, M. M., Munusamy, M., Liang, Z.-X., & Ng, S. B. (2021). Fungal endophytes: A promising frontier for discovery of novel bioactive compounds. *Journal of Fungi*, *7*(10), 786. https://doi.org/10.3390/jof7100786

Ganley, R. J., Sniezko, R. A., & Newcombe, G. (2008). Endophyte-mediated resistance against white pine blister rust in *Pinus monticola*. *Forest Ecology and Management*, *255*(7), 2751–2760. https://doi.org/10.1016/j.foreco.2008.01.052

Gardes, M., & Bruns, T. D. (1993). ITS primers with enhanced specificity for basidiomycetes—Application to the identification of mycorrhizae and rusts. *Molecular Ecology*, *2*(2), 113–118. https://doi.org/10.1111/j.1365-294x.1993.tb00005.x

Gerrits van den Ende, B., & Hoog, S. (1999). Variability and molecular diagnostics of the neurotropic species *Cladophialophora bantiana*. *Studies in Mycology*, *1999*, 151–162.

Gervers, K. A., Thomas, D. C., Roy, B. A., Spatafora, J. W., & Busby, P. E. (2022). Crown closure affects endophytic leaf mycobiome compositional dynamics over time in *Pseudotsuga menziesii* var. *Menziesii*. *Fungal Ecology*, *57–58*, 101155. https://doi.org/10.1016/j.funeco.2022.101155

Ghelardini, L., Pepori, A. L., Luchi, N., Capretti, P., & Santini, A. (2016). Drivers of emerging fungal diseases of forest trees. *Forest Ecology and Management*, *381*, 235–246. https://doi.org/10.1016/j.foreco.2016.09.032

Gloor, G. B., Macklaim, J. M., Pawlowsky-Glahn, V., & Egozcue, J. J. (2017). Microbiome datasets are compositional: And this is not optional. *Frontiers in Microbiology*, *8*. https://www.frontiersin.org/articles/10.3389/fmicb.2017.02224

Gomes, R. R., Glienke, C., Videira, S. I. R., Lombard, L., Groenewald, J. Z., & Crous, P. W. (2013). *Diaporthe:* A genus of endophytic, saprobic and plant pathogenic fungi. *Persoonia : Molecular Phylogeny and Evolution of Fungi*, *31*, 1–41. https://doi.org/10.3767/003158513X666844

González-Montiel, G. A., Kaweesa, E. N., Feau, N., Hamelin, R. C., Stone, J. K., & Loesgen, S. (2020). Chemical, bioactivity, and biosynthetic screening of epiphytic fungus *Zasmidium pseudotsugae. Molecules*, *25*(10), 2358. https://doi.org/10.3390/molecules25102358

Government of BC. (n.d.). *Ministry of Forests, Lands and Natural Resource Operations—Province of British Columbia*. Retrieved January 19, 2024, from https://www.for.gov.bc.ca/hfd/library/documents/treebook/douglasfir.htm

Grabka, R., d'Entremont, T. W., Adams, S. J., Walker, A. K., Tanney, J. B., Abbasi, P. A., & Ali, S. (2022). Fungal endophytes and their role in agricultural plant protection against pests and pathogens. *Plants*, *11*(3), Article 3. https://doi.org/10.3390/plants11030384

Gross, A., Holdenrieder, O., Pautasso, M., Queloz, V., & Sieber, T. N. (2014). *Hymenoscyphus pseudoalbidus* the causal agent of European ash dieback. *Molecular Plant Pathology*, *15*(1), 5–21. https://doi.org/10.1111/mpp.12073

Großkopf, T., & Soyer, O. S. (2014). Synthetic microbial communities. *Current Opinion in Microbiology*, *18*, 72–77. https://doi.org/10.1016/j.mib.2014.02.002

Gruner, K., Esser, T., Acevedo-Garcia, J., Freh, M., Habig, M., Strugala, R., Stukenbrock, E., Schaffrath, U., & Panstruga, R. (2020). Evidence for allele-specific levels of enhanced susceptibility of wheat mlo mutants to the hemibiotrophic fungal pathogen *magnaporthe oryzae* pv. *triticum*. *Genes*, *11*(5), 517. https://doi.org/10.3390/genes11050517

Hansen, E. M., Lewis, K. J., & Chastagner, G. A. (2018). PART III: Diseases of conifers grown as christmas trees. In *Compendium of Conifer Diseases, Second Edition* (pp. 158–162). The American Phytopathological Society. https://doi.org/10.1094/9780890545980.004

Hansen, E. M., Stone, J. K., Capitano, B. R., Rosso, P., Sutton, W., Winton, L., Kanaskie, A., & McWilliams, M. G. (2000). Incidence and impact of Swiss Needle Cast in forest plantations of Douglas-fir in Coastal Oregon. *Plant Disease*, *84*(7), 773–778. https://doi.org/10.1094/PDIS.2000.84.7.773

Henderson, C. (1984). *Applications of linear models in animal breeding*. University of Guelph Press.

Hermann, R. K., & Lavender, D. P. (1999). Douglas-fir planted forests. *New Forests*, *17*(1/3), 53–70. https://doi.org/10.1023/A:1006581028080

Hodgson, S., Cates, C., Hodgson, J., Morley, N. J., Sutton, B. C., & Gange, A. C. (2014). Vertical transmission of fungal endophytes is widespread in forbs. *Ecology and Evolution*, *4*(8), 1199–1208. https://doi.org/10.1002/ece3.953

Hoffmann, W. A., & Poorter, H. (2002). Avoiding bias in calculations of relative growth rate. *Annals of Botany*, *90*(1), 37–42. https://doi.org/10.1093/aob/mcf140

Hood, I. A. (1982). *Phaeocryptopus gaeumannii on pseudotsuga menziesii in southern british columbia*. *12*(3), 415–424.

Horton, M. W., Bodenhausen, N., Beilsmith, K., Meng, D., Muegge, B. D., Subramanian, S., Vetter, M. M., Vilhjálmsson, B. J., Nordborg, M., Gordon, J. I., & Bergelson, J. (2014). Genome-wide association study of *Arabidopsis thaliana* leaf microbial community. *Nature Communications*, *5*(1), Article 1. https://doi.org/10.1038/ncomms6320

Hu, J., Sarrami, F., Li, H., Zhang, G., Stubbs, K. A., Lacey, E., Stewart, S. G., Karton, A., Piggott, A. M., & Chooi, Y.-H. (2018). Heterologous biosynthesis of elsinochrome A sheds light on the formation of the photosensitive perylenequinone system. *Chemical Science*, *10*(5), 1457–1465. https://doi.org/10.1039/C8SC02870B

Huang, Y.-L. (2020). Effect of host, environment and fungal growth on fungal leaf endophyte communities in Taiwan. *Journal of Fungi*, *6*(4). https://doi.org/10.3390/jof6040244

James, T. Y., Stajich, J. E., Hittinger, C. T., & Rokas, A. (2020). Toward a fully resolved fungal tree of life. *Annual Review of Microbiology*, *74*(1), 291–313. https://doi.org/10.1146/annurev-micro-022020-051835

JD Irving. (2017). *Healthier trees grown faster*. Irvingwoodlands.Com. https://www.irvingwoodlands.com/uploadedFiles/Research/37553.pdf

Jeffries, P. (1995). Biology and ecology of mycoparasitism. *Canadian Journal of Botany*, *73*(S1), 1284–1290. https://doi.org/10.1139/b95-389

Johnson, G. R. (2002). Genetic Variation in Tolerance of Douglas-fir to Swiss Needle Cast as Assessed by Symptom Expression. *Silvae Genetica, 51,* 80-86.

Kindt, R., & Coe, R. (2005). *Tree diversity analysis: A manual and software for common statistical methods for ecological and biodiversity studies*. World Agrofirestry Centre.

Lan, Y.-H., Shaw, D. C., Beedlow, P. A., Lee, E. H., & Waschmann, R. S. (2019). Severity of Swiss needle cast in young and mature Douglas-fir forests in western Oregon, USA. *Forest Ecology and Management*, *442*, 79–95. https://doi.org/10.1016/j.foreco.2019.03.063

Lan, Y.-H., Shaw, D. C., Lee, E. H., & Beedlow, P. A. (2022). Distribution of a foliage disease fungus within canopies of mature Douglas-Fir in Western Oregon. *Frontiers in Forests and Global Change*, *5*, 743039. https://doi.org/10.3389/ffgc.2022.743039

Langer, G. J., Fuchs, S., Osewold, J., Peters, S., Schrewe, F., Ridley, M., Kätzel, R., Bubner, B., & Grüner, J. (2022). FraxForFuture—Research on European ash dieback in Germany. *Journal of Plant Diseases and Protection*, *129*(6), 1285–1295. https://doi.org/10.1007/s41348-022-00670-z

Last, F. T. (1955). Seasonal incidence of Sporobolomyces on cereal leaves. *Transactions of the British Mycological Society*, *38*(3), 221–239. https://doi.org/10.1016/S0007-1536(55)80069-1

Letunic, I., & Bork, P. (2007). Interactive Tree Of Life (iTOL): An online tool for phylogenetic tree display and annotation. *Bioinformatics*, *23*(1), 127–128. https://doi.org/10.1093/bioinformatics/btl529

Liebhold, A. M., Brockerhoff, E. G., Garrett, L. J., Parke, J. L., & Britton, K. O. (2012). Live plant imports: The major pathway for forest insect and pathogen invasions of the US. *Frontiers in Ecology and the Environment*, *10*(3), 135–143. https://doi.org/10.1890/110198

Lundberg, D. S., Lebeis, S. L., Paredes, S. H., Yourstone, S., Gehring, J., Malfatti, S., Tremblay, J., Engelbrektson, A., Kunin, V., Rio, T. G. del, Edgar, R. C., Eickhorst, T., Ley, R. E., Hugenholtz,

P., Tringe, S. G., & Dangl, J. L. (2012). Defining the core *Arabidopsis thaliana* root microbiome. *Nature*, *488*(7409), Article 7409. https://doi.org/10.1038/nature11237

Lynch, M., & Walsh, B. (1998). *Genetics and Analysis of Quantitative Traits*. Sinauer Associates.

Maguire, D. A., Kanaskie, A., Voelker, W., Johnson, R., & Johnson, G. (2002). Growth of young Douglas-Fir plantations across a gradient in Swiss Needle Cast severity. *Western Journal of Applied Forestry*, *17*(2), 86–95. https://doi.org/10.1093/wjaf/17.2.86

Manter, D. K., Bond, B. J., Kavanagh, K. L., Rosso, P. H., & Filip, G. M. (2000). Pseudothecia of Swiss needle cast fungus, *Phaeocryptopus gaeumannii,* physically block stomata of Douglas-fir, reducing CO_2 assimilation. *The New Phytologist*, *148*(3), 481–491. https://doi.org/10.1046/j.1469-8137.2000.00779.x

Manter, D. K., Bond, B. J., Kavanagh, K. L., Stone, J. K., & Filip, G. M. (2003b). Modelling the impacts of the foliar pathogen, *Phaeocryptopus gaeumannii*, on Douglas-fir physiology: Net canopy carbon assimilation, needle abscission and growth. *Ecological Modelling*, *164*(2–3), 211–226. https://doi.org/10.1016/S0304-3800(03)00026-7

Manter, D. K., & Kavanagh, K. L. (2003). Stomatal regulation in Douglas-fir following a fungal-mediated chronic reduction in leaf area. *Trees*, *17*(6), 485–491. https://doi.org/10.1007/s00468-003-0262-2

Manter, D. K., Reeser, P. W., & Stone, J. K. (2005). A climate-based model for predicting geographic variation in Swiss Needle Cast severity in the oregon coast range. *Phytopathology*, *95*(11), 1256–1265. https://doi.org/10.1094/PHYTO-95-1256

Manter, D. K., Winton, L. M., Filip, G. M., & Stone, J. K. (2003a). Assessment of Swiss Needle Cast disease: Temporal and spatial investigations of fungal colonization and symptom severity. *Journal of Phytopathology*, *151*(6), 344–351. https://doi.org/10.1046/j.1439-0434.2003.00730.x

Martin, M. (2011). Cutadapt removes adapter sequences from high-throughput sequencing reads. *EMBnet.Journal*, *17*(1), 10. https://doi.org/10.14806/ej.17.1.200

Mbareche, H., Veillette, M., Bilodeau, G., & Duchaine, C. (2020). Comparison of the performance of ITS1 and ITS2 as barcodes in amplicon-based sequencing of bioaerosols. *PeerJ*, *8*, e8523. https://doi.org/10.7717/peerj.8523

McDermott, J. M., & Robinson, R. A. (1989). Provenance variation for disease resistance in *Pseudotsuga menziesii* to the Swiss needle-cast pathogen, *Phaeocryptopus gaeumannii*. *Canadian Journal of Forest Research*, *19*(2), 244–246. https://doi.org/10.1139/x89-034

McMurdie, P. J., & Holmes, S. (2013). phyloseq: An R package for reproducible interactive analysis and graphics of microbiome census data. *PLoS ONE*, *8*(4), e61217. https://doi.org/10.1371/journal.pone.0061217

Mejía, L. C., Herre, E. A., Sparks, J. P., Winter, K., García, M. N., Van Bael, S. A., Stitt, J., Shi, Z., Zhang, Y., Guiltinan, M. J., & Maximova, S. N. (2014). Pervasive effects of a dominant foliar endophytic fungus on host genetic and phenotypic expression in a tropical tree. *Frontiers in Microbiology*, *5*. https://www.frontiersin.org/articles/10.3389/fmicb.2014.00479

Migliorini, D., Ghelardini, L., Tondini, E., Luchi, N., & Santini, A. (2015). The potential of symptomless potted plants for carrying invasive soilborne plant pathogens. *Diversity and Distributions*, *21*(10), 1218–1229. https://doi.org/10.1111/ddi.12347

Milici, M., Tomasch, J., Wos-Oxley, M. L., Wang, H., Jáuregui, R., Camarinha-Silva, A., Deng, Z.-L., Plumeier, I., Giebel, H.-A., Wurst, M., Pieper, D. H., Simon, M., & Wagner-Döbler, I. (2016). Low diversity of planktonic bacteria in the tropical ocean. *Scientific Reports*, *6*(1), 19054. https://doi.org/10.1038/srep19054

Montwé, D., Elder, B., Socha, P., Wyatt, J., Noshad, D., Feau, N., Hamelin, R., Stoehr, M., & Ehlting, J. (2021). Swiss needle cast tolerance in British Columbia's coastal Douglas-fir breeding population. *Forestry: An International Journal of Forest Research*, *94*(2), 193–203. https://doi.org/10.1093/forestry/cpaa024

Mueller, U. G., & Linksvayer, T. A. (2022). Microbiome breeding: Conceptual and practical issues. *Trends in Microbiology*, *30*(10), 997–1011. https://doi.org/10.1016/j.tim.2022.04.003

Müller, D. B., Vogel, C., Bai, Y., & Vorholt, J. A. (2016). The plant microbiota: Systems-level insights and perspectives. *Annual Review of Genetics*, *50*(1), 211–234. https://doi.org/10.1146/annurev-genet-120215-034952

Nakayama, M., Imamura, S., Taniguchi, T., & Tateno, R. (2019). Does conversion from natural forest to plantation affect fungal and bacterial biodiversity, community structure, and co-occurrence networks in the organic horizon and mineral soil? *Forest Ecology and Management*, *446*, 238–250. https://doi.org/10.1016/j.foreco.2019.05.042

National research council (US) committee on metagenomics: challenges and functional applications. (2007). Why metagenomics? In *The New Science of Metagenomics: Revealing the Secrets of Our Microbial Planet*. National Academies Press (US). https://www.ncbi.nlm.nih.gov/books/NBK54011/

Nearing, J. T., Douglas, G. M., Hayes, M. G., MacDonald, J., Desai, D. K., Allward, N., Jones, C. M. A., Wright, R. J., Dhanani, A. S., Comeau, A. M., & Langille, M. G. I. (2022). Microbiome differential abundance methods produce different results across 38 datasets. *Nature Communications*, *13*(1), Article 1. https://doi.org/10.1038/s41467-022-28034-z

Nerva, L., Sandrini, M., Moffa, L., Velasco, R., Balestrini, R., & Chitarra, W. (2022). Breeding toward improved ecological plant–microbiome interactions. *Trends in Plant Science*, *27*(11), 1134–1143. https://doi.org/10.1016/j.tplants.2022.06.004

Newton, A. C., Fitt, B. D. L., Atkins, S. D., Walters, D. R., & Daniell, T. J. (2010). Pathogenesis, parasitism and mutualism in the trophic space of microbe–plant interactions. *Trends in Microbiology*, *18*(8), 365–373. https://doi.org/10.1016/j.tim.2010.06.002

Nguyen, N. H., Song, Z., Bates, S. T., Branco, S., Tedersoo, L., Menke, J., Schilling, J. S., & Kennedy, P. G. (2016). FUNGuild: An open annotation tool for parsing fungal community datasets by ecological guild. *Fungal Ecology*, *20*, 241–248. https://doi.org/10.1016/j.funeco.2015.06.006

Oksanen, J., Simpson, G., Blanchet, F., Kindt, R., Legendre, P., Minchin, P., O'Hara, R., Solymos, P., Stevens, M., Szoecs, E., Wagner, H., Barbour, M., Bedward, M., Bolker, B., Borcard, D., Carvalho, G., Chirico, M., De Caceres, M., Durand, S., … Weedon, J. (2022). *_vegan: Community Ecology Package_* (version 2.6-4) [R package]. <https://CRAN.R-project.org/package=vegan>

Oliva, J., Ridley, M., Redondo, M. A., & Caballol, M. (2021). Competitive exclusion amongst endophytes determines shoot blight severity on pine. *Functional Ecology*, *35*(1), 239–254. https://doi.org/10.1111/1365-2435.13692

Omomowo, I. O., Amao, J. A., Abubakar, A., Ogundola, A. F., Ezediuno, L. O., & Bamigboye, C. O. (2023). A review on the trends of endophytic fungi bioactivities. *Scientific African*, *20*, e01594. https://doi.org/10.1016/j.sciaf.2023.e01594

Pan, A. Y. (2021). Statistical analysis of microbiome data: The challenge of sparsity. *Current Opinion in Endocrine and Metabolic Research*, *19*, 35–40. https://doi.org/10.1016/j.coemr.2021.05.005

Peiffer, J. A., Spor, A., Koren, O., Jin, Z., Tringe, S. G., Dangl, J. L., Buckler, E. S., & Ley, R. E. (2013). Diversity and heritability of the maize rhizosphere microbiome under field conditions. *Proceedings of the National Academy of Sciences*, *110*(16), 6548–6553. https://doi.org/10.1073/pnas.1302837110

Peschel, S., Müller, C. L., von Mutius, E., Boulesteix, A.-L., & Depner, M. (2020). NetCoMi: Network construction and comparison for microbiome data in R. *Briefings in Bioinformatics*, *22*(4), bbaa290. https://doi.org/10.1093/bib/bbaa290

Pojar, J., Klinka, K., & Demarchi, D. A. (1991). Ecosystems of BC. In *Coastal Western Hemlock Zone*. BC Ministry of Forests.

Porras-Alfaro, A., & Bayman, P. (2011). Hidden fungi, emergent properties: endophytes and microbiomes. *Annual Review of Phytopathology*, *49*, 291–315. https://doi.org/10.1146/annurev-phyto-080508-081831

Quan, Y., Muggia, L., Moreno, L. F., Wang, M., Al-Hatmi, A. M. S., Da Silva Menezes, N., Shi, D., Deng, S., Ahmed, S., Hyde, K. D., Vicente, V. A., Kang, Y., Stielow, J. B., & De Hoog, S. (2020). A re-evaluation of the Chaetothyriales using criteria of comparative biology. *Fungal Diversity*, *103*(1), 47–85. https://doi.org/10.1007/s13225-020-00452-8

Quiring, D., Flaherty, L., Adams, G., McCartney, A., Miller, J. D., & Edwards, S. (2019). An endophytic fungus interacts with crown level and larval density to reduce the survival of eastern spruce budworm, *Choristoneura fumiferana* (Lepidoptera: Tortricidae), on white spruce (*Picea glauca*). *Canadian Journal of Forest Research*, *49*(3), 221–227. https://doi.org/10.1139/cjfr-2018-0194

R Core Team. (2015). *R: A Language and Environment for Statistical Computing*.

Rajala, T., Velmala, S. M., Tuomivirta, T., Haapanen, M., Müller, M., & Pennanen, T. (2013). Endophyte communities vary in the needles of Norway spruce clones. *Fungal Biology*, *117*(3), 182–190. https://doi.org/10.1016/j.funbio.2013.01.006

Redondo, M. A., Oliva, J., Elfstrand, M., Boberg, J., Capador-Barreto, H. D., Karlsson, B., & Berlin, A. (2022). Host genotype interacts with aerial spore communities and influences the needle mycobiome of Norway spruce. *Environmental Microbiology*, *24*(8), 3640–3654. https://doi.org/10.1111/1462-2920.15974

Ridout, M., & Newcombe, G. (2015). The frequency of modification of *Dothistroma* pine needle blight severity by fungi within the native range. *Forest Ecology and Management*, *337*, 153–160. https://doi.org/10.1016/j.foreco.2014.11.010

Rigling, D., & Prospero, S. (2018). *Cryphonectria parasitica,* the causal agent of chestnut blight: Invasion history, population biology and disease control. *Molecular Plant Pathology*, *19*(1), 7–20. https://doi.org/10.1111/mpp.12542

Ritóková, G., Shaw, D., Filip, G., Kanaskie, A., Browning, J., & Norlander, D. (2016). Swiss Needle Cast in Western Oregon Douglas-Fir plantations: 20-Year monitoring results. *Forests*, *7*(12), 155. https://doi.org/10.3390/f7080155

Ritóková, G., Shaw, D., & Mainwaring, D. (2020). *Silvicultural decision guide for swiss needle cast in coastal oregon and washington*.

Rivers, A. R., Weber, K. C., Gardner, T. G., Liu, S., & Armstrong, S. D. (2018). ITSxpress: Software to rapidly trim internally transcribed spacer sequences with quality scores for marker gene analysis. *F1000Research*, *7*, 1418. https://doi.org/10.12688/f1000research.15704.1

Roberts, E., & Lindow, S. (2013). Loline alkaloid production by fungal endophytes of *Fescue* species select for particular epiphytic bacterial microflora. *The ISME Journal*, *8*(2), Article 2. https://doi.org/10.1038/ismej.2013.170

Rodriguez, R. J., White Jr, J. F., Arnold, A. E., & Redman, R. S. (2009). Fungal endophytes: Diversity and functional roles. *New Phytologist*, *182*(2), 314–330. https://doi.org/10.1111/j.1469-8137.2009.02773.x

Roe, A. D., Rice, A. V., Bromilow, S. E., Cooke, J. E. K., & Sperling, F. A. H. (2010). Multilocus species identification and fungal DNA barcoding: Insights from blue stain fungal symbionts of the mountain pine beetle. *Molecular Ecology Resources*, *10*(6), 946–959. https://doi.org/10.1111/j.1755-0998.2010.02844.x

Rognes, T., Flouri, T., Nichols, B., Quince, C., & Mahé, F. (2016). VSEARCH: A versatile open source tool for metagenomics. *PeerJ*, *4*, e2584. https://doi.org/10.7717/peerj.2584

Rosso, P. H., & Hansen, E. M. (2003). Predicting Swiss Needle Cast disease distribution and severity in young Douglas-Fir plantations in Coastal Oregon. *Phytopathology®*, *93*(7), 790–798. https://doi.org/10.1094/PHYTO.2003.93.7.790

Sánchez-Cañizares, C., Jorrín, B., Poole, P. S., & Tkacz, A. (2017). Understanding the holobiont: The interdependence of plants and their microbiome. *Current Opinion in Microbiology*, *38*, 188–196. https://doi.org/10.1016/j.mib.2017.07.001

Sanders, H. L. (1968). Marine benthic diversity: A comparative study. *The American Naturalist*, *102*(925), 243–282. https://doi.org/10.1086/282541

Sapkota, R., Knorr, K., Jørgensen, L. N., O'Hanlon, K. A., & Nicolaisen, M. (2015). Host genotype is an important determinant of the cereal phyllosphere mycobiome. *New Phytologist*, *207*(4), 1134–1144. https://doi.org/10.1111/nph.13418

Schardl, C. L., Leuchtmann, A., & Spiering, M. J. (2004). Symbioses of grasses with seedborne fungal endophytes. *Annual Review of Plant Biology*, *55*(1), 315–340. https://doi.org/10.1146/annurev.arplant.55.031903.141735

Schmertmann, L. J., Irinyi, L., Malik, R., Powell, J. R., Meyer, W., & Krockenberger, M. B. (2019). The mycobiome of Australian tree hollows in relation to the *Cryptococcus gattii* and C. neoformans species complexes. *Ecology and Evolution*, *9*(17), 9684–9700. https://doi.org/10.1002/ece3.5498

Schmitz, L., Yan, Z., Schneijderberg, M., de Roij, M., Pijnenburg, R., Zheng, Q., Franken, C., Dechesne, A., Trindade, L. M., van Velzen, R., Bisseling, T., Geurts, R., & Cheng, X. (2022). Synthetic bacterial community derived from a desert rhizosphere confers salt stress resilience to tomato in the presence of a soil microbiome. *The ISME Journal*, *16*(8), Article 8. https://doi.org/10.1038/s41396-022-01238-3

Schoch, C. L., Seifert, K. A., Huhndorf, S., Robert, V., Spouge, J. L., Levesque, C. A., Chen, W., Fungal Barcoding Consortium, Fungal Barcoding Consortium Author List, Bolchacova, E., Voigt, K., Crous, P. W., Miller, A. N., Wingfield, M. J., Aime, M. C., An, K.-D., Bai, F.-Y., Barreto, R. W., Begerow, D., … Schindel, D. (2012). Nuclear ribosomal internal transcribed spacer (ITS) region as a universal DNA barcode marker for *Fungi*. *Proceedings of the National Academy of Sciences*, *109*(16), 6241–6246. https://doi.org/10.1073/pnas.1117018109

Shaw, D. C., Filip, G. M., Kanaskie, A., Maguire, D. A., & Littke, W. A. (2011). Managing an epidemic of Swiss Needle Cast in the Douglas-Fir region of Oregon: The role of the Swiss Needle Cast Cooperative. *Journal of Forestry*.

Shaw, D. C., Ritóková, G., Lan, Y.-H., Mainwaring, D. B., Russo, A., Comeleo, R., Navarro, S., Norlander, D., & Smith, B. (2021). Persistence of the Swiss Needle Cast outbreak in Oregon Coastal Douglas-Fir and new insights from research and monitoring. *Journal of Forestry*, *119*(4), 407–421. https://doi.org/10.1093/jofore/fvab011

Shaw, D. C., Woolley, T., & Kanaskie, A. (2014). Vertical foliage retention in Douglas-Fir across environmental gradients of the Western Oregon Coast range influenced by Swiss Needle Cast. *Northwest Science*, *88*(1), 23–32. https://doi.org/10.3955/046.088.0105

Shearin, Z. R. C., Filipek, M., Desai, R., Bickford, W. A., Kowalski, K. P., & Clay, K. (2018). Fungal endophytes from seeds of invasive, non-native Phragmites australis and their potential role in

germination and seedling growth. *Plant and Soil*, *422*(1), 183–194. https://doi.org/10.1007/s11104-017-3241-x

Sherwood-Pike, M., Stone, J. K., & Carroll, G. C. (1986). *Rhabdocline parkeri*, a ubiquitous foliar endophyte of Douglas-fir. *Canadian Journal of Botany*, *64*(9), 1849–1855. https://doi.org/10.1139/b86-245

Shieh, G., & Jan, S.-L. (2004). The effectiveness of randomized complete block design. *Statistica Neerlandica*, *58*(1), 111–124. https://doi.org/10.1046/j.0039-0402.2003.00109.x

Shivaji, S., Jayasudha, R., Prashanthi, G. S., Arunasri, K., & Das, T. (2022). Fungi of the human eye: Culture to mycobiome. *Experimental Eye Research*, *217*, 108968. https://doi.org/10.1016/j.exer.2022.108968

Singh, B. K., & Trivedi, P. (2017). Microbiome and the future for food and nutrient security. *Microbial Biotechnology*, *10*(1), 50–53. https://doi.org/10.1111/1751-7915.12592

Sowley, E. N. K., Dewey, F. M., & Shaw, M. W. (2010). Persistent, symptomless, systemic, and seed-borne infection of lettuce by *Botrytis cinerea*. *European Journal of Plant Pathology*, *126*(1), 61–71. https://doi.org/10.1007/s10658-009-9524-1

St. Clair, J. B. (1994). Genetic variation in tree structure and its relation to size in Douglas-fir. I. Biomass partitioning, foliage efficiency, stem form, and wood density. *Canadian Journal of Forest Research*, *24*(6), 1226–1235. https://doi.org/10.1139/x94-161

Stone, J. K. (1987). Initiation and development of latent infections by *Rhabdocline parkeri* on Douglas-fir. *Canadian Journal of Botany*, *65*(12), 2614–2621. https://doi.org/10.1139/b87-352

Stone, J. K., Capitano, B. R., & Kerrigan, J. L. (2008). The histopathology of *Phaeocryptopus gaeumannii* on Douglas-fir needles. *Mycologia*, *100*(3), 431–444. https://doi.org/10.3852/07-170R1

Stone, J. K., Hood, I. A., Watt, M. S., & Kerrigan, J. L. (2007). Distribution of Swiss needle cast in New Zealand in relation to winter temperature. *Australasian Plant Pathology*, *36*(5), 445–454. https://doi.org/10.1071/AP07049

Straley, G. B., Taylor, R. L., & Douglas, G. W. (n.d.). *The rare vascular plants of British Columbia.* Nat. Museum Canada.

Sugiyama, A., Ueda, Y., Zushi, T., Takase, H., & Yazaki, K. (2014). Changes in the bacterial community of soybean rhizospheres during growth in the field. *PLOS ONE*, *9*(6), e100709. https://doi.org/10.1371/journal.pone.0100709

Suryanarayanan, T. S. (2013). Endophyte research: Going beyond isolation and metabolite documentation. *Fungal Ecology*, *6*(6), 561–568. https://doi.org/10.1016/j.funeco.2013.09.007

Tanney, J. B., Di Stefano, J., Miller, J. D., & McMullin, D. R. (2023). Natural products from the *Picea* foliar endophytes *Niesslia endophytica* sp. Nov. And *Strasseria geniculata. Mycological Progress*, *22*(3), 17. https://doi.org/10.1007/s11557-023-01869-6

Tanney, J. B., & Seifert, K. A. (2020). Mollisiaceae: An overlooked lineage of diverse endophytes. *Studies in Mycology*, *95*, 293–380. https://doi.org/10.1016/j.simyco.2020.02.005

Taylor, J. E., & Koukol, O. (2023). Towards resolving *Nothophaeocryptopus* and *Rhizosphaera* inhabitants of spruce needles. *Forest Pathology*, *53*(3), e12807. https://doi.org/10.1111/efp.12807

Temel, F., Johnson, G. R., & Adams, W. T. (2005). Early genetic testing of coastal Douglas-fir for Swiss needle cast tolerance. *Canadian Journal of Forest Research, 35*(3), 521-529. https://cdnsciencepub-com.ezproxy.library.uvic.ca/doi/abs/10.1139/x04-183

Temel, F., Johnson, G. R., & Stone, J. K. (2004). The relationship between Swiss needle cast symptom severity and level of *Phaeocryptopus gaeumannii* colonization in coastal Douglas-fir (*Pseudotsuga menziesii* var. *Menziesii*)*. *Forest Pathology*, *34*(6), 383–394. https://doi.org/10.1111/j.1439-0329.2004.00379.x

Tkacz, A., Cheema, J., Chandra, G., Grant, A., & Poole, P. S. (2015). Stability and succession of the rhizosphere microbiota depends upon plant type and soil composition. *The ISME Journal*, *9*(11), Article 11. https://doi.org/10.1038/ismej.2015.41

Toghueo, R. M. K., & Boyom, F. F. (2020). Endophytic *Penicillium* species and their agricultural, biotechnological, and pharmaceutical applications. *3 Biotech*, *10*(3), 107. https://doi.org/10.1007/s13205-020-2081-1

Toju, H., Tanabe, A. S., Yamamoto, S., & Sato, H. (2012). High-coverage ITS primers for the DNA-based identification of ascomycetes and basidiomycetes in environmental samples. *PloS One*, *7*(7), e40863. https://doi.org/10.1371/journal.pone.0040863

Ukrainetz, N. K., Kang, K.-Y., Aitken, S. N., Stoehr, M., & Mansfield, S. D. (2008). Heritability and phenotypic and genetic correlations of coastal Douglas-fir (*Pseudotsuga menziesii*) wood quality traits. *Canadian Journal of Forest Research*, *38*(6), 1536–1546. https://doi.org/10.1139/X07-234

Van Kan, J. A. L. (2006). Licensed to kill: The lifestyle of a necrotrophic plant pathogen. *Trends in Plant Science*, *11*(5), 247–253. https://doi.org/10.1016/j.tplants.2006.03.005

Van Vloten, H. (1932). *Rhabdocline pseudotsugae Sydow, oorzak eener ziwekte van Douglasspar. Proefschrift*. Landbouwhoogschool.

VanWallendael, A., Benucci, G. M. N., da Costa, P. B., Fraser, L., Sreedasyam, A., Fritschi, F., Juenger, T. E., Lovell, J. T., Bonito, G., & Lowry, D. B. (2022). Host genotype controls ecological change in the leaf fungal microbiome. *PLoS Biology*, *20*(8), e3001681. https://doi.org/10.1371/journal.pbio.3001681

Vargas-Hernandez, J., & Adams, W. T. (1991). Genetic variation of wood density components in young coastal Douglas-fir: Implications for tree breeding. *Canadian Journal of Forest Research*, *21*(12), 1801–1807. https://doi.org/10.1139/x91-248

Vorholt, J. A. (2012). Microbial life in the phyllosphere. *Nature Reviews Microbiology*, *10*(12), Article 12. https://doi.org/10.1038/nrmicro2910

Wagner, M. R., Busby, P. E., & Balint-Kurti, P. (2020). Analysis of leaf microbiome composition of near-isogenic maize lines differing in broad-spectrum disease resistance. *New Phytologist*, *225*(5), 2152–2165. https://doi.org/10.1111/nph.16284

Walters, W. A., Jin, Z., Youngblut, N., Wallace, J. G., Sutter, J., Zhang, W., González-Peña, A., Peiffer, J., Koren, O., Shi, Q., Knight, R., Glavina Del Rio, T., Tringe, S. G., Buckler, E. S., Dangl, J. L., & Ley, R. E. (2018). Large-scale replicated field study of maize rhizosphere identifies heritable microbes. *Proceedings of the National Academy of Sciences*, *115*(28), 7368–7373. https://doi.org/10.1073/pnas.1800918115

Wang, J. R., & Kimmins, J. P. (2002). Height growth and competitive relationship between paper birch and Douglas-fir in coast and interior of British Columbia. *Forest Ecology and Management*, *165*(1–3), 285–293. https://doi.org/10.1016/S0378-1127(01)00630-2

White, T. J., Bruns, T., Lee, S., & Taylor, J. (1990). Amplification and direct sequencing of fungal ribosomal RNA genes for phylogenetics. In *Sninsky J and White T. San Diego: CA Academic Press* (Vol. 38, pp. 315–322). https://doi.org/10.1016/B978-0-12-372180-8.50042-1

Wickham, H. (2009). *ggplot2: Elegant Graphics for Data Analysis*. Springer Science & Business Media.

Wijayawardene, N. (2020). Outline of Fungi and fungus-like taxa. *Mycosphere*, *11*(1), 1060–1456. https://doi.org/10.5943/mycosphere/11/1/8

Wijayawardene, N. N., Bahram, M., Sánchez-Castro, I., Dai, D.-Q., Ariyawansa, K. G. S. U., Jayalal, U., Suwannarach, N., & Tedersoo, L. (2021). Current insight into culture-dependent and culture-

independent methods in discovering Ascomycetous taxa. *Journal of Fungi*, *7*(9), 703. https://doi.org/10.3390/jof7090703

Wilhelmi, N. P., Shaw, D. C., Harrington, C. A., St. Clair, J. B., & Ganio, L. M. (2017). Climate of seed source affects susceptibility of coastal Douglas-fir to foliage diseases. *Ecosphere*, *8*(12), e02011. https://doi.org/10.1002/ecs2.2011

Wilson, D. (1995). Endophyte: The evolution of a term, and clarification of its use and definition. *Oikos*, *73*(2), 274–276. https://doi.org/10.2307/3545919

Wilson, L., & Cline, B. (2022, April 18). *Exobasidium leaf and fruit spot of blueberry*. NC State Extension Publications. https://content.ces.ncsu.edu/exobasidium-leaf-and-fruit-spot-of-blueberry#section_heading_16728

Yang, H., Yang, Z., Wang, Q.-C., Wang, Y.-L., Hu, H.-W., He, J.-Z., Zheng, Y., & Yang, Y. (2022). Compartment and plant identity shape tree mycobiome in a subtropical forest. *Microbiology Spectrum*, *10*(4), e01347-22. https://doi.org/10.1128/spectrum.01347-22

Yeh, F. C., & Heaman, J. C. (1987). Estimating genetic parameters of height growth in seven-year old coastal Douglas-Fir from disconnected diallels. *Forest Science*, *33*(4), 946–957. https://doi.org/10.1093/forestscience/33.4.946

Yu, Z., Ding, H., Shen, K., Bu, F., Newcombe, G., & Liu, H. (2021). Foliar endophytes in trees varying greatly in age. *European Journal of Plant Pathology*, *160*(2), 375–384. https://doi.org/10.1007/s10658-021-02250-7

Zahid, M. S., Li, D., Javed, H. U., Sabir, I. A., Wang, L., Jiu, S., Song, S., Ma, C., Wang, D., Zhang, C., Zhou, X., Xu, W., & Wang, S. (2021). Comparative fungal diversity and dynamics in plant compartments at different developmental stages under root-zone restricted grapevines. *BMC Microbiology*, *21*(1), 317. https://doi.org/10.1186/s12866-021-02376-y

Zgadzaj, R., Garrido-Oter, R., Jensen, D. B., Koprivova, A., Schulze-Lefert, P., & Radutoiu, S. (2016). Root nodule symbiosis in *Lotus japonicus* drives the establishment of distinctive rhizosphere, root, and nodule bacterial communities. *Proceedings of the National Academy of Sciences*, *113*(49), E7996–E8005. https://doi.org/10.1073/pnas.1616564113

Zurr, A. F., Leno, E. N., Walker, N. J., Saveliev, A. A., & Graham M.S. (2009). *Mixed Effects Models and Extensions in Ecology with R*. R Springer.

Appendices

Appendix 1.

Table 1. ANOVA of Shannon and Observed Diversity Indices for individual disease phenotypes, phenotype grouping and family (alpha < 0.05). Using dataset with N. gaeumannii (rarefied to depth of 7000) and bottom refers to dataset with out N. gaeumannii (rarefied to depth of 1500).

	Df	Sum Sq	Mean Sq	F value	Pr(>F)
Shannon					
NL 3y 2022	2	0.21	0.11	0.47	0.63
residual	*52*	*11.85*	*0.23*		
SO 2y 2021	2	1.10	0.55	2.56	0.087
residual	*50*	*10.75*	*0.22*		
Female	11	1.71	0.16	0.64	0.78
residual	*43*	*10.36*	*0.24*		
Disease	3	1.35	0.45	2.10	0.11
residual	*49*	*10.51*	*0.21*		
Observed					
NL 3y 2022	2	37.93	18.96	0.11	0.90
residual	*52*	*9244.87*	*177.79*		
SO 2y 2021	2	52.59	26.30	0.15	0.86
residual	*50*	*8630.95*	*172.62*		
Female	11	2163.75	196.70	1.19	0.32
residual	*43*	*7119.05*	*165.56*		
Disease	3	189.41	63.14	0.36	0.78
residual	*49*	*8494.14*	*173.35*		

Appendix 2.

Table 1. Permutational analysis of variance (PERMANOVA) for community dissimilarity based on different data normalization criteria (i.e., rarefied, rarefied without N. gaeumannii, log relative abundance, centered log ration) and different dissimilarity matrices metrics.

	Df	SumOfSqs	R^2	F	Pr(>F)
Rarefied- Bray Curtis					
Family	11	1.38	0.30	1.63	**0.036**
Block	21	1.92	0.41	1.19	0.279
Needle Loss 2nd Year 2021	1	0.018	0.0038	0.23	0.97
Needle Loss 3nd Year 2022	1	0.038	0.0081	0.49	0.81
Stomatal Occlusion 2021	1	0.11	0.023	1.39	0.24
Relative Growth Rate	1	0.025	0.0053	0.32	0.95
Disease Grouping	3	0.16	0.035	0.70	0.77
Residual	*13*	*0.99*	*0.21*		
Total	*52*	*4.64*	*1*		
Rarefied No *N. gaeumannii*- *Bray Curtis*					
Family	11	4.85	0.36	2.28	**0.001**
Block	21	4.58	0.34	1.13	0.196
Needle Loss 2nd Year 2021	1	0.21	0.016	1.10	0.336
Needle Loss 3nd Year 2022	1	0.15	0.011	0.75	0.721
Stomatal Occlusion 2021	1	0.22	0.017	1.15	0.289
Relative Growth Rate	1	0.14	0.010	0.73	0.739
Disease Grouping	3	0.76	0.056	1.31	0.136
Residual	*13*	*2.51*	*0.19*		
Total	*52*	*13.42*	*1*		
Logged Relative Abundance- Bray Curtis					
Family	11	1.47	0.30	1.78	**0.014**
Block	21	1.79	0.36	1.14	0.296
Needle Loss 2nd Year 2021	1	0.029	0.0058	0.38	0.904
Needle Loss 3nd Year 2022	1	0.035	0.0070	0.46	0.894
Stomatal Occlusion 2021	1	0.10	0.021	1.37	0.199
Relative Growth Rate	1	0.034	0.0069	0.45	0.888
Disease Grouping	3	0.18	0.036	0.79	0.698
Residual	*17*	*1.28*	*0.26*		
Total	*56*	*4.92*	*1*		
Centred Log Ratio (CLR)- Euclidean					
Family	11	3348.54	0.28	1.60	**0.001**
Block	21	4372.49	0.36	1.10	0.128

	Df	SumOfSqs	R^2	F	Pr(>F)
Needle Loss 2nd Year 2021	1	186.62	0.015	0.98	0.499
Needle Loss 3nd Year 2022	1	131.29	0.011	0.69	0.939
Stomatal Occlusion 2021	1	166.12	0.014	0.87	0.661
Relative Growth Rate	1	128.74	0.011	0.68	0.96
Disease Grouping	3	584.30	0.048	1.02	0.404
Residual	*17*	*3231.50*	*0.27*		
Total	*56*	*12149.60*	*1*		

Appendix 3.

Table 1. Pearson (r-value) and Spearman (rho value) correlations between clr normalized abundance of Rhizosphaera species, N. gaeumannii, and SNC Disease Symptoms.

Variables	Correlation Coefficient (r-value)	P-value
N. gaeumannii vs *Rhizosphaera* sp. 1	-0.572	0.000*
N. gaeumannii vs *Rhizosphaera* sp. 2	-0.433	0.001*
Rhizosphaera sp. 1 vs *Rhizosphaera* sp. 2	0.680	0.000*
	Correlation Coefficient (rho-value)	
N. gaeumannii vs stomatal occlusion 2021	0.126	0.349
Rhizosphaera sp. 1 vs stomatal occlusion	-0.018	0.895
Rhizosphaera sp. 2 vs stomatal occlusion	-0.068	0.615
N. gaeumannii vs needle loss 2nd year	-0.280	0.032*
Rhizosphaera sp. 1 vs needle loss 2nd year	0.144	0.275
Rhizosphaera sp. 2 vs needle loss 2nd year	-0.037	0.784
N. gaeumannii vs needle loss 3rd year	-0.075	0.573
Rhizosphaera sp. 1 vs needle loss 3rd year	0.241	0.066
Rhizosphaera sp. 2 vs needle loss 3rd year	0.212	0.107

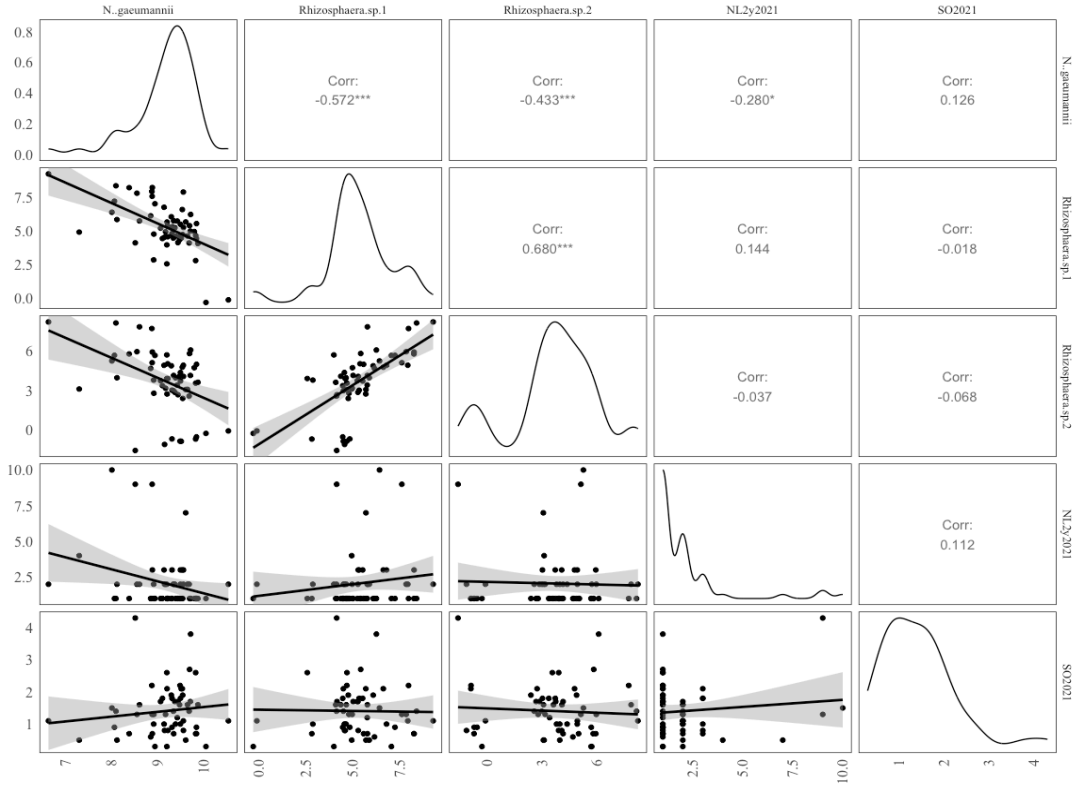

Figure 1. Pearson (r-value) and Spearman (r-value = rho) correlations of Rhizosphaera species and N. gaeumannii) as described in Appendix 3, table 1. Upper triangle reports correlation and lower triangle plots the correlation The diagonal shows density plots for each respective taxa representing the distribution across all (59) samples. Data was clr transformed to account for compositionality.

Appendix 4.

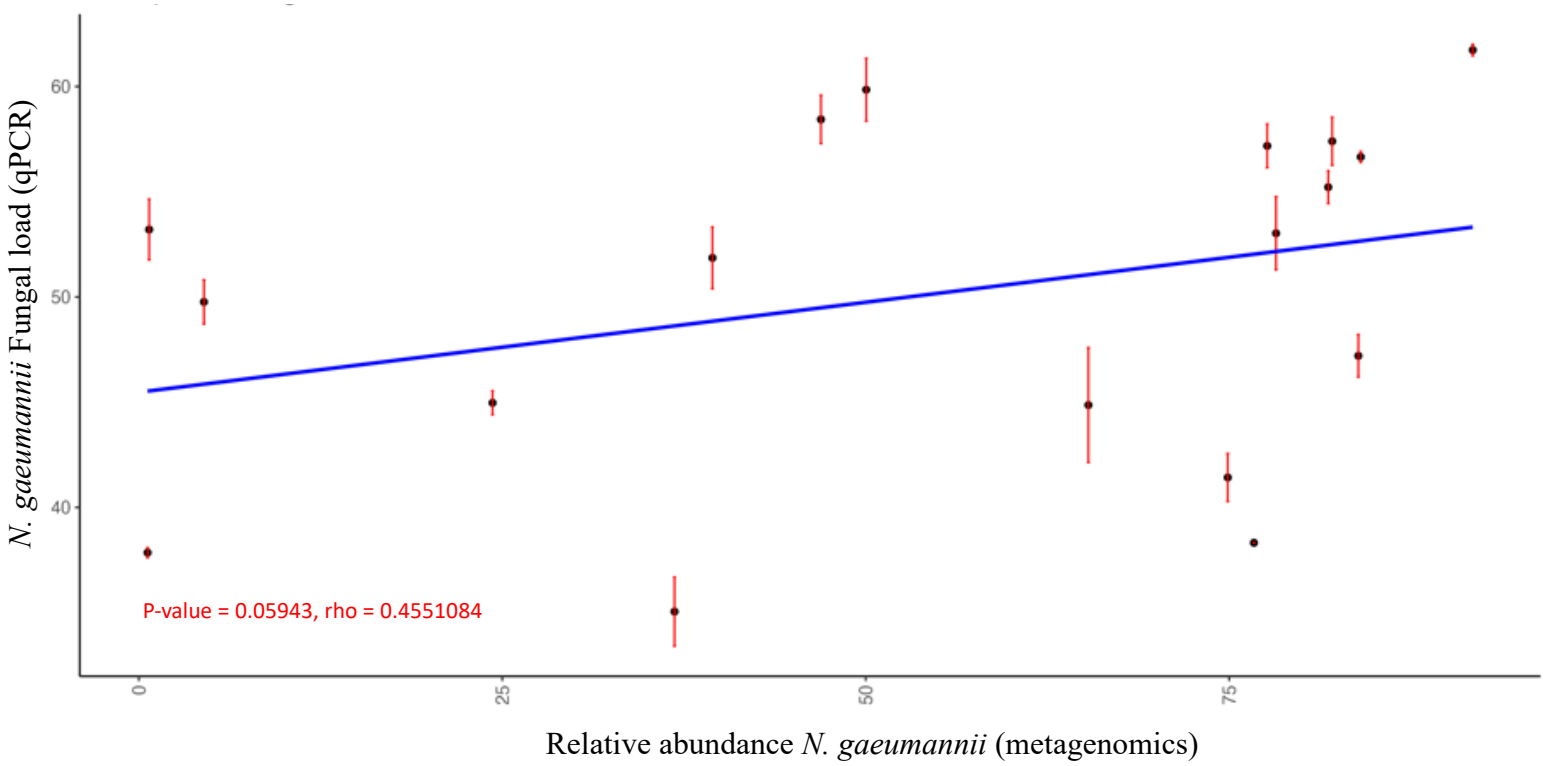

Figure 1. Spearman correlation (r-value = rho) comparing the relative abundance of N. gaeumannii reads from Illumina Miseq metagenomic data with the proportion of N. gaeumannii DNA to P. menziesii DNA determined by qPCR. qPCR methods were as described by Montwé et al. (2021) using Luna qPCR Master Mix (New England BioLabs Inc) and respective primers and probes for amplification and quantification of Douglas-fir and N. gaeumannii DNA (Douglas fir: Leafy probe and primer; N. gaeumannii: beta-tubulin probe and primers).

*Table 1. Table of the top 40 most abundant taxa found across all samples. Given is the relative abundance at which they were found in samples after normalization, accession number for their closest match in genebank (NCBI) and corresponding classification to the genus and species level with scores indicating quality of match. * Indicates nearest classification if genus was not available. Trophic modes and guilds were assigned using FUNguild. Taxon indicates the level at which this classification was made.*

Classification							**FUNguild**		
	Abundance (%)	Accession number	Genus	Species	Query Cover	% Identity	Taxon	Trophic Mode	Guild
OTU1	64.40	ON783984.1	Nothophaeocryptopus	gaeumannii	100	100	Mycosphaerellaceae	Pathotroph-Saprotroph	Plant Pathogen-Undefined Saprotroph
OTU13	0.87	OW986962.1	Penicilium	glaucoalbidum	100	100	Penicillium	Saprotroph	Dung Saprotroph-Undefined Saprotroph-Wood Saprotroph
OTU14	1.24	KY352466.1	Retiarius	bovicornutus	100	81.16	Orbiliaceae	Saprotroph	Wood Saprotroph
OTU17	1.04	KP400572.1	Chaeotothyriales*	sp.	99	98.49	-	-	-
OTU19	0.91	KP400572.1	Chaeotothyriales*	sp.	99	99.5	-	-	-
OTU2	5.64	ON784015.1	Rhizosphaera	merioides,	100	100	Rhizosphaera	Pathotroph	Plant Pathogen
OTU20	0.56	ON787635.1	Exobasidium	sp.	100	98.63	Exobasidium	Pathotroph	Plant Pathogen
OTU23	0.81	KP400572.1	Chaeotothyriales*	sp.	99	98.49	-	-	-
OTU25	0.46	KY424482.1	Exobasidium	uvae-ursi	100	90.83	Exobasidium	Pathotroph	Plant Pathogen
OTU29	0.61	NR_189406.1	Niesslia	endophytica	100	100	Niesslia	Saprotroph	Undefined Saprotroph
OTU3	2.26	ON784044.1	Rhizosphaera	sp.	100	100	Rhizosphaera	Pathotroph	Plant Pathogen
OTU31	0.40	KP400572.1	Chaeotothyriales*	sp.	99	97.49	-	-	-
OTU32	0.44	OL752699.1	Pseudohelotium	pineti	98	86.64	Helotiaceae	Saprotroph-Symbiotroph	Ectomycorrhizal-Fungal Parasite-Plant Pathogen-Wood Saprotroph
OTU33	0.36	MF285231.1	Camptophora	schimae	94	85.05	-	-	-
OTU34	0.34	OP612941.1	Penidiella		82	86.55	Teratosphaeriaceae	Pathotroph-Saprotroph	Animal Pathogen-Plant Pathogen-Undefined Saprotroph
OTU35	0.33	AB845352.1	Penidiella	sp.	99	88.84	Teratosphaeriaceae	Pathotroph-Saprotroph	Animal Pathogen-Plant Pathogen-Undefined Saprotroph
OTU37	0.31	MT548673.1	Cladosporium	delicatulum	100	100	-	-	-
OTU39	0.25	KU559338.1	Acanthobasidium	penicillatum	100	99.51	Acanthobasidium	Saprotroph	Undefined Saprotroph
OTU4	3.56	KP400572.1	Chaeotothyriales*		99	98.99	-	-	-
OTU40	0.19	ON787635.1	Exobasidium	sp.	100	98.17	Exobasidium	Pathotroph	Plant Pathogen
OTU41	0.21	AF462425.1	Rhabdocline	parkeri	100	99.54	Rhabdocline	Pathotroph	Plant Pathogen
OTU44	0.13	AB175249.1	Thysanophora	penicillioides	100	99.53	Thysanophora	Saprotroph	Undefined Saprotroph
OTU45	0.28	MH863133.1	Exophiala	eucalyptorum	100	97.01	Herpotrichiellaceae	Pathotroph-Saprotroph	Animal Pathogen-Fungal Parasite-Undefined Saprotroph
OTU46	0.23	NR_145014.1	Neodevriesia	sardiniae	100	90.71	Neodevriesiaceae	Pathotroph-Saprotroph	Plant Pathogen-Undefined Saprotroph
OTU48	0.25	MT852493.1	Sakaguchia	lamelibrachiae	100	90.74	-	-	-
OTU5	3.22	KY979763.1	Zasmidium	commune	100	97.87	Zasmidium	Saprotroph	Undefined Saprotroph
OTU51	0.15	MN077443.1	Diaporthe	sp.	100	100	Diaporthe	Pathotroph-Symbiotroph	Endophyte-Plant Pathogen
OTU53	0.25	MK536893.1	Ascomycota*	sp.	100	94.26	-	-	-
OTU54	0.19	NR_189986.1	Xenosonderhenia	wangzhenyi	100	91.3	Mycosphaerellaceae	Pathotroph-Saprotroph	Plant Pathogen-Undefined Saprotroph
OTU56	0.17	MH578475.1	Helotiales	sp.	100	88.65	-	-	-
OTU61	0.20	MN894289.1	Tremella	sanguinea	100	89.14	-	-	-
OTU62	0.19	MK577896.1	Pleosporales	sp.	38	84.15	-	-	-
OTU63	0.16	OP612941.1	Lichenostigmatales	sp.	82	87.13	-	-	-
OTU64	0.14	KM216384.1	Dothideomycetes*	sp.	64	98.68	-	-	-
OTU67	0.16	MK794589.1	Orbiliaceae*	sp.	95	100	Orbiliaceae	Saprotroph	Wood Saprotroph
OTU72	0.14	NR_155886.1	Taphrina	vestergrenii	100	100	Taphrina	Pathotroph	Plant Pathogen
OTU79	0.13	KY104495.1	Phaeotremella	skinneri	100	98.29	-	-	-
OTU8	1.94	AF462420.1	Rhabdocline	pseudotsugae	100	98.62	Rhabdocline	Pathotroph	Plant Pathogen
OTU86	0.13	MK460409.1	Venturia	sp.	99	100	Venturiaceae	Pathotroph-Saprotroph-Symbiotroph	Endophyte-Plant Pathogen-Undefined Saprotroph
OTU9	1.38	ON787635.1	Exobasidium	sp.	100	94.98	Exobasidium	Pathotroph	Plant Pathogen

Appendix 6.

Table 1. All OTUs in JR GCA breeding population foliage determined by metagenomics (based on rarefied data; n = 55). The relative abundance of each OTU is given along with their closest taxonomic classification identified with the UNITE Fungal ITS database.

	Percentage	kingdom	phylum	class	order	family	genus	species
OTU1	64.52	Fungi	Ascomycota	Dothideomycetes	Mycosphaerellales	Mycosphaerellaceae	Nothophaeocryptopus	gaeumannii
OTU2	5.64	Fungi	Ascomycota	Dothideomycetes	Dothideales	Dothioraceae	Rhizosphaera	merioides
OTU3	2.23	Fungi	Ascomycota	Dothideomycetes	Dothideales	Dothioraceae	Rhizosphaera	sp.
OTU4	3.59	Fungi	Ascomycota	Eurotiomycetes	Chaetothyriales			
OTU5	3.19	Fungi	Ascomycota	Dothideomycetes	Mycosphaerellales	Mycosphaerellaceae	Zasmidium	
OTU8	1.93	Fungi	Ascomycota	Leotiomycetes	Helotiales	Hemiphacidiaceae	Rhabdocline	pseudotsugae
OTU9	1.36	Fungi	Basidiomycota	Exobasidiomycetes	Exobasidiales	Exobasidiaceae	Exobasidium	
OTU13	0.82	Fungi	Ascomycota	Eurotiomycetes	Eurotiales	Aspergillaceae	Penicillium	glaucoalbidum
OTU14	1.24	Fungi	Ascomycota	Orbiliomycetes	Orbiliales	Orbiliaceae	Retiarius	bovicornutus
OTU17	1.05	Fungi	Ascomycota	Eurotiomycetes	Chaetothyriales			
OTU19	0.91	Fungi	Ascomycota	Eurotiomycetes	Chaetothyriales			
OTU20	0.56	Fungi	Basidiomycota	Exobasidiomycetes	Exobasidiales	Exobasidiaceae	Exobasidium	
OTU23	0.81	Fungi	Ascomycota	Eurotiomycetes	Chaetothyriales			
OTU25	0.45	Fungi	Basidiomycota	Exobasidiomycetes	Exobasidiales	Exobasidiaceae	Exobasidium	
OTU29	0.61	Fungi	Ascomycota	Sordariomycetes	Hypocreales	Niessliaceae	Niesslia	endophytica
OTU31	0.40	Fungi	Ascomycota	Eurotiomycetes	Chaetothyriales			
OTU32	0.44	Fungi	Ascomycota	Leotiomycetes	Helotiales	Helotiales_fam_Incertae_sedis		
OTU33	0.36	Fungi	Ascomycota	Eurotiomycetes	Chaetothyriales			
OTU34	0.36	Fungi	Ascomycota	Ascomycota_cls_Incertae_sedis	Ascomycota_ord_Incertae_sedis	Ascomycota_fam_Incertae_sedis	Ascomycota_gen_Incertae_sedis	
OTU35	0.33	Fungi	Ascomycota	Dothideomycetes	Mycosphaerellales	Teratosphaeriaceae		
OTU37	0.31	Fungi						
OTU39	0.26	Fungi	Basidiomycota	Agaricomycetes	Russulales	Stereaceae	Aleurodiscus	
OTU40	0.18	Fungi	Basidiomycota	Exobasidiomycetes	Exobasidiales	Exobasidiaceae	Exobasidium	
OTU41	0.21	Fungi	Ascomycota	Leotiomycetes	Helotiales	Hemiphacidiaceae	Rhabdocline	parkeri
OTU44	0.14	Fungi	Ascomycota	Eurotiomycetes	Eurotiales	Aspergillaceae	Thysanophora	penicillioides
OTU45	0.28	Fungi	Ascomycota	Eurotiomycetes	Chaetothyriales			
OTU46	0.23	Fungi	Ascomycota	Dothideomycetes	Capnodiales	Neodevriesiaceae	Neodevriesia	
OTU48	0.25	Fungi	Basidiomycota	Cystobasidiomycetes				
OTU51	0.15	Fungi	Ascomycota	Sordariomycetes	Diaporthales	Diaporthaceae	Diaporthe	
OTU53	0.25	Fungi	Ascomycota	Dothideomycetes	Dothideomycetes_ord_Incertae_sedis	Dothideomycetes_fam_Incertae_sedis	Dothideomycetes_gen_Incertae_sedis	
OTU54	0.18	Fungi	Ascomycota	Dothideomycetes	Mycosphaerellales	Mycosphaerellaceae		
OTU56	0.18	Fungi	Ascomycota	Leotiomycetes	Helotiales	Helotiales_fam_Incertae_sedis	Helotiales_gen_Incertae_sedis	
OTU61	0.21	Fungi	Basidiomycota	Tremellomycetes	Tremellales	Tremellales_fam_Incertae_sedis	Tremellales_gen_Incertae_sedis	
OTU62	0.20	Fungi	Ascomycota	Dothideomycetes	Pleosporales	Pleosporales_fam_Incertae_sedis	Pleosporales_gen_Incertae_sedis	
OTU63	0.15	Fungi	Ascomycota	Ascomycota_cls_Incertae_sedis	Ascomycota_ord_Incertae_sedis	Ascomycota_fam_Incertae_sedis	Ascomycota_gen_Incertae_sedis	
OTU64	0.15	Fungi	Ascomycota	Dothideomycetes				
OTU66	0.14	Fungi	Ascomycota	Dothideomycetes	Mycosphaerellales			
OTU67	0.16	Fungi	Ascomycota	Orbiliomycetes	Orbiliales	Orbiliaceae	Orbiliaceae_gen_Incertae_sedis	
OTU68	0.13	Fungi	Basidiomycota	Agaricostilbomycetes	Agaricostilbales	Ruineniaceae	Ruinenia	
OTU71	0.11	Fungi	Basidiomycota	Tremellomycetes	Cystofilobasidiales	Mrakiaceae	Krasilnikovozyma	
OTU72	0.14	Fungi	Ascomycota	Taphrinomycetes	Taphrinales	Taphrinaceae	Taphrina	vestergrenii
OTU74	0.13	Fungi	Ascomycota	Eurotiomycetes	Chaetothyriales			
OTU75	0.12	Fungi	Basidiomycota	Tremellomycetes	Tremellales	Tremellaceae	Tremella	
OTU76	0.12	Fungi	Basidiomycota	Tremellomycetes	Tremellales	Tremellaceae	Tremella	
OTU77	0.12	Fungi	Ascomycota	Dothideomycetes	Dothideales			
OTU78	0.10	Fungi	Basidiomycota	Tremellomycetes	Tremellales	Bulleribasidiaceae	Derxomyces	
OTU79	0.13	Fungi	Basidiomycota	Tremellomycetes	Tremellales	Tremellales_fam_Incertae_sedis	Tremellales_gen_Incertae_sedis	

	Percentage	kingdom	phylum	class	order	family	genus	species
OTU80	0.12	Fungi	Ascomycota	Orbiliomycetes	Orbiliales	Orbiliaceae	Orbiliaceae_gen_Incertae_sedis	
OTU85	0.11	Fungi	Ascomycota	Leotiomycetes	Helotiales			
OTU86	0.13	Fungi	Ascomycota	Dothideomycetes	Venturiales	Venturiaceae		
OTU88	0.11	Fungi	Ascomycota	Sordariomycetes	Xylariales			
OTU89	0.12	Fungi	Ascomycota	Leotiomycetes	Helotiales			
OTU94	0.08	Fungi	Basidiomycota	Microbotryomycetes	Microbotryomycetes_ord_Incertae_sedis	Microbotryomycetes_fam_Incertae_sedis	Microbotryomycetes_gen_Incertae_sedis	
OTU95	0.08	Fungi	Basidiomycota	Tremellomycetes	Tremellales	Tremellaceae	Tremella	
OTU96	0.09	Fungi	Ascomycota	Dothideomycetes	Pleosporales	Pleosporales_fam_Incertae_sedis	Pleosporales_gen_Incertae_sedis	
OTU98	0.08	Fungi	Ascomycota	Eurotiomycetes	Chaetothyriales			
OTU102	0.09	Fungi	Ascomycota	Eurotiomycetes	Chaetothyriales			
OTU103	0.06	Fungi	Ascomycota	Dothideomycetes	Capnodiales	Capnodiales_fam_Incertae_sedis	Microcyclospora	
OTU107	0.07	Fungi	Ascomycota	Dothideomycetes	Capnodiales	Neodevriesiaceae		
OTU108	0.09	Fungi	Ascomycota	Eurotiomycetes	Chaetothyriales	Herpotrichiellaceae		
OTU109	0.04	Fungi	Ascomycota	Dothideomycetes	Dothideales			
OTU110	0.05	Fungi	Basidiomycota	Microbotryomycetes	Sporidiobolales	Sporidiobolaceae	Rhodosporidiobolus	
OTU112	0.08	Fungi	Ascomycota	Dothideomycetes	Zeloasperisporiales	Zeloasperisporiaceae	Zeloasperisporium	
OTU114	0.07	Fungi	Basidiomycota	Tremellomycetes	Tremellales	Tremellaceae	Tremella	
OTU116	0.06	Fungi	Basidiomycota	Microbotryomycetes	Microbotryomycetes_ord_Incertae_sedis	Chrysozymaceae	Pseudohyphozyma	
OTU117	0.08	Fungi	Ascomycota	Candelariomycetes	Candelariales	Pycnoraceae	Pycnora	
OTU118	0.04	Fungi	Basidiomycota	Exobasidiomycetes	Exobasidiales	Exobasidiaceae	Exobasidium	
OTU122	0.05	Fungi	Ascomycota	Dothideomycetes	Capnodiales	Capnodiales_fam_Incertae_sedis	Microcyclospora	
OTU123	0.05	Fungi	Ascomycota	Taphrinomycetes	Taphrinales	Taphrinaceae	Taphrina	
OTU124	0.06	Fungi	Ascomycota	Orbiliomycetes	Orbiliales	Orbiliaceae	Orbiliaceae_gen_Incertae_sedis	
OTU125	0.05	Fungi	Ascomycota	Eurotiomycetes	Chaetothyriales	Herpotrichiellaceae		
OTU126	0.05	Fungi	Basidiomycota	Microbotryomycetes	Microbotryomycetes_ord_Incertae_sedis			
OTU127	0.06	Fungi	Basidiomycota	Tremellomycetes	Tremellomycetes_ord_Incertae_sedis	Tremellomycetes_fam_Incertae_sedis	Tremellomycetes_gen_Incertae_sedis	
OTU128	0.03	Fungi	Ascomycota	Dothideomycetes	Capnodiales	Dissoconiaceae	Ramichloridium	
OTU129	0.06	Fungi	Ascomycota	Orbiliomycetes	Orbiliales	Orbiliales_fam_Incertae_sedis	Orbiliales_gen_Incertae_sedis	
OTU131	0.04	Fungi	Ascomycota	Dothideomycetes	Mycosphaerellales	Mycosphaerellaceae		
OTU139	0.06	Fungi	Basidiomycota	Exobasidiomycetes	Exobasidiales	Exobasidiaceae	Exobasidium	
OTU142	0.04	Fungi	Ascomycota	Eurotiomycetes	Chaetothyriales	Trichomeriaceae	Knufia	
OTU143	0.03	Fungi	Ascomycota	Leotiomycetes	Helotiales			
OTU145	0.06	Fungi	Ascomycota	Dothideomycetes	Zeloasperisporiales	Zeloasperisporiaceae	Zeloasperisporium	
OTU146	0.05	Fungi	Basidiomycota	Agaricostilbomycetes	Agaricostilbales	Chionosphaeraceae	Kurtzmanomyces	
OTU147	0.04	Fungi	Ascomycota	Dothideomycetes				
OTU149	0.04	Fungi	Ascomycota	Dothideomycetes	Capnodiales	Capnodiales_fam_Incertae_sedis	Pseudoramichloridium	henryi
OTU152	0.05	Fungi	Basidiomycota	Agaricomycetes	Cantharellales	Cantharellales_fam_Incertae_sedis	Cantharellales_gen_Incertae_sedis	
OTU156	0.05	Fungi	Basidiomycota	Microbotryomycetes	Microbotryomycetes_ord_Incertae_sedis	Microbotryomycetes_fam_Incertae_sedis	Curvibasidium	
OTU157	0.04	Fungi	Basidiomycota	Microbotryomycetes	Microbotryomycetes_ord_Incertae_sedis			
OTU158	0.03	Fungi	Ascomycota	Dothideomycetes	Mycosphaerellales	Teratosphaeriaceae		
OTU159	0.05	Fungi						
OTU160	0.04	Fungi	Basidiomycota	Tremellomycetes	Filobasidiales	Filobasidiaceae	Naganishia	
OTU161	0.03	Fungi	Basidiomycota	Tremellomycetes	Filobasidiales	Piskurozymaceae	Piskurozyma	
OTU162	0.05	Fungi	Basidiomycota	Microbotryomycetes	Microbotryomycetes_ord_Incertae_sedis	Microbotryomycetes_fam_Incertae_sedis	Microbotryomycetes_gen_Incertae_sedis	
OTU163	0.03	Fungi	Ascomycota	Orbiliomycetes	Orbiliales	Orbiliaceae	Orbiliaceae_gen_Incertae_sedis	
OTU165	0.03	Fungi	Ascomycota	Lecanoromycetes	Lecanorales			
OTU166	0.02	Fungi	Ascomycota	Leotiomycetes	Helotiales			
OTU168	0.04	Fungi	Ascomycota	Orbiliomycetes	Orbiliales	Orbiliaceae	Orbiliaceae_gen_Incertae_sedis	
OTU170	0.04	Fungi	Ascomycota	Eurotiomycetes	Phaeomoniellales	Phaeomoniellaceae		
OTU171	0.03	Fungi	Ascomycota	Dothideomycetes	Pleosporales	Pleosporales_fam_Incertae_sedis	Pleosporales_gen_Incertae_sedis	
OTU172	0.03	Fungi	Ascomycota	Dothideomycetes	Mycosphaerellales	Teratosphaeriaceae		
OTU174	0.02	Fungi	Basidiomycota	Agaricomycetes	Russulales			
OTU175	0.02	Fungi	Basidiomycota	Microbotryomycetes	Leucosporidiales	Leucosporidiaceae	Leucosporidium	
OTU177	0.03	Fungi	Ascomycota	Eurotiomycetes	Chaetothyriales			
OTU178	0.03	Fungi	Ascomycota	Eurotiomycetes	Chaetothyriales	Chaetothyriaceae		
OTU181	0.02	Fungi	Basidiomycota	Exobasidiomycetes	Exobasidiales	Exobasidiaceae	Exobasidium	

	Percentage	kingdom	phylum	class	order	family	genus	species
OTU182	0.02	Fungi	Basidiomycota	Microbotryomycetes	Microbotryomycetes_ord_Incertae_sedis	Chrysozymaceae	Oberwinklerozyma	
OTU183	0.02	Fungi	Basidiomycota	Exobasidiomycetes	Exobasidiales	Exobasidiaceae	Exobasidium	
OTU184	0.03	Fungi	Basidiomycota	Tremellomycetes	Tremellales	Tremellaceae	Tremella	
OTU186	0.02	Fungi	Ascomycota	Sordariomycetes	Hypocreales	Nectriaceae	Nectriaceae_gen_Incertae_sedis	
OTU187	0.02	Fungi	Ascomycota	Dothideomycetes	Mycosphaerellales	Teratosphaeriaceae	Catenulostroma	elginense
OTU189	0.05	Fungi	Ascomycota	Eurotiomycetes	Phaeomoniellales	Phaeomoniellaceae		
OTU191	0.04	Fungi	Ascomycota	Taphrinomycetes	Taphrinales	Taphrinaceae	Taphrina	
OTU196	0.02	Fungi	Basidiomycota	Cystobasidiomycetes	Cystobasidiales	Cystobasidiaceae	Cystobasidium	oligophagum
OTU197	0.02	Fungi	Ascomycota	Eurotiomycetes	Chaetothyriales			
OTU201	0.02	Fungi	Ascomycota					
OTU203	0.05	Fungi	Basidiomycota	Malasseziomycetes	Malasseziales	Malasseziaceae	Malassezia	
OTU204	0.01	Fungi	Basidiomycota	Microbotryomycetes	Microbotryomycetes_ord_Incertae_sedis	Microbotryomycetes_fam_Incertae_sedis	Curvibasidium	
OTU206	0.02	Fungi	Ascomycota	Dothideomycetes	Venturiales	Sympoventuriaceae	Sympoventuriaceae_gen_Incertae_sedis	
OTU208	0.02	Fungi	Ascomycota	Orbiliomycetes	Orbiliales	Orbiliales_fam_Incertae_sedis	Orbiliales_gen_Incertae_sedis	
OTU211	0.02	Fungi	Ascomycota	Dothideomycetes	Mycosphaerellales	Mycosphaerellaceae		
OTU215	0.03	Fungi	Ascomycota	Dothideomycetes	Myriangiales	Myriangiaceae	Myriangium	
OTU220	0.02	Fungi	Ascomycota	Dothideomycetes	Capnodiales	Capnodiales_fam_Incertae_sedis	Capnodiales_gen_Incertae_sedis	
OTU223	0.02	Fungi						
OTU224	0.01	Fungi	Basidiomycota	Microbotryomycetes	Microbotryomycetes_ord_Incertae_sedis	Microbotryomycetes_fam_Incertae_sedis	Curvibasidium	
OTU225	0.02	Fungi	Ascomycota	Dothideomycetes	Dothideales	Dothioraceae		
OTU226	0.01	Fungi	Basidiomycota	Pucciniomycetes	Septobasidiales	Septobasidiaceae	Septobasidium	
OTU227	0.01	Fungi	Ascomycota	Dothideomycetes	Dothideales			
OTU229	0.02	Fungi	Ascomycota	Eurotiomycetes	Chaetothyriales	Chaetothyriaceae		
OTU233	0.02	Fungi	Ascomycota	Orbiliomycetes	Orbiliales	Orbiliaceae	Orbilia	
OTU234	0.02	Fungi	Basidiomycota	Microbotryomycetes	Microbotryomycetes_ord_Incertae_sedis	Chrysozymaceae	Bannozyma	yamatoana
OTU236	0.01	Fungi	Ascomycota	Dothideomycetes	Mytilinidiales	Mytilinidiaceae	Lophium	arboricola
OTU237	0.01	Fungi	Basidiomycota	Cystobasidiomycetes				
OTU239	0.02	Fungi	Basidiomycota	Cystobasidiomycetes				
OTU240	0.01	Fungi	Ascomycota	Sordariomycetes	Hypocreales	Niessliaceae		
OTU242	0.02	Fungi	Basidiomycota	Cystobasidiomycetes				
OTU243	0.01	Fungi	Basidiomycota	Microbotryomycetes	Microbotryomycetes_ord_Incertae_sedis	Chrysozymaceae	Fellozyma	
OTU245	0.01	Fungi	Basidiomycota	Agaricostilbomycetes	Agaricostilbales	Kondoaceae	Bensingtonia	
OTU246	0.02	Fungi	Basidiomycota	Agaricostilbomycetes	Agaricostilbales	Chionosphaeraceae	Kurtzmanomyces	
OTU248	0.02	Fungi	Ascomycota	Orbiliomycetes	Orbiliales	Orbiliaceae	Orbiliaceae_gen_Incertae_sedis	
OTU249	0.01	Fungi	Ascomycota	Orbiliomycetes	Orbiliales	Orbiliales_fam_Incertae_sedis	Orbiliales_gen_Incertae_sedis	
OTU253	0.01	Fungi	Basidiomycota	Cystobasidiomycetes	Cystobasidiomycetes_ord_Incertae_sedis			
OTU255	0.01	Fungi	Ascomycota	Dothideomycetes	Mycosphaerellales	Mycosphaerellaceae	Ramularia	
OTU257	0.01	Fungi	Ascomycota	Dothideomycetes	Pleosporales	Pleosporales_fam_Incertae_sedis	Pleosporales_gen_Incertae_sedis	
OTU258	0.01	Fungi	Basidiomycota					
OTU259	0.02	Fungi	Ascomycota	Taphrinomycetes	Taphrinales	Taphrinaceae	Taphrina	
OTU260	0.01	Fungi	Basidiomycota	Microbotryomycetes				
OTU263	0.01	Fungi	Ascomycota	Leotiomycetes	Helotiales	Sclerotiniaceae		
OTU268	0.02	Fungi	Basidiomycota	Agaricomycetes	Cantharellales	Ceratobasidiaceae		
OTU272	0.01	Fungi						
OTU276	0.01	Fungi	Ascomycota	Leotiomycetes	Helotiales			
OTU278	0.01	Fungi	Ascomycota	Taphrinomycetes	Taphrinales	Taphrinaceae	Taphrinaceae_gen_Incertae_sedis	
OTU280	0.01	Fungi	Basidiomycota	Agaricostilbomycetes	Agaricostilbales	Kondoaceae	Bensingtonia	
OTU281	0.01	Fungi	Ascomycota	Eurotiomycetes	Phaeomoniellales			
OTU282	0.01	Fungi	Basidiomycota	Tremellomycetes	Filobasidiales	Filobasidiaceae	Heterocephalacria	
OTU284	0.01	Fungi	Basidiomycota	Cystobasidiomycetes				
OTU285	0.01	Fungi	Ascomycota					
OTU288	0.01	Fungi	Ascomycota	Dothideomycetes	Venturiales	Sympoventuriaceae	Sympoventuriaceae_gen_Incertae_sedis	
OTU289	0.01	Fungi	Basidiomycota	Microbotryomycetes	Leucosporidiales	Leucosporidiaceae	Leucosporidium	
OTU290	0.01	Fungi	Ascomycota	Leotiomycetes	Helotiales			
OTU291	0.01	Fungi	Ascomycota	Dothideomycetes	Pleosporales	Didymellaceae		
OTU292	0.01	Fungi	Basidiomycota	Agaricomycetes	Cantharellales	Ceratobasidiaceae	Ceratobasidium	

	Percentage	kingdom	phylum	class	order	family	genus	species
OTU298	0.01	Fungi	Basidiomycota	Cystobasidiomycetes				
OTU299	0.02	Fungi	Ascomycota	Eurotiomycetes	Chaetothyriales	Chaetothyriaceae		
OTU301	0.01	Fungi	Ascomycota	Sordariomycetes	Hypocreales	Cordycipitaceae		
OTU304	0.01	Fungi	Ascomycota	Dothideomycetes	Dothideales			
OTU305	0.00	Fungi	Basidiomycota	Agaricomycetes	Agaricales	Strophariaceae	Hypholoma	
OTU308	0.01	Fungi	Ascomycota	Taphrinomycetes	Taphrinales	Taphrinaceae	Taphrinaceae_gen_Incertae_sedis	
OTU310	0.01	Fungi	Ascomycota	Leotiomycetes	Helotiales			
OTU312	0.00	Fungi	Ascomycota	Sordariomycetes	Hypocreales	Nectriaceae	Fusicolla	
OTU314	0.01	Fungi	Ascomycota	Leotiomycetes	Helotiales			
OTU315	0.01	Fungi	Fungi_phy_Incertae_sedis	Fungi_cls_Incertae_sedis	Fungi_ord_Incertae_sedis	Fungi_fam_Incertae_sedis	Fungi_gen_Incertae_sedis	
OTU316	0.02	Fungi	Ascomycota	Eurotiomycetes	Chaetothyriales	Herpotrichiellaceae		
OTU321	0.00	Fungi	Ascomycota	Taphrinomycetes	Taphrinales	Taphrinaceae	Taphrina	
OTU325	0.00	Fungi	Basidiomycota	Cystobasidiomycetes				
OTU326	0.01	Fungi	Ascomycota	Leotiomycetes	Helotiales	Hemiphacidiaceae	Rhabdocline	
OTU327	0.01	Fungi	Ascomycota	Taphrinomycetes	Taphrinales	Taphrinaceae	Taphrina	
OTU328	0.01	Fungi	Basidiomycota	Cystobasidiomycetes				
OTU330	0.01	Fungi	Ascomycota	Taphrinomycetes	Taphrinales	Taphrinaceae	Taphrina	
OTU332	0.01	Fungi	Basidiomycota	Cystobasidiomycetes				
OTU333	0.01	Fungi	Ascomycota	Dothideomycetes	Mycosphaerellales	Mycosphaerellaceae		
OTU335	0.01	Fungi	Ascomycota	Eurotiomycetes	Chaetothyriales	Herpotrichiellaceae	Cladophialophora	
OTU337	0.01	Fungi	Basidiomycota	Pucciniomycetes	Septobasidiales	Septobasidiaceae	Septobasidium	
OTU339	0.01	Fungi	Ascomycota	Dothideomycetes	Dothideomycetes_ord_Incertae_sedis	Dothideomycetes_fam_Incertae_sedis	Dothideomycetes_gen_Incertae_sedis	
OTU348	0.01	Fungi	Ascomycota	Dothideomycetes	Pleosporales	Amorosiaceae	Amorocoelophoma	cassiae
OTU352	0.01	Fungi	Basidiomycota	Tremellomycetes	Tremellales	Tremellales_fam_Incertae_sedis	Tremellales_gen_Incertae_sedis	
OTU353	0.01	Fungi	Basidiomycota	Tremellomycetes	Tremellales	Tremellales_fam_Incertae_sedis	Tremellales_gen_Incertae_sedis	
OTU354	0.00	Fungi	Basidiomycota	Agaricomycetes	Polyporales	Ganodermataceae	Ganoderma	
OTU355	0.00	Fungi	Basidiomycota	Agaricomycetes	Cantharellales	Ceratobasidiaceae	Ceratobasidium	
OTU356	0.01	Fungi	Ascomycota	Dothideomycetes	Mytilinidiales	Mytilinidiaceae	Mytilinidion	
OTU357	0.01	Fungi	Basidiomycota	Cystobasidiomycetes	Sakaguchiales	Sakaguchiaceae	Sakaguchia	
OTU358	0.00	Fungi	Basidiomycota	Exobasidiomycetes	Exobasidiales	Exobasidiaceae	Exobasidium	
OTU362	0.00	Fungi	Ascomycota	Leotiomycetes	Helotiales	Tympanidaceae		
OTU367	0.01	Fungi	Ascomycota	Eurotiomycetes	Chaetothyriales	Trichomeriaceae	Trichomerium	
OTU371	0.00	Fungi	Ascomycota	Leotiomycetes	Helotiales			
OTU374	0.00	Fungi	Ascomycota	Orbiliomycetes	Orbiliales	Orbiliaceae	Orbiliaceae_gen_Incertae_sedis	
OTU375	0.01	Fungi	Basidiomycota	Agaricomycetes	Agaricales	Strophariaceae	Hypholoma	
OTU383	0.01	Fungi	Ascomycota	Ascomycota_cls_Incertae_sedis	Ascomycota_ord_Incertae_sedis	Ascomycota_fam_Incertae_sedis	Ascomycota_gen_Incertae_sedis	
OTU386	0.00	Fungi	Ascomycota	Leotiomycetes				
OTU396	0.01	Fungi	Basidiomycota	Agaricomycetes	Polyporales	Fomitopsidaceae	Fomitopsis	
OTU403	0.00	Fungi	Ascomycota	Dothideomycetes	Dothideales			
OTU406	0.01	Fungi	Basidiomycota	Tremellomycetes	Tremellales	Tremellaceae	Tremella	
OTU407	0.00	Fungi	Ascomycota	Dothideomycetes	Mycosphaerellales	Teratosphaeriaceae	Salinomyces	polonicus
OTU409	0.01	Fungi	Ascomycota	Dothideomycetes	Mycosphaerellales			
OTU410	0.00	Fungi	Ascomycota	Sordariomycetes	Sordariomycetes_ord_Incertae_sedis	Sordariomycetes_fam_Incertae_sedis	Sordariomycetes_gen_Incertae_sedis	
OTU413	0.01	Fungi	Ascomycota	Eurotiomycetes	Chaetothyriales	Herpotrichiellaceae		
OTU415	0.00	Fungi	Ascomycota	Leotiomycetes	Helotiales			
OTU425	0.01	Fungi	Basidiomycota	Agaricomycetes	Russulales			
OTU432	0.00	Fungi	Fungi_phy_Incertae_sedis	Fungi_cls_Incertae_sedis	Fungi_ord_Incertae_sedis	Fungi_fam_Incertae_sedis	Fungi_gen_Incertae_sedis	
OTU442	0.01	Fungi	Ascomycota	Eurotiomycetes	Chaetothyriales	Trichomeriaceae	Knufia	
OTU443	0.00	Fungi	Basidiomycota	Tremellomycetes	Filobasidiales	Piskurozymaceae	Piskurozyma	
OTU458	0.00	Fungi	Ascomycota	Dothideomycetes	Mycosphaerellales	Teratosphaeriaceae	Salinomyces	polonicus
OTU460	0.00	Fungi	Basidiomycota	Agaricostilbomycetes	Agaricostilbales	Chionosphaeraceae	Kurtzmanomyces	
OTU463	0.00	Fungi	Fungi_phy_Incertae_sedis	Fungi_cls_Incertae_sedis	Fungi_ord_Incertae_sedis	Fungi_fam_Incertae_sedis	Fungi_gen_Incertae_sedis	
OTU471	0.00	Fungi	Basidiomycota	Tremellomycetes	Tremellales	Tremellaceae	Tremella	
OTU474	0.00	Fungi	Ascomycota	Leotiomycetes	Helotiales	Hyaloscyphaceae		
OTU475	0.00	Fungi	Ascomycota	Dothideomycetes	Mycosphaerellales	Teratosphaeriaceae	Salinomyces	polonicus
OTU476	0.00	Fungi	Basidiomycota	Microbotryomycetes	Microbotryomycetes_ord_Incertae_sedis	Chrysozymaceae	Slooffia	pilatii

	Percentage	kingdom	phylum	class	order	family	genus	species
OTU478	0.00	Fungi	Ascomycota	Leotiomycetes	Helotiales	Helotiales_fam_Incertae_sedis	Helotiales_gen_Incertae_sedis	
OTU479	0.00	Fungi	Ascomycota	Leotiomycetes				
OTU481	0.00	Fungi	Basidiomycota	Microbotryomycetes	Microbotryomycetes_ord_Incertae_sedis	Chrysozymaceae	Fellozyma	
OTU482	0.00	Fungi	Basidiomycota	Cystobasidiomycetes	Cystobasidiales	Cystobasidiaceae		
OTU491	0.00	Fungi	Ascomycota	Dothideomycetes	Capnodiales	Capnodiales_fam_Incertae_sedis	Capnodiales_gen_Incertae_sedis	
OTU492	0.00	Fungi	Ascomycota	Dothideomycetes	Mycosphaerellales	Teratosphaeriaceae	Devriesia	
OTU499	0.00	Fungi	Ascomycota	Eurotiomycetes	Chaetothyriales	Herpotrichiellaceae	Cladophialophora	
OTU502	0.00	Fungi	Ascomycota	Dothideomycetes	Venturiales	Sympoventuriaceae	Sympoventuriaceae_gen_Incertae_sedis	
OTU518	0.00	Fungi	Ascomycota	Dothideomycetes	Pleosporales	Massarinaceae	Helminthosporium	
OTU521	0.00	Fungi	Basidiomycota	Agaricostilbomycetes	Agaricostilbales	Agaricostilbales_fam_Incertae_sedis	Agaricostilbales_gen_Incertae_sedis	
OTU547	0.00	Fungi	Basidiomycota	Microbotryomycetes	Kriegeriales	Kriegeriales_fam_Incertae_sedis	Kriegeriales_gen_Incertae_sedis	
OTU556	0.00	Fungi	Basidiomycota	Agaricomycetes	Agaricales			
OTU557	0.00	Fungi	Ascomycota	Dothideomycetes	Mycosphaerellales	Teratosphaeriaceae	Teratosphaericola	pseudoafricana
OTU558	0.00	Fungi	Ascomycota	Dothideomycetes	Mycosphaerellales	Teratosphaeriaceae	Salinomyces	polonicus
OTU559	0.00	Fungi	Fungi_phy_Incertae_sedis	Fungi_cls_Incertae_sedis	Fungi_ord_Incertae_sedis	Fungi_fam_Incertae_sedis	Fungi_gen_Incertae_sedis	
OTU565	0.00	Fungi	Ascomycota	Leotiomycetes	Helotiales	Tympanidaceae		